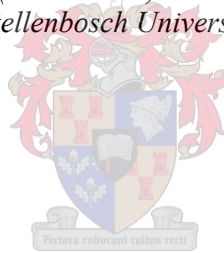


Techno-economic Evaluation of Long-term Energy Storage Options for Variable Renewable Energies in South Africa

by
Johan De Vrye Burger

*Thesis presented in partial fulfilment of the requirements for the degree
of Master of Engineering (Mechanical) in the Faculty of Engineering at
Stellenbosch University*



Supervisor: Prof Thomas Harms
Co-supervisors: Prof Johan van der Spuy
Prof Ben Sebitosi

December 2022

The financial assistance of the National Research Foundation (NRF) towards this research is hereby acknowledged. Opinions expressed and conclusions arrived at are those of the author and are not necessarily to be attributed to the NRF.

Declaration

By submitting this thesis electronically, I declare that the entirety of the work contained therein is my own, original work, that I am the sole author thereof (save to the extent explicitly otherwise stated), that reproduction and publication thereof by Stellenbosch University will not infringe any third party rights and that I have not previously in its entirety or in part submitted it for obtaining any qualification.

Date: 05/09/2022

Copyright ©2022 Stellenbosch University
All rights reserved

Abstract

Techno-economic Evaluation of Long-term Energy Storage Options for Variable Renewable Energies in South Africa

J.D. Burger

*Department of Mechanical and Mechatronic Engineering,
University of Stellenbosch,
Private Bag X1, 7602 Matieland, South Africa.*

Thesis: MEng (Mech)

December 2022

Energy generated by renewable technologies like solar photovoltaics (PV), concentrated solar power (CSP) and wind power, is intermittent (i.e., not dispatchable) and is therefore known as variable renewable energy (VRE). Since the value of electricity is dependent on when it is generated, a dispatchable energy power plant that can deliver electricity when it is needed, is more valuable. With the inclusion of energy storage systems (ESSs), VRE plants can produce dispatchable electricity. This can increase their share of the national energy mix and facilitate the transition away from traditional, greenhouse gas emitting, hence climate change inducing, electricity generation based on fossil fuels like coal or natural gas.

The motivation for this study was to identify the most cost-effective ESS technologies for VREs, based on selected applications. This study sets out to conduct a literature survey of the state-of-the-art ESS, develop a method of comparing their technical and financial performance and based on the results, draw conclusions pertaining to the deployment of such systems. An appropriate solution is proposed for the development of the South African energy mix going forward. The special case of CSP is considered since it includes built-in low-cost thermal energy storage (TES) and electricity generating inertia, which other VREs do not have.

Based on findings in the literature, two energy storage applications are selected, namely peaker replacement and long-term seasonal energy storage, for evaluation in

this study. State-of-the-art ESSs are investigated, and five technologies are selected for comparison: pumped storage hydroelectricity, compressed air energy storage, lithium-ion battery energy storage, vanadium-redox flow batteries and hydrogen power-to-gas energy storage.

A metric like LCOE, levelised cost of energy storage (LCOS), is identified as a suitable method for comparing ESS technologies. A probabilistic model, in the form of Monte Carlo analysis, is developed to account for the uncertainty associated with some of the input variables of the LCOS model. The model is verified and its sensitivity to some of the input variables is determined.

The techno-economic model is used to compare the five ESSs in the peaker replacement and long-term seasonal storage applications. The sensitivity of the LCOS to variance of the discount rate and discharge duration is investigated. A method is developed to compare the cost-competitiveness of CSP (with built-in TES) to PV and wind-powered plants coupled with the five ESSs considered in this study.

It was found that the investment cost had the greatest influence on LCOS, while that of replacement and operational costs were far less. This sensitivity was found to be even more significant for long-term seasonal storage applications. It was also found that the LCOS is more sensitive to changes in the annual cycle frequency than the discharge duration.

While it was found that pumped hydroelectricity and compressed air energy storage proved cost competitive with South African CSP plants (commissioned between 2018-2019), a comparison with the Aurora CSP plant in Australia showed that CSP has a value proposition at storage capacities of 4-8 h. As such, an argument is presented for CSP to be re-introduced in South Africa's integrated resource plan, particularly whenever dispatchable generation is called for.

Uittreksel

Tegno-ekonomiese Evaluasie van Lang-termyn Energiestoor Opsies vir Veranderlike Hernubare Energie in Suid Afrika

J.D. Burger

*Departement Meganiese en Megatroniese Ingenieurswese,
Universiteit van Stellenbosch,
Privaatsak X1, 7602 Matieland, Suid Afrika.*

Tesis: MIng (Meg)

Desember 2022

Energie wat deur hernubare kragopwekkingstechnologieë opgewek word, soos sonfotovoltaïes (PV), gekonsentreerde sonkrag (CSP) en wind krag, is veranderlik (en dus nie versendbaar nie) en staan dus bekend as veranderlike hernubare energie (VRE). Omdat die waarde van elektrisiteit afhanklik is van wanneer dit opgewek word, is 'n versendbare energie kragstasie, wat elektrisiteit kan verskaf wanneer dit benodig word, meer waardevol. Met die byvoeging van energiestoorstelsels (ESSs) kan VRE kragstasies versendbare elektrisiteit produseer. Dit kan hulle aandeel in die nasionale energiemengsel verhoog, en dus die oorskakeling fasiliteer, vanaf tradisionele, kweekhuisgas vrystellende, dus klimaat verandering induserende, elektrisiteit opwekking gebaseer op fossiele brandstowwe soos steenkool of natuurlike gas.

Die motivering vir hierdie studie was om die mees koste-effektiewe ESS tegnologie vir VREs te identifiseer, gebaseer op uitgesoekte toepassings. Hierdie studie mik om 'n literatuurstudie oor die stand-van-sake ESS te voltooi, om 'n metode te ontwikkel om die tegniese en finansiële prestasie daarvan te vergelyk, en, gebaseer op die resultate, gevolgtrekkings oor die aanwending van sulke stelsels te maak. 'n Toepaslike oplossing word voorgestel vir die ontwikkeling van die toekomstige Suid-Afrikaanse energiemengsel. Die spesiale geval van CSP word oorweeg omdat dit goedkoop termiese energiestoor (TES) insluit en ook ander kragopwekkingtraagheids voordele het, wat ander VREs nie het nie.

Gebaseer op die uitkoms van die literatuurstudie, was twee toepassings vir energiestoor geïdentifiseer, naamlik spitskragopwekking vervanging en lang-termyn seisoenale energiestoor, vir verdere oorweging in hierdie studie. Die stand-van-sake ESSs was ondersoek en vyf tegnologieë was gekies vir vergelyking: pompstoorhidroelektrisiteit, druklugenergiestoor, litium-ioon battery energiestoor, vandium-redoks vloeibatterie en waterstof krag-tot-gas energiestoor.

'n Metriek soos LCOE, naamlik gelykgemaakte koste van energiestoor (LCOS), is geïdentifiseer as 'n gepaste metode, om ESS tegnologieë te vergelyk. 'n Waarskynlikheidsmodel, in die vorm van Monte Carlo analise, is ontwikkel om die onsekerheid in ag te neem wat gepaard gaan met van die insetveranderlikes van die LCOS model. Die model is ge-verifieer en sy sensitiwiteit teenoor van die insetveranderlikes is bepaal.

Die tegno-ekonomiese model word gebruik om die vyf ESSs te vergelyk in spitskragvervanging en lang-termyn seisoenale stoortoe toepassings. Die sensitiwiteit van die LCOS teenoor die diskontokoers en die ontladingtydsduur word ondersoek. 'n Metode is ontwikkel om die kostemededingendheid van CSP (met ingeboude TES) te vergelyk met PV en windkragaanlegte gepaard met die vyf ESSs wat in hierdie studie oorweeg is.

Dit was gevind dat die belegingskoste die grootste invloed op LCOS gehad het, meer so as vervanging- en operasionele kostes, wat baie kleiner was. Die sensitiwiteit was nog meer betekenisvol in die geval van lang-termyn, seisoenale stoortoe toepassings. Dit was ook gevind dat die LCOS meer sensitief is vir veranderinge in die jaarlikse laaifrekwensie as die ontladingtydsduur.

Die studie het gevind dat pompstoorhidroelektrisiteit en druklugenergiestoor kostemededingend is met Suid-Afrikaanse CSP kragstasies (in bedryf geneem tussen 2018-2019). In vergelyking met die Aurora CSP kragstasie in Australië, het die studie ook gewys dat CSP steeds goeie waarde kan toe voeg in stoorontladingtydsduur van 4-8 h. Dus, word 'n argument aangebied vir CSP om heroorweeg te word as 'n kandidaat vir versendbare VRE in Suid-Afrika se geïntegreerde hulpbronplan.

Acknowledgements

I could not have undertaken this journey without the invaluable patience and feedback of Prof Thomas Harms. You kindled my passion for energy and concentrated solar power, in particular. Many thanks to Prof Johan van der Spuy for supporting my research and helping with the final push. I would also like to give thanks to Prof Ben Sebitosi and the National Research Foundation for funding my research. Thanks should also go to the Department of Mechanical and Mechatronic Engineering for hosting my research.

Special thanks to my fellow STERG students, particularly those who worked in the "penthouse" with me, for the moral support, camaraderie and quarterly poker games. I am grateful to Dr Matti Lubkoll for his passion and mentorship. Thanks should also go to Leigh van der Merwe at STERG, without whom the group would not be the same.

I am extremely grateful to my parents, Johan and Anita, for their unwavering support throughout my studies. To Skye, who often stayed up with me while I worked, my deepest gratitude and appreciation for always standing by me.

A Quotation

"From a fundamental biophysical perspective, both prehistoric human evolution and the course of history can be seen as the quest for controlling greater stores and flows of more concentrated and more versatile forms of energy and converting them, in more affordable ways at lower costs and with higher efficiencies, into heat, light, and motion." (Smil, 2017)

Contents

Declaration	i
Abstract	ii
Uittreksel	iv
Acknowledgements	vi
Contents	viii
List of Figures	xi
List of Tables	xiii
Nomenclature	xiv
1 Introduction	1
1.1 Background	1
1.2 Motivation	4
1.3 Research objectives	5
1.4 Methodology	5
1.5 Outline of thesis	6
2 Literature Study	7
2.1 Concentrated solar power (CSP)	7
2.1.1 Fundamentals of CSP	7
2.1.2 Existing technology	10
2.1.3 Emerging concepts	12
2.2 Energy storage	12
2.2.1 Definition of an energy storage system	14
2.2.2 Important energy storage metrics	15
2.2.3 Timescales of energy storage	16

2.2.4	Applications of energy storage	17
2.3	Trends in energy storage	18
2.4	Energy storage technologies	21
2.4.1	Thermal energy storage	22
2.4.2	Mechanical energy storage	27
2.4.3	Chemical energy storage	30
2.4.4	Electrochemical energy storage	32
2.4.5	Electromagnetic energy storage	35
2.5	Energy storage technology selection based on literature	35
2.6	Summary of this literature review	37
3	Financial Analysis Method	39
3.1	Definition of financial concepts	39
3.1.1	Time value of money	39
3.1.2	Levelised cost of electricity (LCOE)	40
3.2	Levelised cost of storage (LCOS)	42
3.3	LCOS method considered in this study	45
3.4	Simulation input assumptions	47
3.4.1	Considering inflation	48
3.4.2	Summary of input assumptions	48
3.5	Addressing uncertainty in the model	49
3.5.1	Model sensitivity analysis	49
3.5.2	Model uncertainty analysis	51
3.6	Description of method	52
3.6.1	Sampling strategy	53
3.6.2	Sample inputs for LCOS calculation	53
3.6.3	Determining the minimum sample size	55
3.7	Verification of the model	56
4	Monte Carlo Simulation Results	57
4.1	Interpretation of the results	57
4.2	Comparison of energy storage applications	59
4.2.1	Pumped storage hydroelectricity	59
4.2.2	Compressed air energy storage	60
4.2.3	Lithium-ion energy storage	61
4.2.4	Vanadium redox flow battery energy storage	61
4.2.5	Hydrogen energy storage	63
4.2.6	Peaker replacement: comparison of technologies	63
4.2.7	Seasonal storage: comparison of technologies	64
4.2.8	Summary of results based on energy storage application	65
4.3	Effect of discount rate	66

<i>CONTENTS</i>	xi
4.4 Effect of frequency and discharge duration	68
4.4.1 Pumped storage hydroelectricity	68
4.4.2 Compressed air energy storage	69
4.4.3 Lithium-ion battery energy storage	70
4.4.4 Vanadium redox flow batteries	70
4.4.5 Hydrogen energy storage	71
4.4.6 Practical limitation	71
4.5 Comparison with CSP tariffs	72
4.5.1 Comparison methodology	73
4.5.2 Direct comparison results	74
5 Discussion of Findings and Limitations	76
5.1 Findings of this study	76
5.1.1 Energy storage technology recommendations	76
5.1.2 A case for CSP in SA's integrated resource plan	77
5.2 Limitations of this study	79
5.2.1 The LCOS method	79
5.2.2 Thermal energy evaluation	79
5.2.3 Energy usage modelling	80
6 Summary, Conclusions and Recommendations	81
6.1 Summary	81
6.2 Findings and conclusions	84
6.3 Recommendations for future work	84
Appendices	86
A Inflation Indices and Conversion Rates	87
B Technology Cost Data Used	89
C Matlab Script	92
List of References	96

List of Figures

2.1.1	Schematic of a solar power tower CSP plant with a thermal energy storage system (Pelay <i>et al.</i> , 2017)	8
2.1.2	Worldwide long term average annual direct normal irradiation ((©) 2019 The World Bank, Source: Global Solar Atlas 2.0, Solar resource data: Solargis.)	9
2.1.3	Four mainly accepted technology types of CSP (Gauché, 2016)	10
2.2.1	Electrical power load profile of a large scale energy storage system (Akinyele and Rayudu, 2014)	13
2.2.2	Operational schematic of a general ESS	14
2.2.3	Top six global applications of energy storage (NTESS, 2020)	18
2.3.1	Top six ESS technologies in operation around the globe (NTESS, 2020)	19
2.3.2	Announced and commissioned ESS projects from 1905 to 2020 (cumulative) (NTESS, 2020)	19
2.3.3	Power capacity of announced and commissioned ESS projects from 1905 to 2020 (cumulative) (NTESS, 2020)	20
2.3.4	Power capacity of announced and commissioned ESS projects from 2000 to 2020 (cumulative) (NTESS, 2020)	21
2.4.1	Classification of energy storage	22
2.4.2	Schematic of two tank SPT plant (adapted from Pelay <i>et al.</i> , 2017)	24
2.4.3	Schematic of CAES system (Luo <i>et al.</i> , 2015)	29
2.4.4	Schematic of VRFB system (Luo <i>et al.</i> , 2015)	34
2.5.1	Comparison of ESSs based on power rating, energy capacity and discharge duration (Luo <i>et al.</i> , 2015)	36
3.5.1	Example of a spiderplot, illustrating the sensitivity of LCOS to each input parameter	50
3.5.2	Example of a tornado diagram, illustrating the sensitivity of LCOS to each of the stochastic input parameters	51
3.6.1	Sample plot of relative change in standard deviation of LCOS with growing sample size n	56

*LIST OF FIGURES***xiii**

4.1.1	Simulated cost components of LCOS (n=200)	58
4.1.2	Effect of frequency and discharge duration on LCOS	58
4.2.1	Example of a box plot	59
4.2.2	Levelised cost of pumped storage hydroelectricity	60
4.2.3	Levelised cost of compressed air energy storage	61
4.2.4	Levelised cost of lithium-ion energy storage	62
4.2.5	Levelised cost of vanadium redox flow battery energy storage	62
4.2.6	Levelised cost of hydrogen energy storage	63
4.2.7	Comparison of technologies: simulated LCOS (peaker replacement)	64
4.2.8	Comparison of technologies: simulated LCOS (seasonal storage)	65
4.3.1	Effect of variation in discount rate on LCOS (peaker replacement)	67
4.3.2	Effect of variation in discount rate on LCOS (seasonal storage)	67
4.4.1	LCOS contour plot for pumped storage hydroelectricity	68
4.4.2	LCOS contour plot for compressed air energy storage	69
4.4.3	LCOS contour plot for lithium-ion batteries	70
4.4.4	LCOS contour plot for vanadium redox flow batteries	71
4.4.5	LCOS contour plot for hydrogen	72

List of Tables

2.2.1	Storage applications considered in this study and the corresponding technical requirements	18
2.4.1	PSH plants in South Africa	28
2.6.1	Energy storage systems and their corresponding applications considered in this study	38
3.2.1	Comparison of economic and technical factors considered in recent studies	44
3.4.1	Summary of key input assumptions	49
3.6.1	Stochastic inputs with sample values	54
3.6.2	Fixed inputs with sample values	54
3.6.3	Key inputs based on peaker replacement application	55
4.2.1	Simulation results for peaker replacement and seasonal storage	66
4.5.1	South African CSP plants considered (Lilliestam <i>et al.</i> , 2020)	73
4.5.2	CSP tariff comparison with ESSs charged with other VRE	74
A.0.1	Average annual exchange rates: ZAR per USD	87
A.0.2	Inflation indices for EUR, USD and ZAR	88
B.0.1	Stochastic inputs for pumped storage hydroelectricity	89
B.0.2	Stochastic inputs for compressed air energy storage	90
B.0.3	Stochastic inputs for lithium-ion batteries	90
B.0.4	Stochastic inputs for vanadium redox flow batteries	91
B.0.5	Stochastic inputs for hydrogen energy storage	91

Nomenclature

Abbreviations

AA-CAES	Advanced adiabatic compressed air energy storage
CAES	Compressed air energy storage
CF	Capacity factor
CSP	Concentrated solar power
CPI	Consumer price index
D-CAES	Diabatic compressed air energy storage
DD	Discharge duration
DHI	Diffuse horizontal irradiance
DNI	Direct normal irradiance
DoD	Depth of discharge
DoE	Department of Energy
EES	Electrical energy storage system
ESS	Energy storage system
FES	Flywheel energy storage
FLH	Full load hours
GHI	Global horizontal irradiance
HTF	Heat transfer fluid
IEA	International energy agency
IRP	Integrated resource plan
IRP1	Scenario 1 of the integrated resource plan
LCOE	Levelised cost of electricity
LCOS	Levelised cost of (energy) storage
LFR	Linear Fresnel reflectors
LHS	Latin hypercube sampling
LI-ION	Lithium-ion

NOMENCLATURE

xvi

LOHC	Liquid organic hydrogen carrier
MGA	Miscibility gap alloy
NERSA	National energy regulator of South Africa
NPV	Net present value
NREL	National renewable energy laboratory
PCM	Phase change material
PDC	Parabolic dish collector
PEC	Photoelectrochemical
PPA	Power purchase agreement
PSH	Pumped storage hydroelectricity
PTC	Parabolic trough collector
PtG	Power-to-gas
PtGtP	Power-to-gas-to-power
PV	Photovoltaic
RE	Renewable energy
REIPPPP	Renewable energy independent power producer procurement programme
RMIPPPP	Risk mitigation independent power producer procurement programme
RTE	Round-trip efficiency
sCO ₂	Supercritical carbon dioxide
SES	Super conductor energy storage
SMES	Superconducting magnetic energy storage
SOC	State of charge
SPT	Solar power tower
SRS	Simple random sampling
STERG	Solar thermal energy research group
TcES	Thermochemical energy storage
TES	Thermal energy storage
TIT	Turbine inlet temperature
TVM	Time value of money
SU	Stellenbosch University
VRE	Variable renewable energy
VRFB	Vanadium redox flow battery

WACC Weighted average cost of capital

Symbols

A_t	Annual cost	[\$USD]
$CAPEX$	Capital expenditure	[\$USD]
C_D	Cost of debt	[%]
C_E	Cost of equity	[%]
C_{elec}	Price of electricity	[\$USD/kWh]
c_p	Specific heat capacity	[J/(kg K)]
D	Value of debt	[\$USD]
DoD	Depth of discharge	[%]
E_{nom}	Nominal energy capacity	[kWh]
E	Value of equity	[\$USD]
EoL	End-of-life cost	[\$USD]
f	Cycle frequency	[1/a]
f_{deg}	Cyclical degradation factor	[-]
g	Gravitational acceleration constant	[m/s ²]
H	Reservoir height	[m]
h	Heat transfer coefficient	[W/m ² K]
i	Interest rate	[%]
I_E	Energy specific investment cost	[\$USD /kWh]
I_P	Power specific investment cost	[\$USD /kW]
I_T	Total investment cost	[\$USD]
k	Thermal conductivity	[W/(m K)]
n	Repayment period	[a]
N	Financial lifetime	[a]
OM	Operation and maintenance cost	[\$USD]
P_{nom}	Nominal power rating	[kW]
q	Heat capacity	[J]
r	Discount rate	[%]
r_{tax}	Corporate tax rate	[%]
rep	Replacement period	[a]
R_n	Expected net cash flow	[\$USD]
t_{deg}	Temporal degradation factor	[-]

NOMENCLATURE

xviii

T_c	Construction time	[a]
T_r	Replacement interval	[a]
V	Volume	[m ³]
W_{in}	Charging cost	[\$ _{USD} /kWh]
W_{out}	Energy discharged annually	[kW h]

Greek letters

η_{RT}	Round-trip efficiency	[%]
ΔT	Temperature difference	[K]
ρ	Density	[kg/m ³]
σ	Standard deviation	[–]

Subscripts

E	Energy specific costs
P	Power specific costs

Chapter 1

Introduction

1.1 Background

South Africa is blessed with significant natural resources. Abundant stores of coal allowed for cheap electricity generation for many decades. The motivation to replace the country's coal-driven generation fleet with renewable technologies was purely driven by environmental concerns. Renewable energy (RE) has become synonymous with sustainable carbon-conscious growth, and rising international pressures to de-carbonise the electricity sector make it difficult for anyone to advocate the installation of coal based generation plants in 2022.

Traditionally, there exists a direct relationship between the demand for electricity and its generation; when a light is switched on, somewhere a turbine driving an electricity generator is working a little harder. Without energy storage, generation must follow demand and power plants adjust their production accordingly. The ability to adjust generation to meet varying demand is known as dispatchable generation and examples of this include coal, nuclear, hydroelectric and natural gas powered plants.

The generation of electricity from variable renewable energy (VRE), however, is intermittent and can be described as stochastic - meaning that its availability has a random probability distribution or pattern (Akinyele and Rayudu, 2014). This pattern can be analysed statistically but cannot be precisely predicted, which is why electricity generated by VRE sources is generally not dispatchable (renewable energy power generating plants with some storage are, to the extent of the storage, dispatchable power suppliers) and must be used as it is generated. A distinction is made here between variable renewable energy sources (like wind and solar power) and other renewable sources that are not intermittent (like geothermal power and

biofuels).

As stated by Akinyele and Rayudu (2014), energy storage systems (ESSs) are one of many possible solutions to mitigating the effects that VRE has on power networks. Besides dispatchability, these effects include curtailment of generation due to inability of the grid to accommodate the peak RE generation capacity at the point of common connection at peak generation periods. These factors inhibit the growth of RE penetration into the market. ESSs allow us to decouple energy supply from demand by storing energy in various forms.

Economically, increased curtailment of VRE can be described as an increase in costs or a decrease in value since more reliance is placed on fossil fueled generation, which decreases the economic and environmental value of renewable energies (Denholm and Mai, 2019). This effect can also be described as an increase in the levelised cost of electricity (LCOE), since fewer units of electricity are sold, while the capital and operating costs remain fixed.

Data published by the international energy agency (IEA) shows that South Africa's energy mix, in terms of electricity generated in 2020, consists of 87.7% non-renewables like coal, gas, diesel and oil based generation (IEA, 2021). Nuclear power plants contributed 5.17 %, while 7.06 % of the country's electricity was generated by hydro, biofuel, wind and solar energy. The solar energy category comprises of photovoltaic (PV) and concentrated solar power (CSP).

The last integrated resource plan (IRP) 2019, outlines a strategy to install new VRE capacity each year until 2030 and beyond. The IRP is a document published by the South African national Department of Energy (DoE), the national electricity supply system operator, Eskom, and the National Energy Regulator of South Africa (NERSA), which sets out the national level long-term electricity sector plan. The IRP outlines seven scenarios that make projections, based on key assumptions, of the electricity demand over the coming years and how the energy sector should develop in response.

Across all seven of the scenarios, deployment of PV, wind and flexible dispatchable capacity is consistent. Flexible dispatchable capacity in this context refers to natural gas-powered peaking plants. This means that regardless of the input assumptions, all plans will make provision for new-built installation of these technologies. The first scenario, IRP1, imposes no annual build limits on VRE based installed capacity and identifies PV, wind and flexible dispatchable capacity as the least cost option as existing coal-powered capacity is set to be increasingly decommissioned over the coming years. Projections for IRP1 include 25 % renewables-based by 2030

and the least-cost combination of new-build options (R 10-15 Bill. less than other scenarios, per year) (Wright *et al.*, 2018).

Interestingly, at the time of writing, the South African government has finally given notice that the IRP (2019) is to be revised (Mantashe, 2022), in part significantly motivated by the electricity supply constraints experienced by the country but also appropriate given rapid technological developments in this field.

When PV and wind energy was first introduced, it was too expensive and could not compete with coal power (IRENA, 2017). However, technological developments have brought down the costs of these renewable technologies to a point where they can compete with, and even out-price coal power in certain cases. The major obstacle, preventing VRE from attaining greater penetration into the energy mix is storage and dispatchability of the power generated from these sources.

The prominent renewable energy based generation capacities in South Africa are solar (500 MW CSP and 2292 MW PV) and wind energy (3357 MW), both of which are limited by the same obstacle, intermittent power delivery (Eberhard and Naude, 2016). This intermittency poses a problem for the technology's integration into the national grid since existing coal and nuclear plants operate at base load conditions and are constrained to fluctuate with the change in demand caused by these renewable sources.

An infamous example of this is known as the "duck-curve" phenomena (Maize, 2017) which was first noticed in 2013 by the California Independent System Operator and it represents the effect that the energy harvested from the sun using PV has on the electrical load curve. Without PV the curve would resemble something closer to a plateau, with a steady increase in consumption after office hours. The consumption would also vary depending on the specific grid and the time of year. The boost of electricity production from PV during the day looks like a drop in electricity demand from the perspective of the coal based electricity power plants, meaning they need to decrease their output to avoid overloading the grid.

A large portion of existing power plants in South Africa operate as baseload plants (mostly coal but also a significant nuclear based contribution with nominal generation of 2000 MW) which take time to reach full load generation and are not able to ramp production up and down as quickly as and to the extent as required when intermittent power sources come online (Huggins, 2016).

Another problem that occurs with the use of renewable energy is over-generation - producing more energy at a given time than required by the grid (Maize, 2017).

This can be easily solved by de-focusing some heliostat mirrors in the case of CSP, disconnecting PV panels from the grid or rotating (feathering) wind turbine blades, but this curtailment means discarding energy and decreasing the economic and environmental benefits for which these plants were initially designed. One way to solve the problem of the varying load would be to retrofit existing power plants to be flexible and be able to adapt to the fluctuations of renewable technologies, but this would only be a temporary fix to a larger and ever-growing problem. However, both of the previously mentioned problems could be addressed by introducing a storage mechanism into the electricity generation system.

1.2 Motivation

The most popular storage systems in use today for PV systems are electrical batteries, whereas existing CSP plants make use of molten salt and rock beds as a thermal energy storage media (Stein and Buck, 2017). Although electrical battery technology is relatively efficient, it is expensive and limited in terms of required manufacturing materials (IRENA, 2017). Rock bed and molten salt thermal storage are highly efficient and cost-effective when it comes to thermal storage (Allen *et al.*, 2016), but costs increase significantly when trying to insulate these storage media for longer than 8 hours. These types of storage systems usually deploy a thermal power cycle, converting heat to electricity, and are therefore also referred to as a Carnot battery. While a previous record of 15 hours was held by Gemasolar (commissioned in 2011), a pilot plant commissioned in 2019 in Hamburg by Siemens Gamesa, is capable of storing 130 MWh of thermal energy for up to a week (Siemens Gamesa, 2019).

Other terms used to describe Carnot batteries include: pumped heat electricity storage, pumped thermal electricity storage, electro-thermal electricity storage and thermal batteries. The energy storage and power generation components of these systems are identical to those found in modern CSP plants, the differentiating factor being the source of heat energy. CSP plants harvest thermal energy from the sun's rays, while Carnot batteries, e.g. can use a heat pump powered by low value electricity from the grid (McTigue, 2019). When comparing the cost of energy stored and electricity supplied by Carnot batteries to CSP plants, the capital investment of the former would be added to the cost of buying electricity from the grid. In contrast, these costs are already included in the price of electricity generated by a CSP plant.

As previously stated, the stochastic nature of renewable energy generation limits its potential for a greater share of the energy generation market. Traditional

generation methods like coal and nuclear power plants are not sustainable in the climate and political trajectory of 2022, and provisions need to be made that facilitate a greater adoption of VRE. Finding suitable storage technologies is one way of achieving said goal. By selecting the most suitable storage technologies for wind, PV and CSP, it is possible to move away from fossil fuel technologies in the coming decades and solidify their place in the future energy mix.

1.3 Research objectives

The aim of this study can be summarised as follows:

- Conduct literature survey of the state-of-the-art ESS technologies.
- Develop a method of comparing the technical and financial performance of selected ESSs.
- Apply the method to selected ESSs and from the result draw conclusions pertaining to the deployment of such systems.
- Based on an understanding gained of the economics of energy storage technologies, propose an appropriate solution for the development of the South African energy mix going forward.
- Formulate a summary of the work undertaken, present insights and conclusions made, and offer recommendations for further work.

1.4 Methodology

The methodology used in this study consists of two parts. Firstly, a broad literature review, focused on identifying state-of-the-art energy storage technologies within the application of long-term energy storage. Secondly, a techno-economic model that considers several selected technology types, their costs and technical performance characteristics. This model consists of a levelised cost of energy storage analysis as well as a sensitivity analysis to determine the effect of variance in each input parameter.

To deal with the unique nature of CSP technology, which allows for incorporation of cost-effective and significant short term energy storage, a special comparison was made: using performance and costing figures from CSP plants operating in South Africa, a comparison was made between the levelised cost of electricity generated by CSP plants (with thermal energy storage included) and a combined cost of

renewable sources like wind and photovoltaic plants and electrical energy storage systems like lithium-ion batteries.

1.5 Outline of thesis

Chapter 2 presents a background of CSP and energy storage, explores trends in storage technologies and selects appropriate technologies based on the literature. Chapter 3 investigates methods of comparing various energy storage technologies and presents the financial and statistical tools used in the levelised cost analysis performed in this study. Chapter 4 presents the results of the levelised cost analysis and compares these results to tariffs achieved by CSP plants in South Africa. Chapter 5 presents an overview of the significant findings from the literature review, recommendations of energy storage technologies, and presents a case for CSP in South Africa's IRP. Limitations of this study are also presented. Chapter 6 summarises the findings of this study and proposes potentially fruitful further research.

Chapter 2

Literature Study

This literature study aims to identify advancements in energy storage and build a knowledge base from which further investigation can be launched. The content of the literature review, as well as topics to be explored, are set out below.

2.1 Concentrated solar power (CSP)

In an exploration of energy storage in the context of renewable energy, concentrated solar power (CSP) holds a unique place and is therefore given special consideration in this chapter. This uniqueness arises out of the fact that the storage of (solar) heat is still considerably cheaper than the storage of electricity, and such plants already have the equipment to convert heat into electrical energy. State of the art CSP plants are therefore always equipped with constantly advancing thermal heat storage technology, allowing some desirable mitigation of typical renewable energy issues like intermittency, curtailment and peak loads (see also Chapter 1).

2.1.1 Fundamentals of CSP

Concentrated solar power technology, as the name implies, generates electrical power using concentrated solar irradiation from the sun. While there have been several iterations of the technology since its first commercial installation in 1984 in California, United States, the fundamental principle remains the same, in that a reflective surface is used to direct and focus the solar irradiation from the sun to a target area. The concentration of the solar flux on this area yields high quality thermal energy, which is used to produce useful work. The amount of power generated depends on the magnitude of the incoming solar flux, the concentrating effect of the reflective surfaces, and several related efficiencies.

A modern CSP plant consists of four main components; the concentrator, high temperature solar receiver, a heat transfer fluid (HTF) transport system and a power block. The power block, also known as the heat engine, generates electricity and is typically comprised of a steam generator and a turbine. This component also dictates the temperature that the solar concentrator, receiver and storage must provide. It is also the component that has the greatest effect on total system efficiency and, by extension, the cost of the generated electricity (Stein and Buck, 2017). Total system efficiency refers to the ratio of electrical energy generated by the system to the input energy used to generate useful work, which is solar radiation in this case.

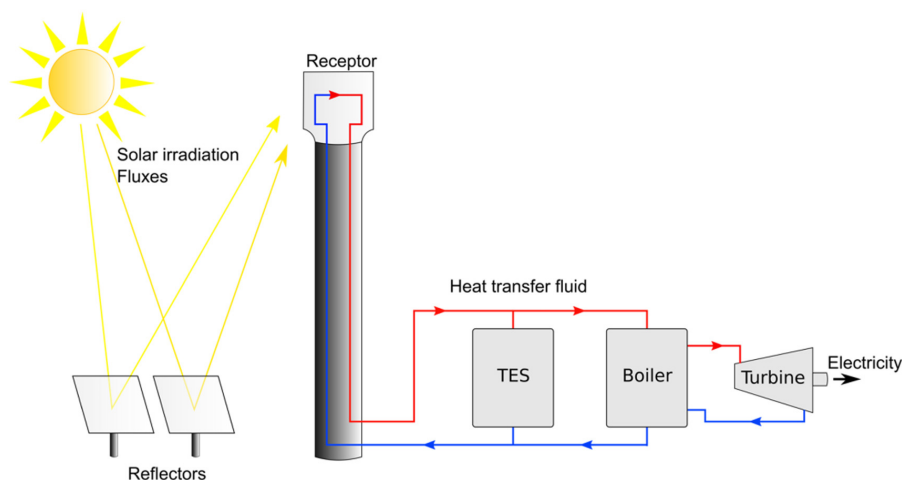


Figure 2.1.1: Schematic of a solar power tower CSP plant with a thermal energy storage system (Pelay *et al.*, 2017)

There exist a wide variety of CSP technologies, mostly differing in the manner in which the solar flux is concentrated and how the heat is transported to the power block. Existing technologies are discussed in Section 2.1.2.

Energy from the sun can be split into three broad categories. The global horizontal irradiance (GHI) is the total radiation from the sun, striking a flat surface on Earth. Diffuse horizontal irradiance (DHI) is the portion of GHI that is scattered by the atmosphere. The direct normal irradiance (DNI), also known as beam irradiance, represents the portion of GHI that excludes DHI. From Figure 2.1.2, it is evident that South Africa has some of the highest annual average DNI in the world. In most parts of the country, the annual total DNI exceeds 2000 kWh/m^2 , with some parts in the Northern Cape exceeding 3000 kWh/m^2 (Gauché, 2016).

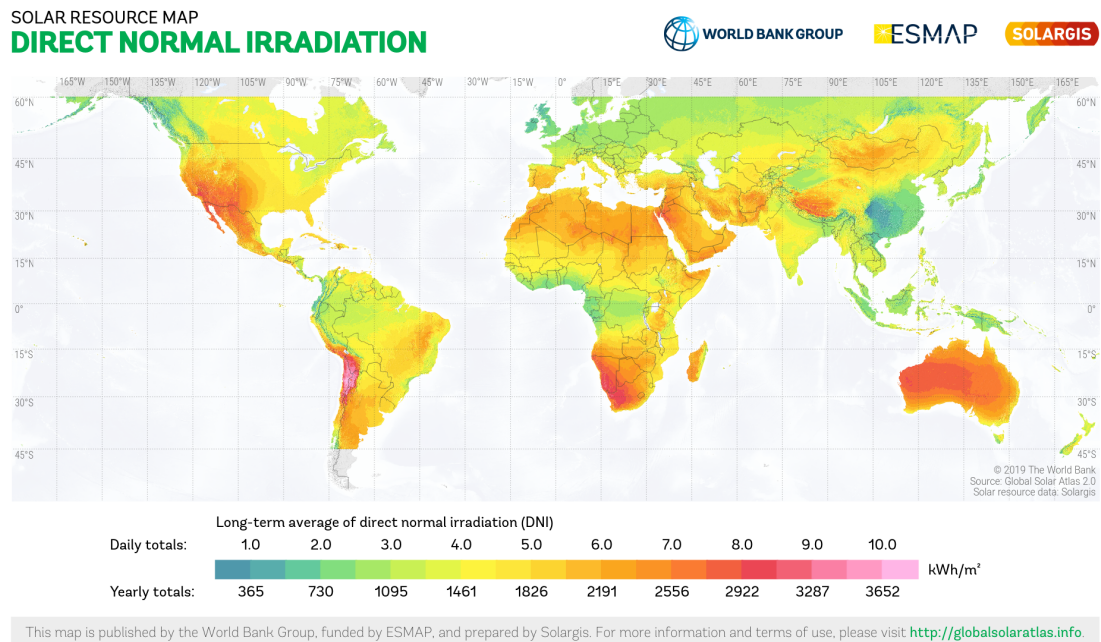


Figure 2.1.2: Worldwide long term average annual direct normal irradiation (© 2019 The World Bank, Source: Global Solar Atlas 2.0, Solar resource data: Solargis.)

The portion of DNI available depends on the time of day, the weather and the geographical location of the plant. The energy input into a CSP plant is dependent on the available DNI. As a result, CSP plant performance is sensitive to weather patterns and time of day and hence provisions need to be made to ensure that the full load hour (FLH) requirements are met.

One way to smooth out these transient effects is by supplementing CSP plants with backup generating capacity, usually in the form of fossil-fuelled generation (i.e. coal, natural gas or diesel). Other common supplements include biomass or photovoltaic (PV) plants, which are able to utilise both DNI and GHI, and can provide support in overcast weather conditions. Another approach is to use thermal energy storage (TES), which allows increased FLH for electricity generation, and in some scenarios, optimisation of electricity generation and resale (Pelay *et al.*, 2017). Due to powerblock downtime at night and during cloudy conditions, CSP plants without energy storage or backup boilers have capacity factors (CFs) of around 20%. The addition of energy storage can increase the CF to 75% or more (Lovegrove and Stein, 2021).

2.1.2 Existing technology

As of 2022, there are 6 commercial CSP plants in service in South Africa (with a seventh, the state-of-the-art 100 MW Redstone plant due for commissioning 2023 and neighbour Botswana going out to tender on two 100 MW plants in 2022) and 109 around the world (Saunyama, 2022; RenewAfrica, 2022). The largest plant being Ivanpah Solar Electric Generating System (ISEGS) in California, United States, with a net turbine capacity of 377 MW (NREL, 2020). The most well known CSP technologies are parabolic trough collectors (PTC), linear Fresnel reflectors (LFR), solar power towers (SPT) and parabolic dish collectors (PDC). Figure 2.1.3 illustrates these technologies.

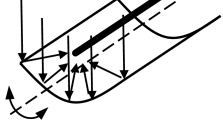

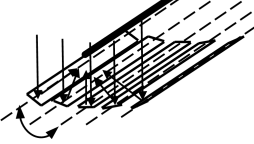
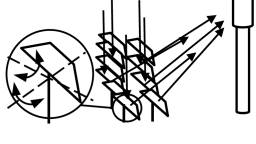
Reflector type	Focus type	
	Line focus (single axis, 2D concentrating)	Point focus (2 axis, 3D concentrating)
Continuous (continuously curved to axes)	Parabolic trough 	Parabolic dish 
Discrete (multiple, near flat)	Linear Fresnel 	Central receiver 

Figure 2.1.3: Four mainly accepted technology types of CSP (Gauché, 2016)

While PTC and SPT are the most common technologies used in operating plants, trends for future plants indicate a greater preference for SPT plants (Pelay *et al.*, 2017). PTC based plants operate at 20–400 °C, have relatively low installation costs and large experimental feedback, but have lower thermodynamic efficiencies and require large portions of land (Pelay *et al.*, 2017). Existing PTC use a synthetic oil as the receiver HTF, which has a maximum operating temperature of 395 °C. Combined with a sub-critical steam turbine (at 380 °C and 100 bar), the thermal conversion efficiency of a PTC based plant is around 37.5 % (Stein and Buck, 2017). Thermal conversion efficiency is the ratio of electrical energy generated by the system to the input thermal energy.

SPT using molten salt or steam as HTF are able to achieve higher steam turbine inlet conditions and have a net turbine inlet efficiency of 41.5 % (Stein and

Buck, 2017). Net turbine inlet efficiency is the ratio of mechanical energy output to the input energy. On the downside, SPT also require relatively large portions of land, are relatively expensive to install and have high heat losses (Pelay *et al.*, 2017).

Proving to be a reliable technology, the average generating capacity of CSP plants have grown by a factor of six, from 21 MW_{elec} (for plants commissioned before 2000) to 120 MW_{elec} (for plants in the construction and planning phase) (Pelay *et al.*, 2017). This growth can be attributed to a well documented phenomenon associated with steam turbine systems: the net turbine inlet efficiency and specific costs (\$/kWh) typically improve with increasing capacity (Stein and Buck, 2017).

Supplementary generation, previously a necessity, is decreasing globally due to the increasing costs of fossil fuels and the rise of TES adoption. This is demonstrated by the fact that around 47 % of existing plants in operation make use of TES, while more than 70 % of plants in construction and planning phases include TES systems (Pelay *et al.*, 2017). This increase can partly be attributed to the technological progress of TES and the dependance of CSP plants on these systems to remain cost-competitive with competing electricity generation technologies. CSP plants with storage can sell more electricity, which makes them more profitable, allowing them to reduce their tariffs. In addition to the previously mentioned greater power capacity of 120 MW_{elec}, the average storage capacity of TES systems has increased from 3 h to 7 h (for plants installed after 2010), with 8 h planned for future projects (Pelay *et al.*, 2017).

Sensible heat storage, the most dominant and mature TES technology in CSP, has a large variety of low-cost material options, but low energy density compared to other TES technologies. Latent heat storage and thermochemical storage are not yet commercially viable, but show potential due to their higher energy density and heat storage capabilities.

Depending on the power purchase agreement (PPA), a CSP plant could either prioritise meeting baseload demand (generating at full capacity during the day) or peak demand (charging the storage system for generation during a peak consumption period). Peaker plants run for shorter durations at higher tariffs, while baseload plants run for longer durations (>12 h) at lower tariffs (Schöniger *et al.*, 2021). The desired operating strategy influences the solar multiple specification for the solar field and receiver, which affects the initial capital cost of the project. Solar multiple is the ratio of the thermal energy collected by the solar field and receiver to the amount of energy required by the powerblock to operate at its nameplate capacity (Lovegrove and Stein, 2021).

2.1.3 Emerging concepts

A key focus in CSP research is the development of more advanced thermodynamic cycles and machinery, since there is great potential for thermal conversion efficiency improvement and cost reduction (Stein and Buck, 2017). One method of improving the system efficiency is by increasing the turbine inlet temperature (TIT); Stein and Buck (2017) showed that the cost of solar electricity (\$/kWh) generated by a conventional CSP plant with low solar efficiency and medium temperature steam turbines is nearly double that of advanced plants using supercritical carbon dioxide (sCO₂) cycles with TIT of 700 °C. Solar efficiency is the ratio of electrical energy generated by the system to the input solar radiation. Existing technologies used in pilot plants are able to achieve temperatures of around 1000 °C, with upper limits set by properties of available materials and HTFs (Stein and Buck, 2017).

Closed loop sCO₂ Brayton cycles combine the best attributes of both Rankine and standard air Brayton cycles. Supercritical CO₂ is favoured due to its chemical stability at the desired operating point, industry handling knowledge and reduced turbine dimensions that are an order of magnitude smaller than steam turbines. As a result, sCO₂ based cycles offer high efficiencies at smaller capacities where steam would not be suitable and a greater market penetration due to a range of turbine capacities (Stein and Buck, 2017).

2.2 Energy storage

The interest in energy storage is driven by the need to account for the non-dispatchable nature of renewable energy sources in general, i.e. beyond CSP applications. The concept of energy storage, however, is as old as mankind's relationship with one of the earliest sources of energy; namely wood. As the old adage goes, mankind has been gathering and storing firewood during the warmer months to ensure that there is enough during winter where gathering might not be as convenient (Smil, 2017). Appropriately, it is worthwhile to remember that wood is also a form of stored solar energy.

That same motivation is what drives the development of storage in 2022: gathering enough energy when it is more convenient or cheaper, so that there is enough during times of low availability. With wider adoption of renewable energy sources, which are often intermittent in nature, e.g. wind and solar, the energy demand is not synchronized with availability. If there was no delay between the demand and generation capability, there would be no need for storage. This would likely never be the case for intermittent renewable power generation, since it is also impossible

to predict the transient power requirements of a large energy network.

Large differences in demand and supply can be addressed through peak-shifting, where storage systems are charged during periods of low demand (and prices), and then discharged to supply the grid when demand rises during peak load hours (Huggins, 2016). Figure 2.2.1 illustrates this concept for a large scale power network using storage with baseload generation. Seasonal mismatches in generation hold great potential for energy storage; the largest of which occurs in spring, when wind and solar generation is higher and electricity demand is lower (Denholm and Mai, 2019).

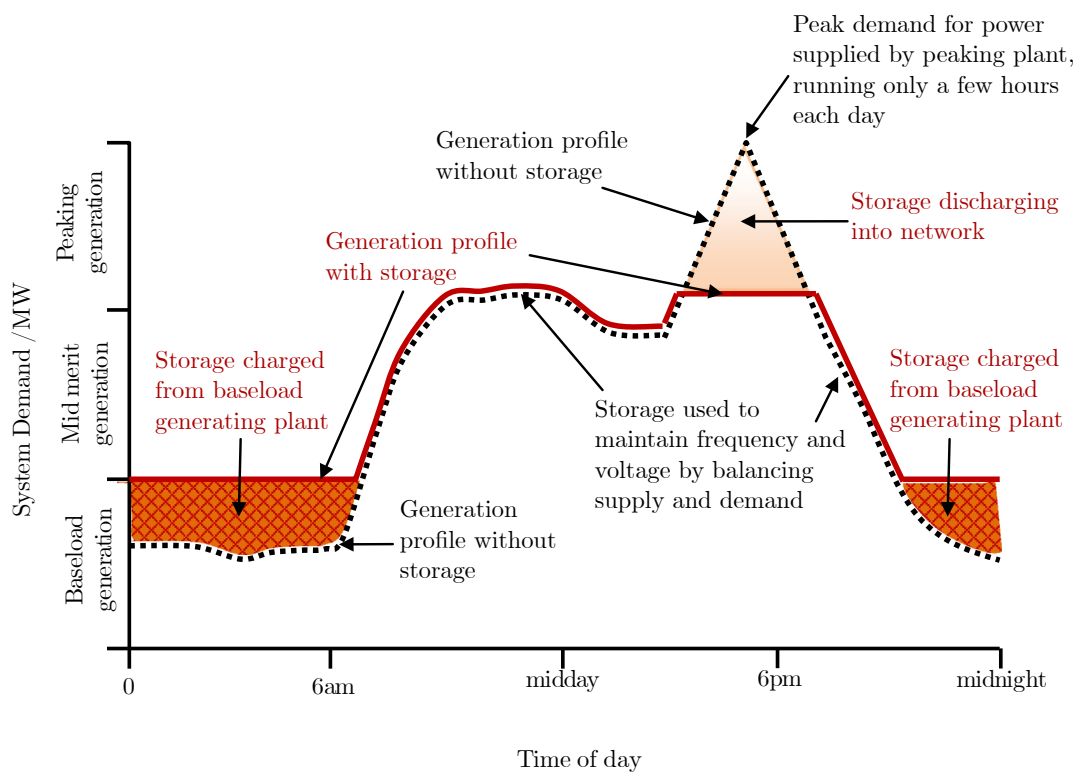


Figure 2.2.1: Electrical power load profile of a large scale energy storage system (Akinyele and Rayudu, 2014)

Smaller variations in generation and demand, also known as transients, can cause generator rotor instabilities, which can lead to unwanted oscillations and unstable operating conditions. Similarly, voltage instability, which occurs when the load and the coupled transmission systems draw large amounts of reactive power, can cause

a sudden voltage drop, causing costly short-term power outages (Huggins, 2016).

Before the more complex characteristics of energy storage are discussed, two fundamental statements about energy and storage should be considered. The first law of thermodynamics states that, in a closed system, energy cannot be created nor destroyed, only converted from one form to the other (Çengel and Boles, 2006). In other words, all forms of energy are either collected from an external source, like the sun or ocean currents, or converted from one form to the other within the system, like burning coal to generate usable heat. This ties into the second statement about energy, which is that energy can be stored in a reversible or non-reversible mode. In the former, energy can be stored, extracted and replaced. In the latter storage mode, energy that is present, can be harnessed through a one-way conversion process into another form. An example of an irreversible mode of storage is the chemical energy stored in wood that is converted to heat energy by means of an irreversible combustion process. (Huggins, 2016).

2.2.1 Definition of an energy storage system

An energy storage system (ESS) converts energy from one form to another (typically electrical energy) and stores it internally, to be discharged at a later time. The electrical energy can be converted to several classes or categories of energy (like thermal, chemical or mechanical), examples of which are discussed in Section 2.4. The operation of a general ESS is described by Figure 2.2.2.

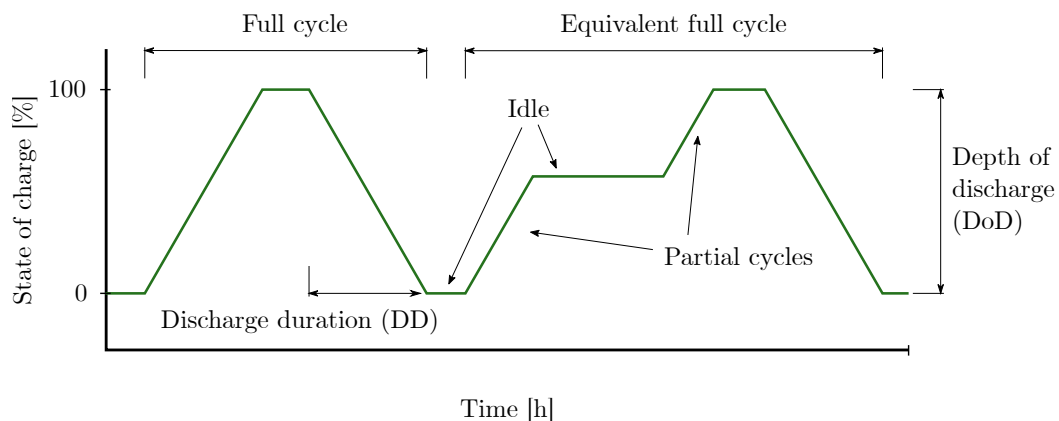


Figure 2.2.2: Operational schematic of a general ESS

A cycle is defined from an initial state of charge (SOC) by four phases: charge, pause, discharge and new pause; returning to the initial SOC. Pause (or idle) is a

period of zero active charging or discharging (DNVGL, 2017).

Full and full equivalent cycles are illustrated in Figure 2.2.2. A full cycle, or nominal cycle, is when the ESS is charged from 0 % to 100 % SOC and after a relatively short idle period, discharged to 0 % SOC. Any ESS operation where the initial and final charge levels are the same are considered full equivalent cycles. A partial cycle is when the initial and the final SOC are different. Unless otherwise specified, *cycle* refers to full and full equivalent cycles in the context of this study.

The size of an ESS is defined by its power capacity and discharge duration (DD). The former being the rate at which the system can be discharged and the latter refers to the amount of time over which the ESS can deliver at the rated capacity. Related to these parameters is the energy capacity of a ESS, which is defined as the amount of energy that it can deliver at the rated power capacity between the fully charged and empty state (DNVGL, 2017). Due to system inefficiencies, this is not the same as the amount of energy needed to charge the system from an empty to fully charged state. The ratio of energy discharged from the system to input energy used to charge the system, over one cycle, is known as the round-trip efficiency (RTE).

Depth of discharge (DoD) refers to the percentage of the total energy storage capacity that can be discharged safely in one cycle, before the lifetime of the system is damaged. Cycle durability at DoD refers to the lifetime of a system operating at the optimal DoD. The self discharge rate is the amount of stored energy lost due to system inefficiencies and other parasitic losses while the system is on standby. Cycle frequency describes the number of full charge-discharge cycles completed in a year; Figure 2.2.2 illustrates an ESS with a cycle frequency of two.

2.2.2 Important energy storage metrics

For stationary storage technologies, for use with large energy generation and transmission networks, there are several important characteristics to consider. Not only are the capacity of storage and ramp rate important factors to consider, but also the calendar life, the rate of self discharge and the life cycle costs, to name a few. Ramp rate is selected based on the application, e.g. network frequency regulation requires faster ramp rates compared to hourly or daily storage (Chueh, 2018).

Other important parameters include cycle life, energy cost and safety, where the weighting of these parameters shift depending on the specific storage application (Chueh, 2018). In the case of transient response, ramp rate becomes more important than storage duration or capacity. When looking at mobile energy storage, as

is required in electric vehicles for instance, other factors are important to consider, like gravimetric and volumetric energy density and round-trip efficiency.

Important technical parameters considered in this study include: depth of discharge, cycle durability, self-discharge and cycle frequency. Cycle frequency, along with rated power and discharge duration, limits suitable ESS based on the selected application. Selection of application and its related requirements are discussed in Section 2.2.4.

2.2.3 Timescales of energy storage

As mentioned in Chapter 1, greater penetration of variable renewable energies (VRE) is inhibited by curtailment. An important question to be asked is how much storage is necessary to reduce or eliminate curtailment and whether that point is dependent on storage capacity or duration. This is also known as the timescale of storage, which is the duration of energy storage per unit of power capacity.

The relationship between timescale of storage and curtailment was investigated by Denholm and Mai (2019), and they found that there is an optimal return on investment with durations between 4–8 h. Using historical load data, they simulated the average curtailment of wind and PV generation in the US over a period of 6 years and found that the duration and capacity of storage needed for effective curtailment reduction is a function of both the ratio of PV to wind generation and the resulting demand and supply patterns (i.e. the curtailment function). That is to say that the ESS specifications required to reduce curtailment are highly dependent on the type of VRE and its share of the VRE energy mix, as this determines the curtailment function.

It was demonstrated that various ratios of wind to PV installed capacity (at 55 % total penetration) resulted in curtailment events of varying duration, average power and total energy. By adjusting to a 4:1 wind to solar PV ratio, the amount of non-transmission related curtailment could be reduced to 12 % before the addition of any storage. An optimal ratio results in reduced curtailment due to the difference in PV and wind generation patterns, with wind generators able to deliver power at night. They also showed that for VRE penetration of 55 % or less, there is little benefit in storage durations greater than 4–8 h with the greatest benefit reached at 4 h and significantly smaller returns on investment after 8 h. It was found that until the cost of storage decreases, the return on investment of ESS with capacity greater than 4 hours is not enough to motivate their use. Storage in this context refers to electrical energy storage systems (EESSs). Denholm and Mai (2019) also found that the timescales needed are dependent on the application, with storage of

several hours being used for peaking capacity and peak shifting and storage greater than 19 h being used for daily shifting.

Abdon *et al.* (2017) investigated the economic and environmental performance of various stationary EESS technologies at several timescales. They specified three distinct durations for storage: 0.01 h, 4.5 h and 2160 h as short, medium and long, respectively. The shortest timescale corresponds to 21 cycles/h and is best suited for transient applications like frequency control. Medium timescale storage is appropriate for daily peak shifting applications and corresponds to 1 cycle/day. Long-term storage was specified at 1 cycle/year and is suitable for season shifting technologies (e.g. long-term seasonal storage).

2.2.4 Applications of energy storage

Energy storage systems are useful for the whole spectrum of electrical power systems and can be used for a wide range of applications, from energy balance, reserve and arbitrage to frequency regulation, voltage control and peak shaving (Akinyele and Rayudu, 2014). From the Global Energy Storage Database, the top six cases globally are shown in Figure 2.2.3; the top three being electric energy time-shift, electric supply capacity and renewable capacity firming.

Electric energy time-shift, also known as wholesale arbitrage, entails buying and storing energy during low price periods and discharging (and selling) during peak periods where prices are higher (Schmidt *et al.*, 2019). Electric supply capacity, also known as peaker replacement, reduces reliance on power from other regions and ensures that there is sufficient generation. Renewable capacity firming, also known as secondary response, utilises storage to dampen the effect of rapid variations in generation output from VRE sources. Another application to consider is long-term seasonal storage, which aims to smooth out seasonal differences in generation and accommodate extended disruptions in generation (Schmidt *et al.*, 2019).

The scope of this study is limited to long-term storage and energy storage durations that will increase the penetration of VRE in South Africa. Since peak loads are most expensive to service from otherwise idle power plants, energy storage to serve peak loads would be the most profitable. Additionally, to minimize energy losses through curtailment and undesirable fossil fuel backup power protecting against intermittancy, the largest energy storage is also of interest. Therefore, only technologies that are suitable for peaker replacement and so-called seasonal storage applications will be considered in this study. The key technical characteristics of these energy storage applications are described by Akhil *et al.* (2015) and IEA (2014) and are summarised in Table 2.2.1.

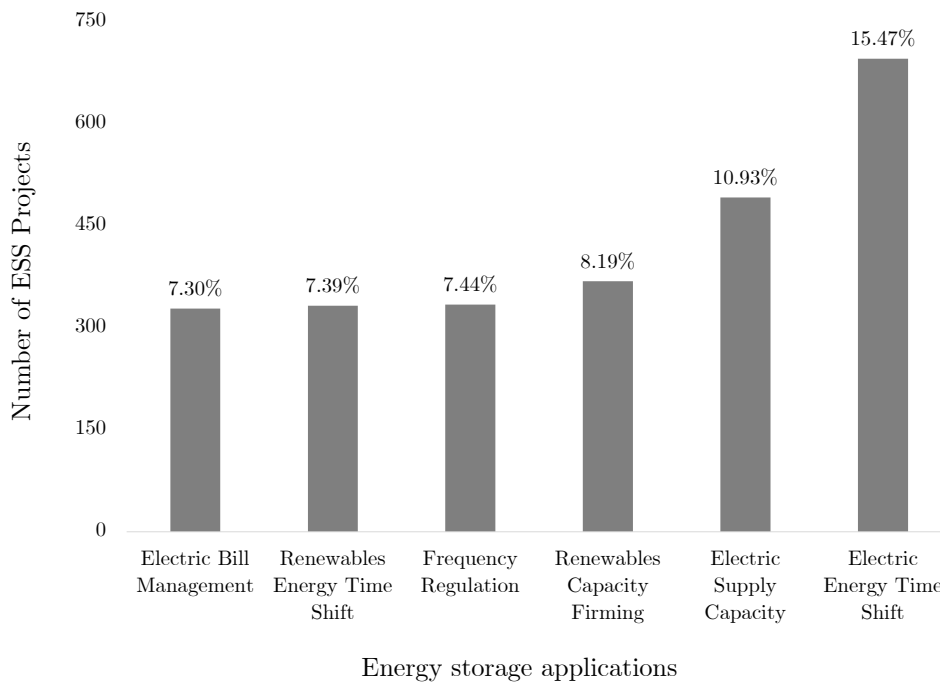


Figure 2.2.3: Top six global applications of energy storage (NTESS, 2020)

Table 2.2.1: Storage applications considered in this study and the corresponding technical requirements

Application	Key technical characteristics		
	Size (MW)	Discharge (h)	Annual cycles
Peaker replacement	1–500	2–6	5–100
Seasonal storage	500–2000	24–2000	1–5

2.3 Trends in energy storage

Figures 2.3.1 and 2.3.2 illustrate the top six ESSs in operation worldwide and the cumulative announced or commissioned ESS projects since 1905. Figure 2.3.3 illustrates the cumulative power capacity of ESSs installed in the period between 1905 and 2020, with Figure 2.3.4 highlighting only the last twenty years.

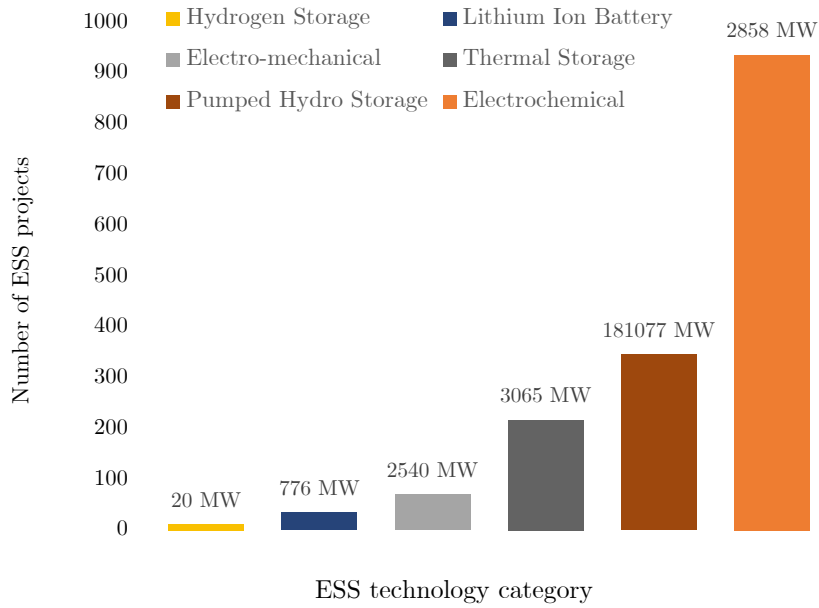


Figure 2.3.1: Top six ESS technologies in operation around the globe (NTESS, 2020)

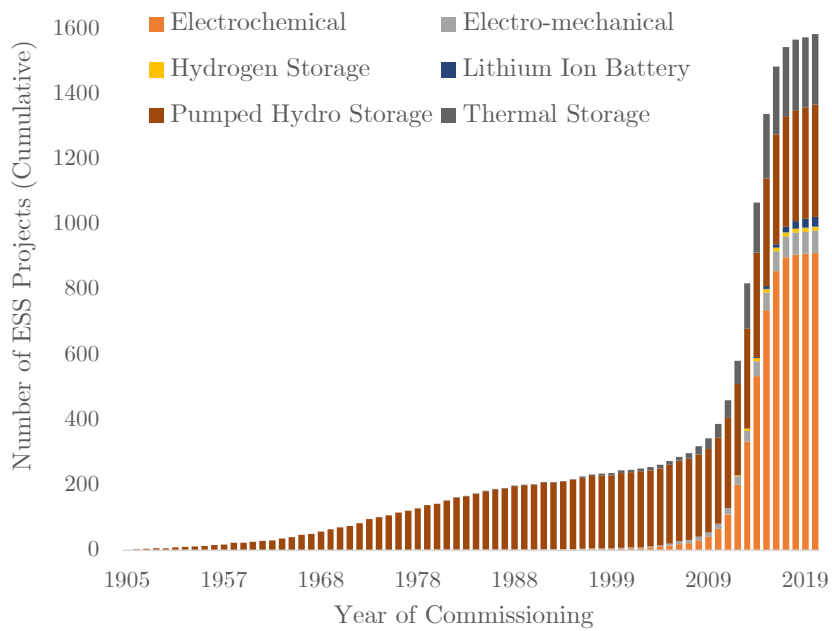


Figure 2.3.2: Announced and commissioned ESS projects from 1905 to 2020 (cumulative) (NTESS, 2020)

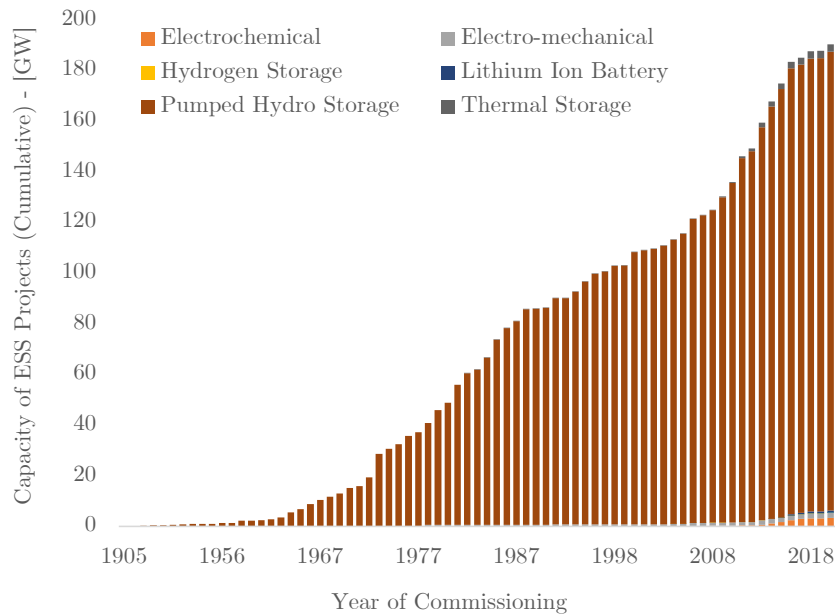


Figure 2.3.3: Power capacity of announced and commissioned ESS projects from 1905 to 2020 (cumulative) (NTESS, 2020)

In terms of the number of new projects each year, it is clear that there occurred a rapid growth in the energy storage sector between 2008 and 2014. From 2014 to 2019, Figures 2.3.2 and 2.3.3 indicate a decline in both the count and power capacity of new projects each year. The latter more significantly so, pointing to an overall decrease in ESS power capacity per project. This decline in average power capacity could be explained by the introduction of smaller capacity electrochemical ESS technologies. From Figures 2.3.2 and 2.3.4 it appears that the largest contribution (in terms of quantity and power capacity) between 2014 and 2019, was made by electrochemical, electro-mechanical and thermal ESSs, while more mature technologies like pumped storage hydroelectricity (PSH) remained constant.

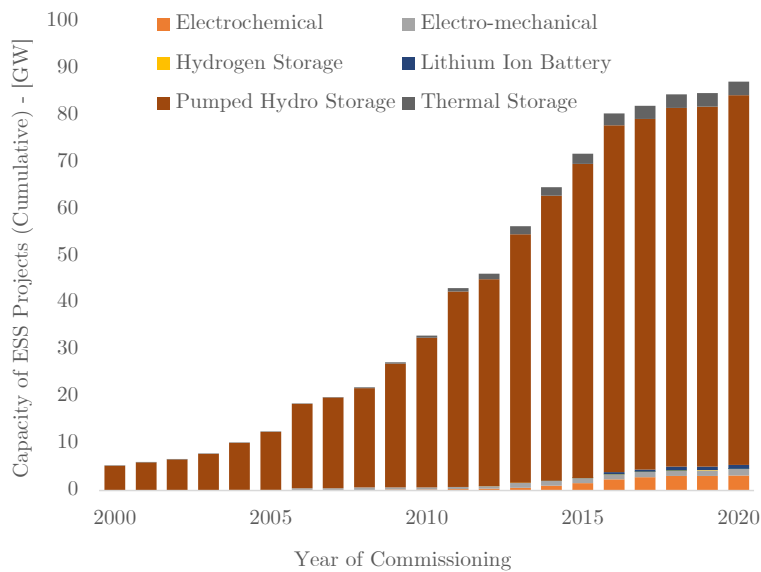


Figure 2.3.4: Power capacity of announced and commissioned ESS projects from 2000 to 2020 (cumulative) (NTESS, 2020)

2.4 Energy storage technologies

ESSs can be divided into five categories based on the underlying physics of the technology and this is presented in Figure 2.4.1. From literature, it is apparent that some of these technologies are better suited for specific applications, e.g. fly-wheel energy storage (FES) and superconducting magnetic energy storage (SMES) are best used for frequency control because of their rapid response and relatively short discharge duration required.

Other technologies like pumped storage hydroelectricity (PSH), compressed air energy storage (CAES), lithium-ion (li-ion) batteries and power-to-gas (PtG) technologies are viable for more than one application (Abdon *et al.*, 2017). More specifically, these technologies meet the requirements for the two timescales of storage considered in this study: daily and long-term seasonal storage. The fundamentals of each of these categories are discussed in greater detail in the following section, along with examples of ESSs used commercially as well as new developments in the field.

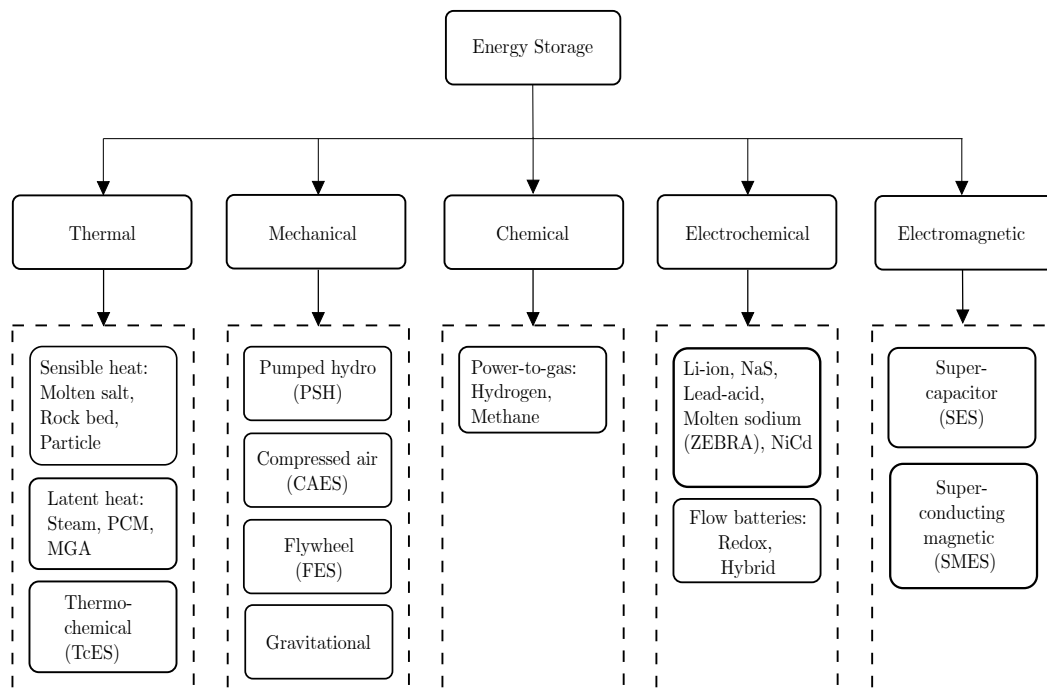


Figure 2.4.1: Classification of energy storage

2.4.1 Thermal energy storage

Thermal energy storage involves the transport of heat by means of conduction, convection or radiation from a generating source to a storage medium. TES can be split into three subcategories, namely; sensible, latent and thermo-chemical storage.

Sensible heat is the energy required to change the temperature of a substance and is proportional to the product of the specific heat, c_p , and the temperature change, ΔT . The thermal storage capacity of a sensible heat system is given by

$$q = \rho c_p V \Delta T \quad (2.4.1)$$

where ρ is the material density and V is the volume of the storage medium (Huggins, 2016). An example of this would be heating water by a few degrees without any phase change occurring. Solids (stone, concrete, metal or earth) and liquid (water, thermal-oil, molten-salt) mediums are used for this type of storage (Guney and Tepe, 2017).

Latent heat is the energy absorbed or released from a substance during a phase change, as when the substance water is melted or evaporated (or boiled). Thermal

conductivity k is a key parameter when selecting a suitable material as well as its density and latent heat absorbed or released during the phase change, as this determines the volumetric energy density (Guney and Tepe, 2017).

Absorption and adsorption systems store heat indirectly by means of physiochemical processes that absorb and release heat through charging and discharging modes. These processes have high energy densities (around 1000 MJ/m^3), resulting in relatively compact storage systems, compared to sensible heat materials. The performance of these mechanisms depends on the material and chemical composition of the storage materials involved, and it is often the case that specific materials are selected based on the desired temperature range of the application. As such, there exists a wide range of heat storage technologies, suited for low ($50\text{--}90^\circ\text{C}$) to high temperature applications ($800\text{--}1200^\circ\text{C}$).

Sensible heat

Sensible heat TES systems can be classified as active or passive. In the former, the storage medium flows to absorb or release heat through forced convection. In the latter, the storage medium, usually a solid, is stationary and is passively heated or cooled by a HTF (Pelay *et al.*, 2017). Active storage can further be classified as direct or indirect. Active direct systems use the same material as the primary HTF and storage media and therefore do not require a heat exchanger between the HTF and the storage media. Active indirect systems use a HTF and heat exchanger to heat and cool the storage media, which is stored in two separate tanks for hot and cold storage. Another approach is to use one tank with the hot and cold materials separated by a thermocline - a zone separating materials at different temperatures (Pelay *et al.*, 2017).

Molten salt

Molten salt is a term that covers a wide variety of HTFs and is mainly used as storage medium on CSP plants. Its excellent thermal stability at high temperatures, low vapor pressure, low viscosity and high thermal conductivity makes it very suitable for CSP applications (Pelay *et al.*, 2017). Other favourable characteristics include non-flammability and non-toxicity. The salt has a high heat capacity and traditionally operates in the temperature range of $220\text{--}1000^\circ\text{C}$, depending on the chemical composition of the salt (Barlev *et al.*, 2011).

In almost all CSP plants (typically PTC based), molten salt is used in an active indirect TES configuration with a synthetic oil being used as the HTF in a two tank system, as depicted in Figure 2.4.2.

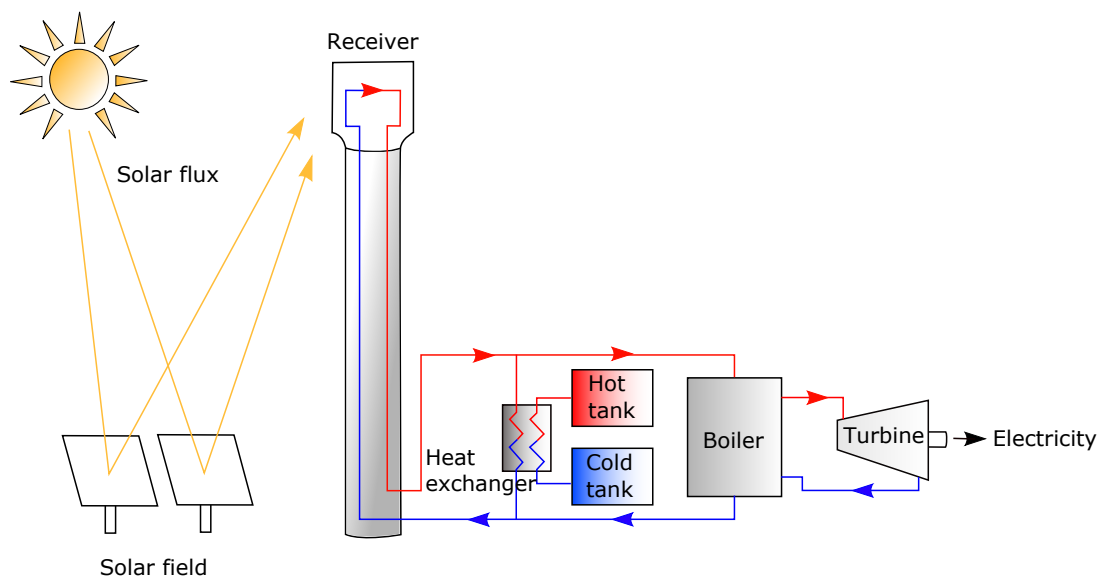


Figure 2.4.2: Schematic of two tank SPT plant (adapted from Pelay *et al.*, 2017)

As a technology advancement, both in PTC and SPT plants, the direct use of molten salt as HTF is considered, removing the need for an intermediary heat exchanger and improving the thermal conversion efficiency of the system (Pan *et al.*, 2019).

With a melting point of 220 °C, commercial plants require some provision for electric trace heating to prevent the salt from freezing in the pipes which is a costly problem to fix and can delay operation of the plant for several weeks. Newer molten salt compositions have been proposed with lower melting points between 76–80 °C (Pelay *et al.*, 2017).

Rock bed

Rock bed thermal storage is an example of a passive TES system that utilises low-cost materials in a packed bed structure. An immediate advantage of this technology lies in the abundance and cost-effectiveness of the material. Using air as a high temperature HTF, Zanganeh *et al.* (2012) demonstrated the feasibility of the concept, reaching temperatures of 500–600 °C. Allen *et al.* (2016) found that rock bed storage could be cost-competitive with two tank molten salt storage systems with costs lower than 20 \$/kWh_{th} at capacities above 100 MW h_{th}.

The first pilot scale plant was commissioned in 2014 in Morocco and was able to demonstrate good performance within the operating temperature range of 20–

650 °C and thermal efficiencies of 95 %.

Particle receiver

In the field of concentrated solar technologies, particle receivers are a promising candidate for new high temperature applications (> 700 °C). One of the main challenges with high temperature power tower technologies is the material choices for the receiver.

As receiver temperatures reach 1000 °C, uneven heat distribution causes warping and corrosion, leading to material degradation. Uneven heating is caused by non-uniform distributions of incoming solar flux, causing high temperature gradients and resulting stresses which reduce the component lifetime (Landman, 2017). Particle receivers completely sidestep this problem by replacing a traditional receiver with a curtain of falling particles (ceramic or sand) which are heated by the incoming solar flux as they pass through the focal zone.

Solid particles act as the receiver, HTF and storage material since they can be collected in large insulated bins at the base of the tower. There are still several concepts being developed around the best method of storing these particles and extracting the heat from them at a later stage. A natural feature of this technology is that the particles can be collected on the site and shipped to a nearby customer for use in process heating applications. Research in this field is focused on particle material composition, receiver tower design and particle dispenser mechanisms (Ho *et al.*, 2020).

While this technology is not yet ready for commercial applications, Sandia National Laboratories have developed and demonstrated a 1 MW_{th} particle receiver system that achieved particle temperatures over 700 °C (Ho *et al.*, 2020). Advantages of next-generation in particle receivers include: greater operating temperature ranges (below zero to over 1000 °C), no risk of freeing HTF, use of inert and non-corrosive materials, direct storage of particles and direct heating of particles (Ho *et al.*, 2020).

Latent heat

Phase change materials (PCMs)

Phase change materials operate on the basis of latent heat storage and the material is designed for a specific temperature range and working point and as such there are a wide variety of designs and material choices available. Metallic PCM materials, like miscibility gap alloys (MGAs), are attractive for CSP applications due

to the high melting point and thermal conductivity of the material. MGAs consist out of PCM pockets dispersed inside a matrix material which has a higher melting temperature (Cuskelly *et al.*, 2019). Both metals are selected for their high thermal conductivity as well as high latent and specific heat properties.

During operation, the matrix delivers heat to the embedded PCM particles by means of conduction and power is delivered isothermally, meaning that the output temperature (T_{out}) remains constant. This is advantageous for CSP applications since the MGA will smooth out any drops in solar flux received from the field due to its thermal inertia and the ability to discharge heat isothermally. The immiscibility of the two materials allows for thermal cycling with minimal structural degradation and through selection of specific material pairs, specific operating temperatures can be designed for (Cuskelly *et al.*, 2019). Additionally, the MGA remains macroscopically solid during operation due to the higher melting point of the matrix material.

MGA storage blocks are capable of performing multiple roles in a CSP plant, including: solar receiver, heat exchanger, boiler and super heater. This flexibility enables MGAs to meet the demand of supercritical CO₂ (sCO₂) CSP plants. Other advantages include zero risk of freezing HTF and safe and effective storage due to chemical and thermal stability. One disadvantage of PCMs is that it is an unproven technology and hence lacks technology readiness.

Steam

Steam is a widely used working fluid in the power generation industry. Its suitability is proven by its use in coal power plants for decades, and it is still used in most modern power plants that generate power using turbines. Steam is also used for storage, e.g. in Khi Solar One in Upington, South Africa which is a direct steam generating plant with saturated steam storage for two hours of full load operation (NREL, 2021).

Thermochemical

Thermochemical energy storage (TcES) enables higher energy density as well as the possibility for heat storage at room temperature, in the form of stable solid materials. Isothermal heat release at restitution temperature is set through achieving reaction equilibrium. Selection criteria for TcES include a high energy conversion and reaction rate, as well as complete irreversibility of the reaction. By design, the reactions occur in the appropriate temperature range for the desired applications.

2.4.2 Mechanical energy storage

Pumped storage hydroelectricity (PSH)

Pumped storage hydroelectricity is one of the largest forms of energy storage in use today, both in terms of physical scale and energy storage potential. The technology relies on the gravitational energy potential between two reservoirs of water and extracts useful work by converting gravitational potential energy to kinetic energy. The energy storage capacity of PSH is described by Equation 2.4.2, where ρ , g and V are the density of water, the gravitational acceleration constant and the volume of water stored, respectively (Akinyele and Rayudu, 2014). The vertical difference in height between the two reservoirs is captured by $H_{upper} - H_{lower}$.

$$E_{storage} = \rho g V (H_{upper} - H_{lower}) \quad (2.4.2)$$

Fundamentally, the electricity generation technology is the same as used in hydroelectric power plants, except that the water is pumped back up to the higher level reservoir during off-peak periods using electricity from the grid. During peak load periods, water is driven through large turbines at the base of the system, which drive electricity generators. Due to the nature of this technology, its adoption is limited by geographical features, water availability and large investment costs. Due to the low self-discharge rates of PSH, it is suitable for long-duration storage applications (hours to months). As of 2022, the largest technology of this kind is the Fengning Pumped Storage Power Station in the Hebei province of China, which is able to store 6612 GWh of energy, with 12 pump-turbine generators, each rated at 300 MW (Bellini, 2022).

According to Akinyele and Rayudu (2014), PSH remains a mature option for large-scale applications, while technologies like sub-surface and seawater storage systems could potentially reduce the environmental impacts of traditional PSH. Equipped with variable-speed drives, PSH could offer ancillary services to networks and thus increase the range of suitable applications.

PSH plants are often used as peaker plants due to their ability to connect and synchronise with the grid in a matter of minutes and are typically used during relatively short periods of maximum demand electricity consumption periods. In South Africa, these periods typically occur in the morning and in the early evening periods. In addition to utilising off-peak periods to charge, PSH also allow for peak shifting of midday solar PV power generation to delivery of power generation during the evening or early morning (i.e. peak shifting). In South Africa, the value of PSH plants has further been demonstrated during bouts of load-shedding in 2017–2022, where Cape Town faced less severe outages due to the Steenbras PSH plant. The

PSH plants in South Africa are listed in Table 2.4.1 below.

Table 2.4.1: PSH plants in South Africa

	Plant name			
	Steenbras	Palmiet	Ingula	Drakensberg
Location	Gordon's Bay	Grabouw	Van Reenen	Bergville
Operator	City of Cape Town	Eskom	Eskom	Eskom
Capacity (MW)	180	400	1332	1000
Storage (h)	9.6	22.5	16	10
Commissioned	1979	1988	2018	1982

Compressed air energy storage (CAES)

CAES uses air as an energy storage media and consists of two distinct phases. The charging (or compression) phase uses electricity to drive compressors, injecting air into storage vessels. In the discharging (or expansion) phase, the air is released and heated by a heat source and used to drive a turbine, generating electricity; illustrated in Figure 2.4.3.

The first utility scale CAES based plant, the Huntorf plant in Germany, was commissioned in 1978. It makes use of two salt domes as storage vessels and operates at 290 MW on a daily 8 h charging and 2 h discharging cycle (Raju and Kumar Khaitan, 2012). Advantages of CAES systems include: low energy capital cost, long lifetime (20–40 years or 13000 cycles), high discharge efficiency (70–90 %) and negligibly small self-discharge rates (Mostafa *et al.*, 2020; Luo *et al.*, 2015; Ould Amrouche *et al.*, 2016). Discharge efficiency is the ratio of energy discharged by the system to the energy stored by the system. The product of charge and discharge efficiency is equivalent to the round-trip efficiency.

The heat source used in the expansion phase can be a combustion process or heat stored from the compression process. From this, two categories of CAES emerge; diabatic (D-CAES) and advanced adiabatic (AA-CAES). The former requiring fossil-fuels as a heat source. The total system efficiency of D-CAES systems are relatively low (42 %) but can be improved (~ 54 %) by recuperating the exhaust

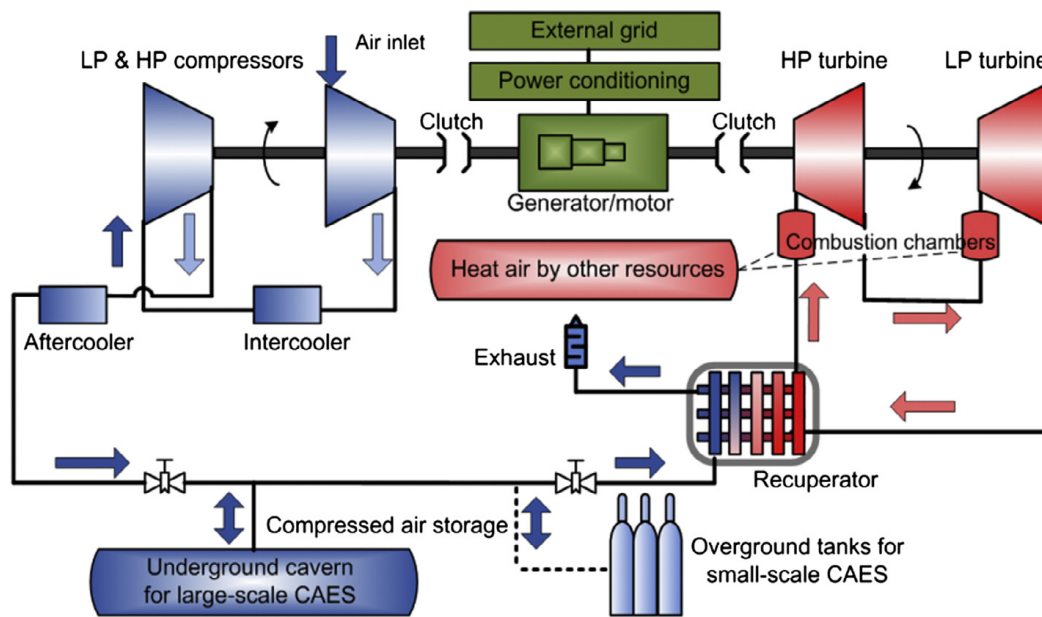


Figure 2.4.3: Schematic of CAES system (Luo *et al.*, 2015)

heat energy (Zakeri and Syri, 2015).

Since 2014, studies are focused on AA-CAES, which incorporates a TES subsystem to capture heat generated in the compression phase, removing the reliance on the combustion of fuel in the expansion phase, increasing the system efficiency to 70 % but also increasing the system cost by 30–40 % (Luo *et al.*, 2015; Zakeri and Syri, 2015). Isothermal CAES, another possible alternative to D-CAES, compresses the air without increasing its temperature, reducing the work required for compression and increasing the RTE ($\sim 70\text{--}80\%$) (Akinyele and Rayudu, 2014).

CAES can also be classified as aboveground and underground. The latter has greater capacity (5–400 MW), longer discharge durations (1–24 hours) and utilises naturally occurring underground cavities (Luo *et al.*, 2015). The most cost-efficient solutions for underground storage are salt caverns, natural aquifers and depleted natural gas reservoirs (Zakeri and Syri, 2015). Aboveground systems typically use pressure vessels, have smaller capacities (3–15 MW) and shorter discharge durations (2–4 hours).

Adoption of CAES is limited by geographical requirements, since the storage vessel is the primary contributor of investment cost of the plant (Luo *et al.*, 2015). Another limiting factor is the relatively low round-trip efficiency of traditional CAES

(44 %) compared to PSH and Li-ion (78 % and 86 %, respectively) (Schmidt *et al.*, 2019).

Luke (1996) identified CAES as a cost-competitive energy storage option for South Africa, compared to PSH, and found that storage volume was a limiting factor in both cases. It was also found that the province of Gauteng would be the most suitable due to the number of mining shafts in the area that could be used to store the air and their proximity to areas of high energy consumption.

CAES plant costs consist of power and storage related costs. The former includes the turbine, compressor and other equipment related to the powertrain, which are mature technologies; meaning limited potential for future cost reduction. The latter includes all costs related to the storage vessel, which might be relatively inexpensive if existing salt caverns are used (Zakeri and Syri, 2015).

New research is also focused on identifying alternative geological features for use in underground systems. Underwater/ocean-CAES makes use of an underwater storage vessel installed on the seabed which removes the need for an underground storage cavern and can be readily integrated with offshore generation like wind or PV (Akinyele and Rayudu, 2014; Lim *et al.*, 2012).

2.4.3 Chemical energy storage

There are several viable chemical storage media, the most well-known of which are hydrogen and methane storage. They are often classified as power-to-gas (PtG) and power-to-gas-to-power (PtGtP) since they are used as intermediary energy carriers. Synthetic fuels produced using hydrogen and carbon also fall in this category.

Hydrogen

Hydrogen is popular for many reasons such as its high energy density and its natural abundance in the world. With an energy density of 33.32 kWh/kg, more than double that of natural gas and gasoline (13.9 and 12.7 kWh/kg respectively), hydrogen fuel has one of the highest energy densities of all fuels (Zhang *et al.*, 2014). There is also the added commercial motivation to produce hydrogen as an export to countries like Japan, which aim to launch a hydrogen driven economy by 2030 and commit to reaching a carbon-neutral status by 2050 (Kelly-Detwiler, 2020).

Another attractive quality of hydrogen is its established position as a power source of electric vehicles in the form of hydrogen fuel cells. Fuel cells produce electrical energy from a chemical fuel input, such as hydrogen, through a conversion process

that strips electrons off hydrogen atoms (Zhang *et al.*, 2014).

Hydrogen can be produced through several methods such as steam-methane reforming reactions, electrolysis and more recently, polymer exchange membrane electrolysis. Electrolyzers are often used to break down water into hydrogen and oxygen by means of an electrochemical reaction. Zhang *et al.* (2014) found that the industry standard electrolyzers, using platinum catalysts, are able to achieve hydrogen production efficiencies of nearly 70%. The cost of electricity and platinum electrodes used in this process significantly increases the cost of hydrogen fuel.

Hydrogen production can alternatively be powered by PV plants through a method known as solar water splitting, which splits water into oxygen and hydrogen. Solar water splitting is a thermodynamically uphill reaction, meaning that a minimum potential voltage is required to initiate the reaction (Zhang *et al.*, 2014). Solar panels could be used to generate the necessary electricity, but current performance limitations set the solar efficiency at 20%. The production of so-called green hydrogen, i.e. using either wind or direct solar PV energy, will therefore be expensive and probably only be feasible at very large scale. The 2022 investigation of 350 000 t annual production of green hydrogen production by Hyphen Hydrogen Energy in Namibia comes to mind (Creamer, 2022a).

Another method of generating green hydrogen is through photocatalytic and photoelectrochemical (PEC) methods. PEC technologies use semiconductors to generate hydrogen directly, eliminating the need for costly electrolyzers. As described by Zhang *et al.* (2014), PEC utilizes a photochemical reaction and hydrogen is generated when the energy of the incident light is larger than the bandgap energy of the semiconductor. Photo-excited electrons are created in the conduction band and holes are formed in the valence band. Water is reduced by electrons in the conduction band to form hydrogen, and oxidised by holes in the conduction band to form oxygen gas.

More advanced semiconductors have been developed that are able to spontaneously split water into hydrogen and oxygen when they are illuminated with light energy greater than the bandgap energy of the semiconductor. The performance of these semiconductors can be further improved with the introduction of element doping, but the instability of these oxides limit the practical applications of this technology, (Zhang *et al.*, 2014). Although the production of hydrogen is well-understood, the challenge lies in producing it in a sustainable and renewable manner.

A further economic motivator for hydrogen production is that it can be sold for its various applications in many industrial applications. Some of these applications

include the production of agricultural fertilizer, plastics and other pharmaceuticals. A disadvantage of hydrogen is that it has very poor density, meaning that it needs to be stored under immense pressure or very low temperatures to achieve the same energy per unit volume as traditional fuels. These extreme conditions make it very costly and dangerous to transport hydrogen. Both of these obstacles can be overcome by improvements in storage and material technology.

Reuß *et al.* (2017) investigated flexible hydrogen supply chain models in a seasonal storage application and found that underground storage and liquid organic hydrogen carriers (LOHCs) offer an economical solution to the storage of large amounts of hydrogen at low charge cycles.

It was also found that seasonal storage systems have high investments costs, while continuous liquefaction plants have higher electricity costs and carbon emissions. With low hydrogen demand, it was found that LOHC is more economic, while hydrogen gas benefits from economies of scale by using gas pipelines and networks.

Methane storage

A second promising technology is the use of methane as storage medium of energy. A benefit of this would be that plants would draw carbon dioxide (along with oxygen) from the environment to create methane, creating a carbon-neutral process. The stored methane could be pumped along in pipelines in a reasonably safe manner and can be used in a combustion process to generate heat and ultimately electricity if necessary.

2.4.4 Electrochemical energy storage

Electrochemical storage includes all the storage systems under the more common name of "battery", which is a system that stores electrical energy as chemical potential energy and typically consists out of one or more cells containing an electrode and an electrolyte. This section briefly discusses and describes batteries of various chemical compositions and configurations of electrode and electrolyte.

Lithium-ion (Li-ion)

Lithium-ion batteries were first commercially produced in the 1990s. Originally developed for portable applications, the technology has rapidly improved over a relatively short time and is now also used for electric vehicle and grid scale storage applications (Zakeri and Syri, 2015). In 2015, 85.6% of newly deployed ESSs were Li-ion batteries (worldwide).

Advantages of Li-ion include: low self discharge rate (5–10 % per month), long cycle durability (1000–10000 cycles), high RTE ($\sim 97\%$) and low maintenance requirements (compared to other batteries). Compared to other battery technologies, the capital cost of Li-ion is very high but due to its round-trip efficiency and lifetime, it has the lowest cost per cycle (Ould Amrouche *et al.*, 2016). Disadvantages include high capital costs and low DoD (requiring frequent charging to prevent reduction of lifespan). The cost of these batteries is further increased by the need for electronic controllers that manage the charge levels (Mostafa *et al.*, 2020; Luo *et al.*, 2015). Studies from 2015 and 2018 focused on finding better electrode materials, improving energy density, increasing the available power and reducing safety concerns of the technology (Luo *et al.*, 2015; Gür, 2018).

A substantial South African project which comes to mind is the Scatec Kenhardt 150 MW, 7.6 hours of lithium-ion storage plant (contracted at 0.12\$/kWh). This project was awarded under the Risk Mitigation Independent Power Producer Program (RMIPPP) and reported financial funding closure in 2022 (Creamer, 2022b).

Flow batteries

Flow batteries are unique compared to other batteries; liquid electrolytes are used which are stored in separate external storage tanks. During charging, the electrolytes are pumped to a cell stack where a reduction-oxidation reaction takes place, converting electrical to electrochemical energy (Luo *et al.*, 2015). As illustrated in Figure 2.4.4, one of the electrolytes is oxidised at the anode while the other is reduced at the cathode. During energy discharge, the above process is reversed.

An advantage of flow batteries is that the power output is independent of the storage capacity. The power is determined by the size of the electrodes and the number of cells in a stack, while the storage capacity is determined by the concentration and volume of electrolyte in the tanks (Luo *et al.*, 2015; Zakeri and Syri, 2015). This means that the capacity can be readily expanded by installing larger electrolyte tanks. The rate of self-discharge is also negligible compared to other batteries due to the separation of the electrolytes (Schmidt *et al.*, 2019; Luo *et al.*, 2015; Akinyele and Rayudu, 2014).

There are two types of flow batteries: redox, which have two electrolyte solutions in two separate tanks, and hybrid, where only one solution is in a separate tank. Vanadium redox flow batteries (VRFB) are an example of the former and are the most mature of the flow battery technologies (Luo *et al.*, 2015). VRFB have long dis-

charge (up to 12h), long life cycles (> 5000 deep cycles) due to high electrochemical reversibility, slow self discharge and low maintenance costs (Ould Amrouche *et al.*, 2016). VRFB also have demonstrated high efficiencies ($\sim 85\%$) and are capable of longer discharge durations (up to 24h) (Schmidt *et al.*, 2019).

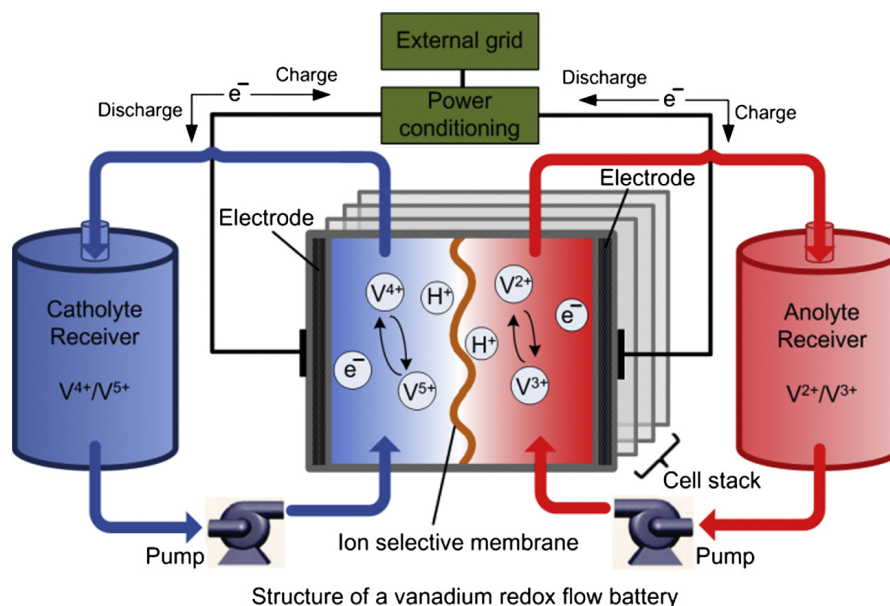


Figure 2.4.4: Schematic of VRFB system (Luo *et al.*, 2015)

Limitations of VRFB include low energy density (10–75 W h/kg) compared to other battery technologies like Li-ion (150–500 W h/kg); limited operating temperature range 10–35 °C and high capital costs (Luo *et al.*, 2015; Mostafa *et al.*, 2020).

Other battery technologies

Other commercially available battery technologies include: nickel cadmium (NiCd), lead-acid, sodium-sulfur (NaS) and sodium nickel chloride (Zebra). Ould Amrouche *et al.* (2016) found that NiCd batteries had the lowest capital cost of all the electrochemical battery systems. Lead acid batteries traditionally suffered from technical limitations: short life cycle (< 500), low DoD (20%), limited lifetime (2 – 4 years), slow charging and high maintenance requirements (Ould Amrouche *et al.*, 2016). However, as of 2022, state-of-the-art lead-acid batteries use carbon in the cathode, resulting in better performance and longer lifetimes.

Compared to other battery technologies, NaS batteries have high energy density,

high charge and discharge efficiencies (89–92%), long life cycles and inexpensive material requirements. An operating temperature of 350 °C makes NaS unsuitable for household applications, but it remains a strong contender with Li-ion batteries in the large scale energy storage market (Ould Amrouche *et al.*, 2016). The Zebra battery is a suitable candidate for bulk storage with a long lifetime (4500 cycles) and an average round-trip efficiency of 75%, long discharge time and fast response. The molten electrolyte requires external heat input and operates between 270–350 °C, which limits its adoption.

2.4.5 Electromagnetic energy storage

There are two technologies in the electromagnetic category: super capacitor (SES) and superconducting magnetic energy storage (SMES). SES have high round-trip efficiencies of 95% and are often used in wind energy conversion applications to dampen transient fluctuations in power (Ould Amrouche *et al.*, 2016). SMES offers instantaneous discharge of energy, resulting in high power output capability; making it a good option for rapid response to transient fluctuations (Ould Amrouche *et al.*, 2016).

2.5 Energy storage technology selection based on literature

This section summarises several studies that investigated energy storage technologies and their suitability for specific energy storage applications. The arguments presented below guided the selection of the energy storage technologies further investigated in this study.

A study by Guney and Tepe (2017) compares features, advantages, environmental considerations and variations in the application of several ESS technologies. They found that mechanical storage systems allowed for the greatest storage capacity, while batteries were preferable in stand-alone systems. Mobile storage applications were found to be the most compatible with batteries and fuel-cells.

Ould Amrouche *et al.* (2016) investigated various storage mechanisms for use with PV and wind power plants. They found that for the application of energy management the most suitable technologies were: PSH, CAES, electrochemical batteries, flow batteries, fuel cells, solar fuels and TES. Super conductors, flywheels, batteries and capacitors were more suitable for power quality and short duration storage applications.

Akinyele and Rayudu (2014) also note that increased penetration of RE would require a unique mix of ESSs for each application and that it is unlikely that a single technology would be able to meet all the requirements due to the range of characteristics that each technology is equipped with. A combination of technologies, each with varying charging and discharging properties, and cycle duration, would be selected for a specific application. Akinyele and Rayudu (2014) also suggest that an important avenue of investigation would be the possible combination of various ESSs in a single "system" which could provide multiple storage services.

A comparison of several ESSs can be seen in Figure 2.5.1 by Luo *et al.* (2015), from which the most suitable technologies can be selected for the applications considered in this study as motivated in Section 2.2.4 and described in Table 2.2.1.

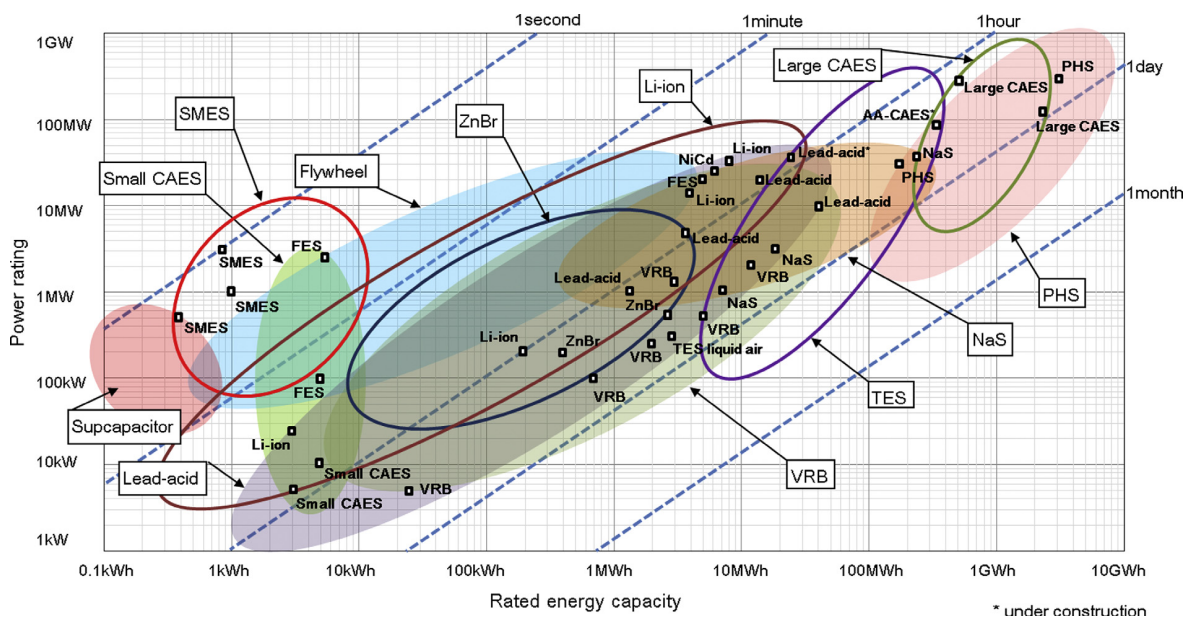


Figure 2.5.1: Comparison of ESSs based on power rating, energy capacity and discharge duration (Luo *et al.*, 2015)

The applications considered are peaker replacement and long-term seasonal storage (also see Section 2.2.4). The former requires an ESS in the range of 1–500 MW with a DD of 2–6 h. Applying these requirements to Figure 2.5.1, identifies several suitable technologies like: PSH, NaS, CAES, VRFB, FES, TES and Li-ion. The same approach was used for long-term seasonal storage, which requires a capacity in the range of 500–2000 MWh with a DD of 24–2000 h. Only CAES and PSH were identified to meet the criteria on the lower bound of 24 h and 500 MWh.

In a 2019 study, Schmidt *et al.* (2019) identified hydrogen energy storage as a viable candidate for peaker replacement applications, capable of discharge durations of up to 24 h. Schmidt *et al.* identified the following technologies as suitable for the same application: PSH, CAES, Li-ion, NaS, Lead-acid and VRFB. For the application of seasonal storage, Schmidt *et al.* identified the following suitable technologies: PSH, CAES, VRFB and hydrogen based energy storage options.

Based on these findings reiterated in the literature as to best-for-purpose energy storage types, a decision was taken to investigate the storage types listed below in Table 2.6.1. Thus PSH, CAES, Li-ion, VRFB and Hydrogen may be suitable candidates to be considered further.

2.6 Summary of this literature review

In this literature study the background of CSP was investigated, as well as new developments in the field, since, in the RE context, CSP already provides short term cost-effective energy storage. The need for storage was identified, as well as an internationally growing trend in the type and amount of storage technologies installed in the context of all renewable energy harvesting technologies. The technical parameters of a storage system were investigated, as well as the timescales of storage necessary for various applications. Discharge duration timescales of 4.5 h and 2160 h were identified (Section 2.2.3) for the purposes of medium (daily) and long-term (seasonal) energy storage.

The various application of energy storage were reviewed, with peaker replacement and long-term seasonal storage selected for further investigation due to their suitability to the scope of this study. The major categories of energy storage were discussed, with examples of each given. Commercial and developing technologies were also discussed. Based on literature findings, and their suitability to the storage applications considered in this study, as outlined in Section 2.5, five storage technologies were identified and are summarised in Table 2.6.1 below.

Table 2.6.1: Energy storage systems and their corresponding applications considered in this study

Application	Technologies considered				
	PSH	CAES	Li-ion	VRFB	Hydrogen
Peaker replacement	✓	✓	✓	✓	✓
Seasonal storage	✓	✓		✓	✓

Chapter 3

Financial Analysis Method

This chapter discusses the method of evaluation used in this study. A brief introduction is given to levelised cost of (energy) storage, followed by an explanation of the calculation method and the approach used to deal with uncertainty.

3.1 Definition of financial concepts

3.1.1 Time value of money

Time value of money (TVM) is the potential earning capacity of capital today compared to its expected future value. The value of an investment can be determined by its net present value (NPV) which is the present value of expected annual expenses and returns. Equation 3.1.1 calculates the NPV of an investment by discounting the expected net cash flow (R_n) during a period (n), over the lifetime of the investment (N). The interest rate used for discounting is often referred to as discount rate (r). If the net present value is greater than zero, the project is financially viable (Fernando, 2021).

$$NPV = \sum_{n=1}^N \frac{R_n}{(1+r)^n} \quad (3.1.1)$$

The levelised cost of electricity (LCOE) calculation, discussed in the following section, is based on NPV and calculates the ratio of (discounted) system costs to (discounted) electrical energy supplied by the system over its lifetime.

The discount rate is determined by factors like the cost of capital, the balance between debt and equity financing and the financial risk assessment of the loan. Schmidt *et al.* (2019) found that discount rates used for industry projects depend

on the maturity of the energy storage system (ESS) technology and the business case. Several studies found that discount rate significantly influences LCOE (Lai and McCulloch, 2017; Schmidt *et al.*, 2019; Pan, 2020). Pawel (2014) found that a 5 % increase in discount rate resulted in a 50 % increase in LCOE; implying that choosing an appropriate discount rate is vital for any such analysis.

An approach used by several studies (Jülch, 2016; Lazard, 2019; Pawel, 2014; Pan, 2020) is to assume the discount rate to be equal to the *weighted average capital cost* (*WACC*); calculated using Equation 3.1.2. The *WACC* accounts for equity (E), debt (D), cost of equity (C_E), cost of debt (C_D) and the corporate tax rate (r_{tax}).

$$WACC = \frac{E}{E + D} \cdot C_E + \frac{D}{D + E} \cdot C_D \cdot (1 - r_{tax}) \quad (3.1.2)$$

Since interest and tax rates are dependent on the country and its investment climate, the WACC is often significantly higher in developing countries like South Africa. For example, for a debt/equity ratio of 70/30, the nominal WACC in South Africa is 11.45 % compared to 3 % for the *Dubai Electricity and Water Authority* (DEWA) which leads to significantly higher levelised cost of electricity (Lilliestam and Pitz-Paal, 2018; Pan, 2020).

As highlighted by Pawel (2014), correctly calculating the WACC is complicated and there exists multiple methodologies, generally unique within the context of each project and its investors, therefore this approach cannot be followed in this study. Instead, a discount rate of 8 % for projects in South Africa will be used, as was done by Lai and McCulloch (2017); Schmidt *et al.* (2019); Zakeri and Syri (2015), and Battke *et al.* (2013), although Pan (2020) cites somewhat higher values between 11 and 12 % for Southern Africa. As mentioned previously, the discount rate is influenced by each technology's financial risk assessment; in practice, mature technologies will benefit from lower rates compared to their newer competitors (Schmidt *et al.*, 2019). For the purposes of this study, the same discount rate will be applied across all the considered technologies and sensitivities to it will be tested. The effect of discount rate was investigated and is discussed in Section 4.3.

3.1.2 Levelised cost of electricity (LCOE)

The high variability of technical and economic factors involved with storage plant technologies, as well as the ever-growing range of applications, makes it challenging to compare the costs of storage technologies (Jülch, 2016). Costing research presently focuses on two approaches: profitability analysis of a technology for a specific application and calculation of cost per stored unit of electrical energy (kWh).

The former being well suited to analyse a single storage technology under a niche application and the latter being more appropriate when a broad overview of multiple technologies is desired, allowing for comparison of technologies with different costing structures (Jülch, 2016).

At the time of writing, terms used in literature to evaluate ESSs are; levelised cost of electricity (LCOE), levelised cost of (energy) storage (LCOS) and life cycle cost. All of these terms refer to the ratio of discounted ESS charging costs (including capital investment, maintenance costs, etc.) to the amount of electrical energy discharged over the expected lifetime of the system. In the context of this study, "electricity" refers to units of electrical energy (kWh).

The LCOE approach is a proven method for comparing the cost of power generation technologies. It calculates the minimum price of electrical energy supplied over the project lifetime so that the net present value of all future expenses, capital and revenue streams is zero. From this, project planners and financiers are able to select the most cost-effective technology based on the price of supplied electricity instead of capital cost or technical performance.

Based on Equation 3.1.1, the LCOE equation can be derived by setting NPV to zero (i.e. $NPV_{expenses} = NPV_{revenue}$), where revenue (R_n) is calculated as the product of the amount of electricity generated in a year (E_t) and the cost of electricity (C_{elec}).

$$NPV_{expenses} = NPV_{revenue} = \sum_{n=1}^N \frac{E_t \cdot C_{elec}}{(1+r)^n} \quad (3.1.3)$$

Equation 3.1.3 can be simplified to the equation below since the cost of electricity is constant through the system's lifetime.

$$NPV_{expenses} = C_{elec} \cdot \sum_{n=1}^N \frac{E_t}{(1+r)^n} \quad (3.1.4)$$

Arranging Equation 3.1.4 in terms of C_{elec} (equivalent to LCOE), and expanding the expense terms, results in Equation 3.1.5, below

$$LCOE = C_{elec} = \frac{NPV_{expenses}}{\sum_{n=1}^N \frac{E_t}{(1+r)^n}} = \frac{\sum_{n=1}^N \frac{I_t + M_t + F_t}{(1+r)^n}}{\sum_{t=n}^N \frac{E_t}{(1+r)^n}} \quad (3.1.5)$$

where I_t , M_t and F_t are the total investment, operations and maintenance and input energy costs in a year (n). The annual costs are discounted at each year of operation using the discount rate (r) over the lifetime (N) of the system.

3.2 Levelised cost of storage (LCOS)

LCOS is a variation of Equation 3.1.5 which considers the charging cost of the ESS and the amount of energy discharged over the project lifetime. Jülch (2016) and Abdon *et al.* (2017) found that it was important that the investment and operational costs for the full life cycle of energy storage is also taken into account. A study by Schmidt *et al.* (2019) found the key input parameters for LCOS to be: nominal power capacity (energy discharge rate), discharge duration (energy storage capacity), cycle frequency (the number of equivalent annual cycles) and price of electricity (used for charging of ESSs).

As pointed out by Mayr and Beushausen (2016), it is easy to become overwhelmed by the complexities of energy storage costs. To successfully compare technologies it is necessary to be meticulous with input assumptions across all the technologies. Additionally, there are several cost influencers to consider when comparing the costs of ESS technologies. For instance, it is important to consider all upfront costs required to install and connect the system to the grid; shipping and installation costs are often overlooked and do not always appear in the initial quote. The physical dimensions of a technology will influence the cost and complexity of the shipping process.

Other important cost influencers include: operation and maintenance costs, charging costs (price of electricity used to charge the ESS), usable energy over the project lifetime, end-of-life value (re-sale value of individual components) and financing costs (the time value of all cash flows during the project lifetime). The usable energy of a project is determined by the relevant number of annual cycles, the round-trip efficiency and the corresponding DoD. It may be the case that the cycle life exceeds the project calendar life of the project, in which case only the relevant cycle count should be considered. For example, if an ESS delivers 200 cycles per year for 25 years, a cycle life greater than 5000 cycles does not add extra value and should not be considered in the calculation of LCOS (Mayr and Beushausen, 2016).

Battke *et al.* (2013) found that most literature on battery systems only account for initial investment and operating costs and suggest that a fair basis for comparison of battery technologies should include life-cycle costs since these costs vary across storage applications, in particular when life time requirements vary considerably.

Several academic and industry parties have conducted LCOS analyses and published their findings, but the input parameters are not always defined or are vague, making it difficult to replicate their results and develop a verified model. Publica-

tions from 2019 have pushed for a more transparent approach, making their input assumptions, methods and datasets publicly available and even creating free online tools for users to manipulate input variables and compare with their own results (Schmidt *et al.*, 2019).

As with LCOE, there are several input parameters to consider in the calculation of LCOS and through a survey of the literature, it is clear that not all studies use the same approach. Schmidt *et al.* (2019) conducted a comparison of economic and technical LCOS input parameters considered in studies from 2013–2019; a summary of which can be found in Table 3.2.1.

Table 3.2.1: Comparison of economic and technical factors considered in recent studies

LCOS components	Studies reviewed						
	<i>a</i>	<i>b</i>	<i>c</i>	<i>d</i>	<i>e</i>	<i>f</i>	<i>g</i>
Investment cost	✓	✓	✓	✓	✓	✓	✓
Replacement cost	✓	✓	✓				✓
Operating cost	✓	✓	✓	✓	✓	✓	✓
Power cost	✓	✓	✓	✓	✓	✓	✓
End-of-life cost	✓	✓			✓		✓
Discount rate	✓	✓	✓	✓	✓	✓	✓
Nominal capacity	✓	✓	✓	✓	✓	✓	✓
Depth of discharge	✓	✓	✓		✓	✓	✓
Round-trip efficiency	✓	✓	✓	✓	✓	✓	✓
Cycle life	✓	✓				✓	✓
Shelf life	✓	✓		✓	✓	✓	✓
Construction time							✓
Degradation rate			✓	✓			✓
Self-discharge		✓					✓

^aZakeri and Syri (2015)

^bJülch (2016)

^cLazard (2019)

^dLai and McCulloch (2017)

^ePawel (2014)

^fBattke *et al.* (2013)

^gSchmidt *et al.* (2019)

3.3 LCOS method considered in this study

Compared to other recent studies (from 2013–2019), the evaluation by Schmidt *et al.* (2019), is the most comprehensive; taking economic factors like construction time, replacement costs, and end-of-life costs into consideration. Technical factors overlooked by other studies include: cycle life, construction time and self-discharge rate. For these reasons, the LCOS calculation methodology presented by Schmidt *et al.* (2019) is followed for the purposes of this study and is described in the following section.

The equation used to calculate levelised cost of storage, is described in Equation 3.3.1 and consists of four major terms, namely: investment (I), operation and maintenance (OM), charging (W_{in}) and end-of-life (EoL) costs which are described using Equations 3.3.2 to 3.3.5. The total annual energy discharged (W_{out}) is discounted using Equation 3.3.6. The LCOS components listed in Table 3.2.1 and used in Equations 3.3.1–3.3.6 will be described in this section. The discount rate (r) is used to calculate the present value of the system after each year of operation (n) across the project lifetime (N).

$$LCOS = \frac{I + \sum_{n=1}^N \frac{OM}{(1+r)^{n+T_c}} + \sum_{n=1}^N \frac{W_{in}}{(1+r)^{n+T_c}} + \frac{EoL}{(1+r)^{N+1}}}{\sum_{n=1}^N \frac{W_{out}}{(1+r)^{n+T_c}}} \quad (3.3.1)$$

The investment cost, as described in Equation 3.3.2, consists of overnight capital costs that are related to the system's power and energy capacity (P_{nom} and E_{nom} , respectively) as well as discounted replacement costs over the system lifecycle.

$$I = I_P \cdot P_{nom} + I_E \cdot E_{nom} + \sum_{rep=1}^R \frac{C_{P-r} \cdot P_{nom}}{(1+r)^{T_c+rep \cdot T_r}} \quad (3.3.2)$$

The overnight cost is the cost of construction, without considering the interest accrued during construction time (as if the plant had been built overnight). Instead of being incorporated into operation costs (which are discounted annually), the replacement costs are discounted from the end of each replacement interval (rep), which might only occur once every 3 years for a total number of replacements (R) in a project's lifetime. The replacement cost also includes a power specific component cost (C_{P-r}). The total number of replacements are determined by the system lifetime and the replacement interval (T_r) which is specific to each technology. The discounting impact of construction time (T_c) is also accounted for by adding it at

each replacement interval (expressed as $T_c + rep \cdot T_r$ in Equation 3.3.2). The construction time is also taken into account when discounting operating costs, charging costs and discharged energy.

The operation and maintenance costs, as described in Equation 3.3.3, consists of power and energy specific costs. The power related costs are fixed, but energy costs vary with the amount of energy stored by the system in a year. The first term is a product of the system's rated power and a power specific OM cost (C_{P-OM}). The second term is a product of an energy specific OM cost (C_{E-OM}), the total energy discharged per annum and two performance factors. The annual energy discharge is calculated as the product of discharge frequency, depth of discharge (DoD) and nominal energy capacity. The two performance factors are governed by cyclical (f_{deg}) and temporal (t_{deg}) degradation of the system. As the terms suggest, the former is a function of the cycle frequency (f) and the latter of the system lifetime only.

$$O\&M = C_{P-OM} \cdot P_{nom} + C_{E-OM} \cdot (f \cdot DoD \cdot E_{nom}) \cdot (1 - f_{deg})^{(n-1) \cdot f} \cdot (1 - t_{deg})^{(n-1)} \quad (3.3.3)$$

The charging cost of the system, described by Equation 3.3.4, is a function of the system round-trip efficiency (η_{RT}), the price of electricity (C_{elec}) and the total annual energy discharged from the system (discounted), which is described in Equation 3.3.6.

$$\sum_{n=1}^N \frac{W_{in}}{(1+r)^{n+T_c}} = \frac{C_{elec}}{\eta_{RT}} \cdot \left(\sum_{n=1}^N \frac{W_{out}}{(1+r)^{n+T_c}} \right) \quad (3.3.4)$$

The end-of-life costs, described by Equation 3.3.5, are the costs associated with recycling or disposing the storage system at the end of its life and consists of energy and power specific end-of-life costs (EoL_E and EoL_P , respectively). These costs are discounted from the end of the system lifetime (N).

$$EoL = \frac{(EoL_P \cdot P_{nom} + EoL_E \cdot E_{nom})}{(1+r)^{N+1}} \quad (3.3.5)$$

Equation 3.3.6 is used to calculate the discharged electricity (W_{out}) and considers annual energy stored (discussed above), round-trip efficiency (η_{RT}), self-discharge rate (η_{self}), cycle degradation and temporal degradation of the system.

$$\sum_n^N \frac{W_{out}}{(1+r)^n} = f \cdot DoD \cdot E_{nom} \cdot (1 - \eta_{self}) \cdot \sum_{n=1}^N \frac{(1 - f_{deg})^{(n-1)} \cdot f \cdot (1 - t_{deg})^{(n-1)}}{(1+r)^{n+T_c}} \quad (3.3.6)$$

3.4 Simulation input assumptions

For certain technologies, there exists a large discrepancy between the values obtained from literature and those obtained from the market (Jülch, 2016). Often, insufficient exposure of a technology to the market results in unreliable data, in which case it is more appropriate to use values from literature.

The input data used for this study was sourced from a database created by Schmidt *et al.* (2019) which was derived from a review of academic publications and industry, and verified with industry experts. Each ESS technology's technical and economic data is summarised in Appendix B along with relevant references. Values in the database are presented as a mean value with a standard deviation (assumed to be normally distributed). Given the source of the input parameters of this study, it can be expected that certain technologies might be more expensive in South Africa. However, since this type of information was not accessible, it was assumed that the input parameters are representative of global trends in technology cost and performance.

Several of the ESS technologies considered in this study store electrical energy in another form (mechanical, chemical, etc.) and therefore the price of the electricity used to charge the system affects the LCOS. This is also known in the literature as the charging cost or charging electricity price. Previous research indicates that the LCOS is significantly influenced by the variability of electricity prices (used for charging the ESS) and annual operation hours for different technologies across the literature (Jülch, 2016). Following the procedure set out by Schmidt *et al.* (2019), a fixed price was assumed for charging electricity and the number of operational hours were selected based on values most suitable for the application of peaker replacement and long-term seasonal storage. It is then assumed, that this fixed price represents an optimum available for given charging needs and e.g. varying time-of-day tariffs.

As mentioned previously, the key input parameters are nominal power capacity (P_{nom}), discharge duration (DD), cycle frequency (f) and electricity price (C_{elec}).

The selection of these parameters are dependent on the storage application (discussed in Section 2.2.4); for instance, peaker replacement applications require a system with power capacity, discharge duration and cycle frequency of 1–500 MW, 2–6 h, and 5–100 annual cycles, respectively.

Cost projections for technologies like pumped storage hydroelectricity (PSH), which are mature and well established, were assumed to remain constant (Jülch, 2016).

3.4.1 Considering inflation

Data from various sources and currencies were used for this study. Before any comparison could be made, costs were converted to a reference currency and adjusted for inflation; the 2022 USD ($\$_{2022}$) is used for the purposes of this study. Costing data published in other currencies were first converted to USD using the yearly average exchange rate for the year of publication and then inflation adjusted to 2022. Unless otherwise specified, all costs in this study can be assumed to be in $\$_{2022}$. This approach follows the work of Pan (2020), Schmidt *et al.* (2019) and Lilliestam *et al.* (2020).

A cost from a year besides 2022 can be adjusted using the relevant consumer price indices (CPIs) and Equation 3.4.1, where $CPI_{initial}$ and CPI_{final} are the indices for the initial and final years in consideration. The conversion rates and inflation indices used can be found in Appendix A.

$$\$_{final} = \$_{initial} \times \frac{CPI_{final}}{CPI_{initial}} \quad (3.4.1)$$

Inflation rates differ for each currency, so all inflation adjustments were made using USD inflation indices; no additional inflation was considered when presenting results in currencies other than $\$_{2022}$.

3.4.2 Summary of input assumptions

Table 3.4.1 below summarises all key input assumptions made in this section. While the effect of electricity price and discount rate on LCOS was investigated, these values remained constant for the rest of the analysis.

Table 3.4.1: Summary of key input assumptions

Parameter	Description	Value	Units	Source
r	Discount rate	8	%	<i>a, b, c, d</i>
C_{elec}	Price of electricity	0.05	\$/kWh	<i>d</i>

^aZakeri and Syri (2015)

^bLai and McCulloch (2017)

^cBattke *et al.* (2013)

^dSchmidt *et al.* (2019)

3.5 Addressing uncertainty in the model

Due to the probabilistic nature of LCOS input parameters used in this study, it is important to consider the variance introduced into the model as well as its sensitivity to each input. The input values sourced from literature and industry are often presented as ranges, and this introduces uncertainty into the model and its results. Battke *et al.* (2013) found that the uncertainty in input parameters were often overlooked in the literature, but could be addressed by investigating the impact this uncertainty has on the cost of ESS.

While it is possible to use the mean of these input ranges, the end result is a discrete value and any statistical information is lost. Sensitivity and uncertainty analysis also serve to inform readers how robust the conclusions of the study are and where future research can be focused to improve the analysis (Hauschild *et al.*, 2018).

3.5.1 Model sensitivity analysis

With sensitivity (or perturbation) analysis, an input parameter is numerically varied while observing the relative change in the resulting output. One at a time, input parameters are varied by a predefined amount (usually within a range of ± 5 – 10 %). A model is considered sensitive to a parameter if a relatively small change to the input results in a large change in the model output (Hauschild *et al.*, 2018). Some studies vary a parameter between a pessimistic, optimistic and realistic value (Abdon *et al.*, 2017), while others use a range of ± 20 % from the initial value (Jülch, 2016; Kost *et al.*, 2018).

The analysis results are often presented in the form of spiderplots or tornado di-

agrams, as seen in Figures 3.5.1 and 3.5.2, respectively, illustrating the relative change in output for each input that was varied. Both of these sample plots were generated using the LCOS model described in Section 3.3. In the spiderplot, each line represents one of the input parameters which passes through the base case configuration (zero relative change). In the given example, LCOS is most sensitive to round-trip efficiency and power specific costs.

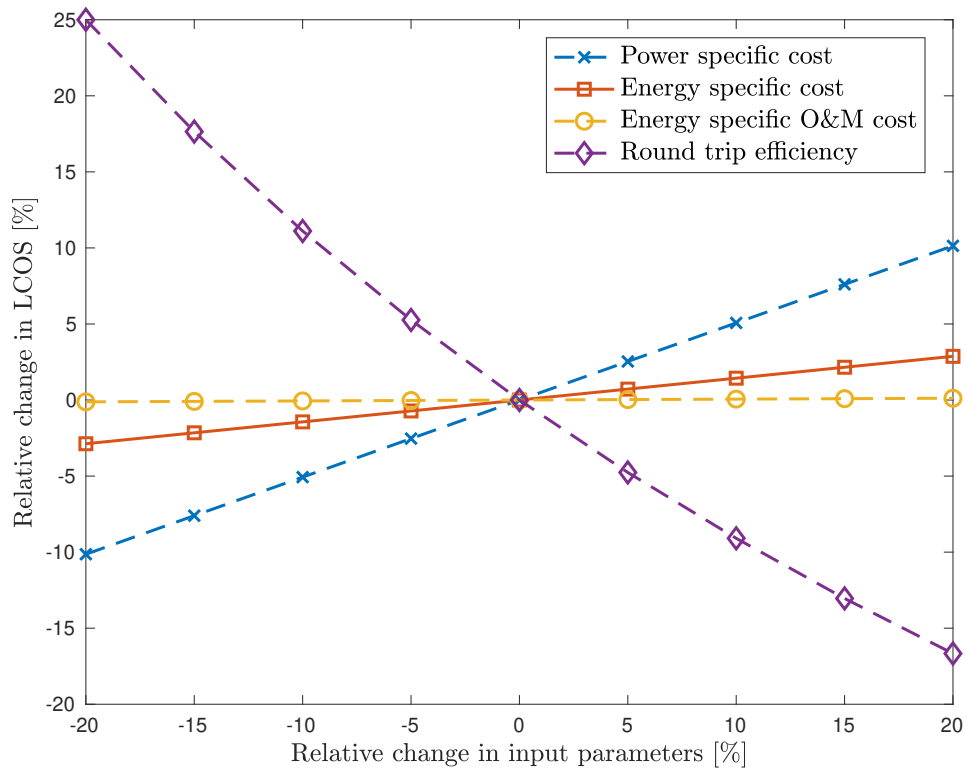


Figure 3.5.1: Example of a spiderplot, illustrating the sensitivity of LCOS to each input parameter

Each bar in the tornado diagram represents one input parameter, arranged by the magnitude of its impact on the LCOS. The striped blocks indicate an increase in the variable (or higher value compared to baseline) and the solid black blocks indicate a decrease in the variable (or lower value compared to baseline). For example, an increase in the specific power cost lead to an increase in the LCOS, while an increase in round-trip efficiency, resulted in a decrease in LCOS. Similar to the spiderplot, the tornado diagram illustrates that LCOS is most sensitive to the specific power cost and the round-trip efficiency. Higher efficiency resulted in lower LCOS, creating a negative nett change. This form of analysis is known as local sensitivity analysis and serves as a useful first approximation, highlighting

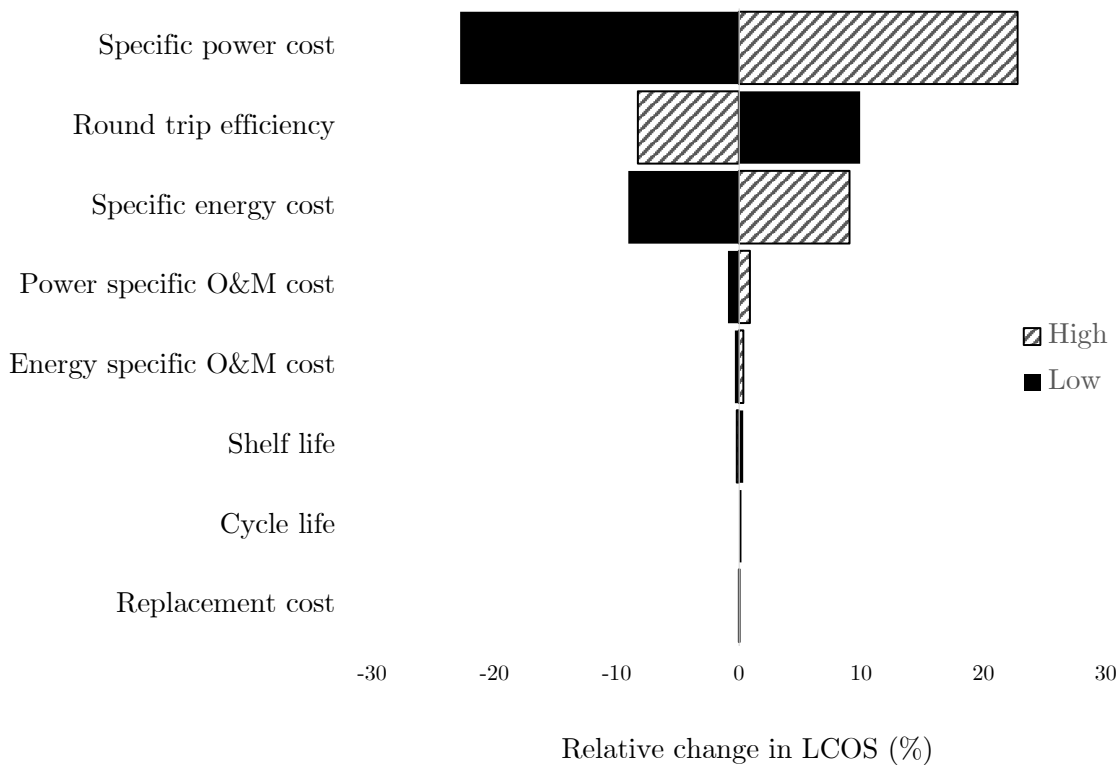


Figure 3.5.2: Example of a tornado diagram, illustrating the sensitivity of LCOS to each of the stochastic input parameters

input parameters with the greatest influence on the model output. However, these tools are limited since they only include a small sample set of all possible input parameter permutations and do not consider the uncertainty of inputs.

3.5.2 Model uncertainty analysis

Global sensitivity analysis (also known as uncertainty analysis) includes the effect of input uncertainty. In contrast to local sensitivity analysis, all inputs are varied simultaneously.

A commonly used method of addressing this uncertainty is the Monte Carlo simulation, which is a numerical approach that estimates the model output using the principles of inferential statistics (Hauschild *et al.*, 2018). Several studies on the LCOS of ESSs have used a Monte Carlo simulation to determine the most likely

cost of a specific technology within a certain confidence interval (Zakeri and Syri, 2015; Battke *et al.*, 2013; Obi *et al.*, 2017).

A Monte Carlo simulation is conducted by generating a sample of input values, randomly selected, from within the distribution range of an input parameter. The model is applied to the generated input and the resulting output is analysed using statistical methods. A good sample set tends to exhibit the same properties as the whole population on the condition that the sample is random (Guttag *et al.*, 2016). This process generates a probability distribution instead of a discrete value, meaning that a result can be given within a certain level of confidence.

The confidence interval of a sample set depends on the sample size and the variance of the sample; with higher variance requiring greater sample sizes (Guttag *et al.*, 2016). Each input value generated (and corresponding output) represents one iteration (or one sample) of the simulation. In this context, "sample size" can be used interchangeably with "number of iterations". The accuracy of the Monte Carlo simulation is based on the law of large numbers (also known as Bernoulli's law), which states that as the size of the dataset grows, the variance between data points will decrease and the distribution of the output will converge to its theoretical distribution (Battke *et al.*, 2013).

Generally, the intricacy of the model is related to the amount of computational work required to perform the simulation (Hauschild *et al.*, 2018). For example, a model with a large set of input variables would be more computationally expensive to simulate than one with fewer variables. For the purposes of this study, the sample size was determined as the number of samples at which the change in standard deviation between the results approached zero (within a 5% margin of error). This was done by gradually increasing the number of samples until the results satisfy the convergence criteria. The procedure used to calculate this number is described in more detail in Section 3.6.3.

3.6 Description of method

A probabilistic model was developed using the equations set out by Schmidt *et al.* (2019) and verified using their interactive LCOS calculator (Schmidt, 2019). Once verified, it was adapted to facilitate the Monte Carlo simulation. The initial model and verification (discussed in Section 3.7) was created using Microsoft Excel (Version 16.55) (Microsoft Corporation, 2021). The Monte Carlo simulations were performed using a self-generated Matlab script (see Appendix C) due to its computational load and need for automation (The MathWorks Inc., 2020). The input

values used for the calculation is based on a random value within an 80 % confidence interval of the normal distribution, which was calculated from the mean and standard deviation (as discussed in Section 3.4).

3.6.1 Sampling strategy

There is more than one method of sampling values from within the distribution of input parameter, the simplest is called simple random sampling (SRS). The SRS method selects one random sample value from within the entire distribution range for each iteration. In contrast, Latin hypercube sampling (LHS) pre-samples values from segments of equal probability within the distribution from which one is selected at random as the input value. While LHS allows for better representation of extreme values and usually requires fewer iterations, it adds no significant value compared to SRS unless the number of input parameters are less than five (Hauschild *et al.*, 2018). Since the number of input parameters considered in this study is greater than five, the SRS strategy is sufficient.

3.6.2 Sample inputs for LCOS calculation

The following tables illustrate a sample input used for calculating the LCOS for PSH. As mentioned in Section 3.4, the input data was sourced from a database created by Schmidt (2019), which is a collection of information from relevant sources in the literature. Each ESS technology's technical and economic data is summarised in Appendix B along with relevant references, and is assumed to be representative of global trends in cost and performance of energy storage technologies. Table 3.6.1 lists the variables with associated uncertainty, which includes a mean and standard deviation (σ). Table 3.6.2 lists inputs with constant values. The key ESS inputs used in the calculation of LCOS were selected to meet the requirements of a peak-shifting application and are listed in Table 3.6.3

Table 3.6.1: Stochastic inputs with sample values

Parameter	Symbol	Mean	σ [%]	Units
Investment cost - Power	I_P	1129	45	\$/kW
Investment cost - Energy	I_E	80	63	\$/kWh
Operation cost - Power	C_{P-OM}	8	26	\$/kW-yr
Operation cost - Energy	C_{E-OM}	0.001	60	\$/kWh
Replacement cost	C_{REP}	116	5	\$/kW
Round-trip efficiency	η_{RT}	78	9	%
Lifetime(100% DoD)	$cyclife$	33250	43	cycles
Shelf life	T_{shelf}	55	9	years

Table 3.6.2: Fixed inputs with sample values

Parameter	Symbol	Value	Units
Replacement interval	cyc_R	7300	1/a
Energy specific end-of-life cost	EoL_E	0	%
Discount rate	r	8	%
Self-discharge	η_{self}	0	%/day
Time degradation	t_{deg}	0.4	%/year
Cycle degradation	f_{deg}	0.0007	%/cycle
Construction time	T_C	3	years

Table 3.6.3: Key inputs based on peaker replacement application

Parameter	Symbol	Value	Units
Rated power	$cap_{nom,P}$	10000	kW
Discharge duration	DD	4	hours
Energy capacity	$cap_{nom,E}$	40000	kWh
Annual cycles	f	100	-
Electricity Price	C_{elec}	0.05	\$/kWh

3.6.3 Determining the minimum sample size

The procedure followed to determine the minimum sample size is described below, where the change in standard deviation between sample size is calculated using $\Delta\sigma = \sigma_n - \sigma_{n-1}$. While each sample uses a random subset of input variables, the significance of this procedure is to determine how the variance of each sample set changes compared to the previous (smaller) sample set. As mentioned in Section 3.5.2, when $\Delta\sigma \rightarrow 0$, the distribution of the model's output will converge to its theoretical distribution.

- The variables are selected from a normal distribution at a random probability.
- The levelised cost is calculated using Equation 3.3.1.
- The variance is calculated of n samples and compared to the previous run.
- The process is repeated until $\Delta\sigma \rightarrow 0$ (within 5 % margin).

A typical plot of simulation convergence can be seen in Figure 3.6.1, where it converges to within a 5 % error margin at a sample size of 500. This demonstrates that, for the LCOS model used in this study, 500 iterations are sufficient to represent its theoretical distribution. This finding is consistent with Schmidt *et al.* (2019) who also used 500 samples. All results represented in this study use this number as a minimum sample size, unless otherwise stated.

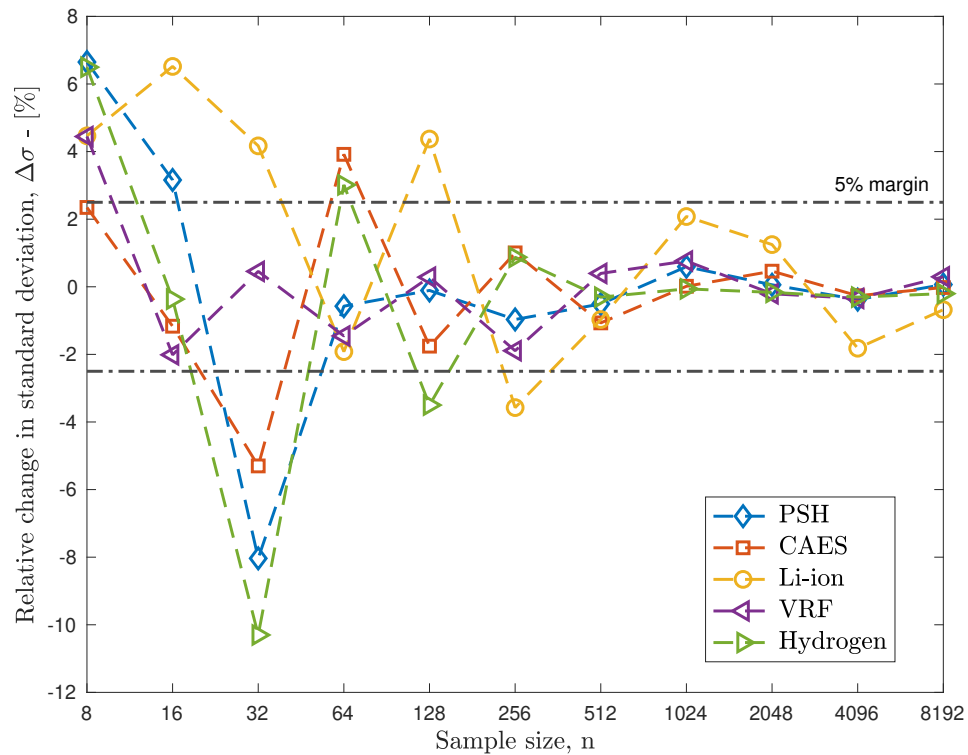


Figure 3.6.1: Sample plot of relative change in standard deviation of LCOS with growing sample size n

3.7 Verification of the model

The LCOS model used in this study was developed using the equations set out in Section 3.3, following the method of Schmidt *et al.* (2019) who also created an online LCOS tool (Schmidt, 2019). The LCOS cost components (replacement, investment, charging, etc.) for each technology was gathered from the tool (Schmidt, 2019) and compared, using the same input parameters, to the results of the model used in this study. A 5 % margin of error between the two was allowed. By varying and randomising the inputs, and comparing the results, the robustness of the model was ensured.

Since its publication in 2019, Schmidt *et al.* (2019) made some improvements to the online tool and these were confirmed and incorporated into the model used in this study, through electronic mail communications with the author (Schmidt, 2020).

Chapter 4

Monte Carlo Simulation Results

4.1 Interpretation of the results

Following the methodology described in Section 3.3, 500 data points were collected for each technology and application. This chapter presents the findings of the Monte Carlo simulation and uses several graphical tools to do so. This section presents samples of some of these graphical tools and describes how to interpret them.

Although it was previously demonstrated that the levelised cost of storage (LCOS) model converges at $n = 500$, the differences between each technology and storage application are better visually represented using smaller samples of $n = 200$. This is demonstrated in Figure 4.1.1 where each vertical bar represents one simulated LCOS value as a stacked bar graph of five major cost components. These components being: investment, replacement, operation and maintenance, charging and end-of-life costs. The composition of the average LCOS is shown to the right of the graph. The plot also indicates the 90th and 10th percentile of the results, highlighting the statistical spread of the results. In this sample case, it is apparent that the levelised cost most greatly affected by the investment cost and is less sensitive to variations of charging and operation costs.

Contour plots are also used to communicate the effect of two variables on the LCOS. Figure 4.1.2 is an example of this, where the black curves between each shaded area indicate a level on the three-dimensional surface, where the z-axis represents the LCOS. As there are only 8760 hours in a year, the graph as been trimmed accordingly.

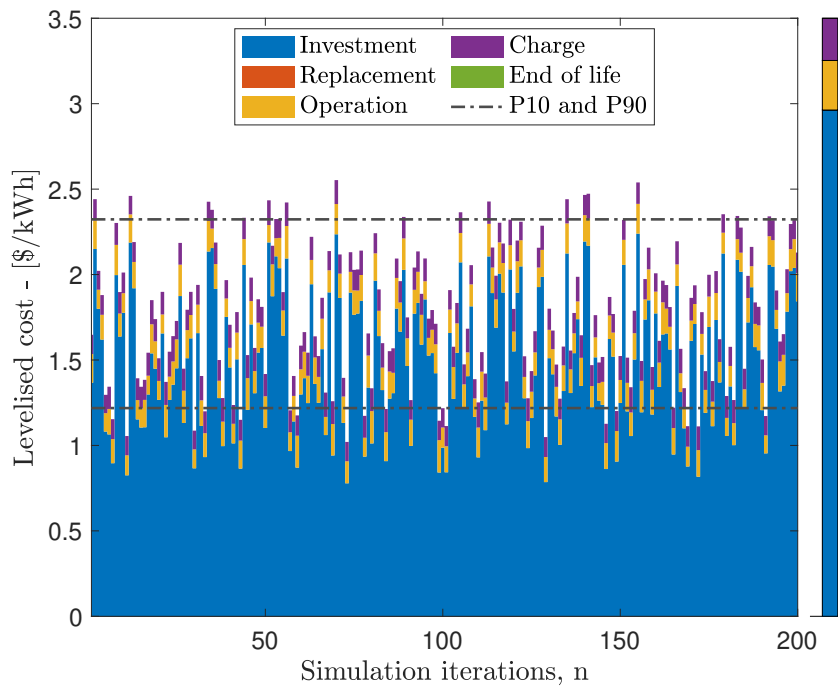


Figure 4.1.1: Simulated cost components of LCOS (n=200)

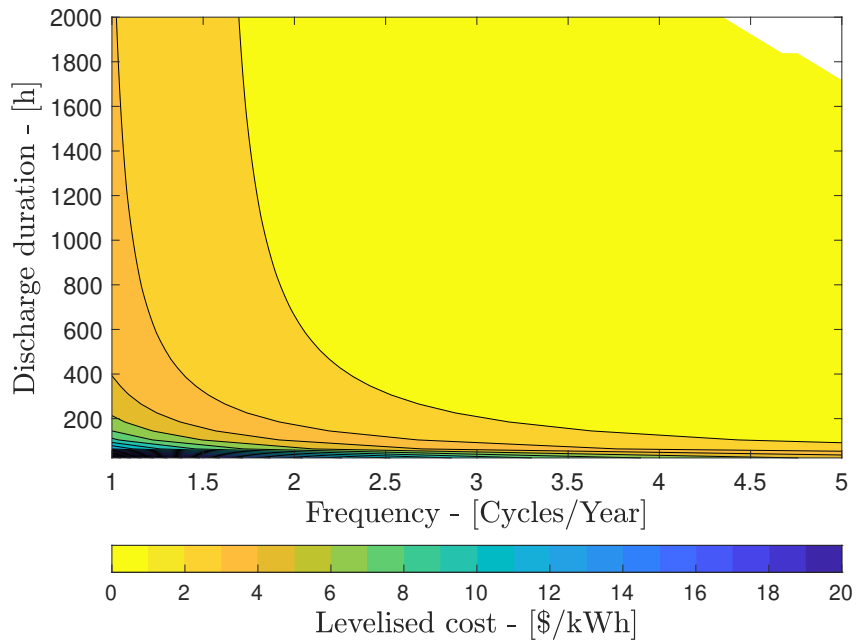


Figure 4.1.2: Effect of frequency and discharge duration on LCOS

4.2 Comparison of energy storage applications

The simulated LCOS for each of the five technologies are presented and discussed in Sections 4.2.1 to 4.2.5 with each section discussing both energy storage applications considered in this study (peaker replacement and long-term seasonal energy storage).

Across the considered technologies and storage applications, the replacement and end-of-life costs were found to have an insignificantly small influence on the LCOS, and have been omitted from the resulting figures presented. It should be noted that these costs are still important to consider with other energy storage system (ESS) applications. For example, in the voltage support application, the replacement cost contribute to 14-17 % of the LCOS cost.

Sections 4.2.6 and 4.2.7 present a comparison of each of the technologies for each energy storage application. The results are presented with box plots (also known as box-and-whisker plots), which are a statistical summary of a data set, using five values: minimum, maximum, first quartile (Q_1), median and third quartile (Q_3), as demonstrated in Figure 4.2.1. Any values in the dataset that lie outside 1.5 times the interquartile range from Q_1 or Q_3 , is classified as an outlier (Chambers, 2017).

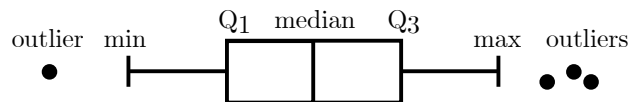


Figure 4.2.1: Example of a box plot

A summary of the results is presented in Section 4.2.8. From the individual simulation runs presented in each figure, the variance in each technology's cost can be seen, as well as the relative contribution of each component to the levelised cost.

4.2.1 Pumped storage hydroelectricity

From Figure 4.2.2, it is apparent that the energy storage application has an affect on the LCOS of pumped storage hydroelectricity (PSH). The mean LCOS of PSH for peaker replacement was 0.51 \$/kWh, compared to 1.69 \$/kWh for seasonal storage. The variance also differs between applications, with 46 % and 54 % for peaker replacement and seasonal storage applications, respectively. In the case of

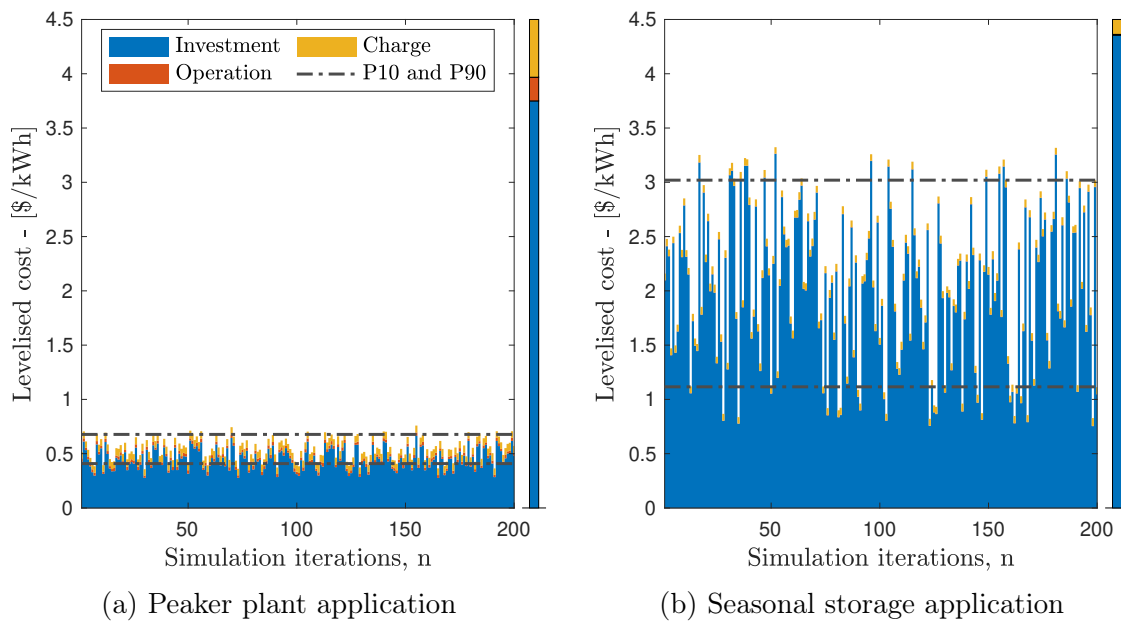


Figure 4.2.2: Levelised cost of pumped storage hydroelectricity

each application, the variance is high and is most greatly effected by the investment cost of the system. This is to be expected from the high power and energy specific investment costs of PSH, relative to other technologies, as shown in Appendix B. The change in composition of the average LCOS between the two energy storage applications indicates that its sensitivity to investment costs is amplified by increases in the system's power and energy capacity.

4.2.2 Compressed air energy storage

The mean LCOS of CAES is 0.42 \$/kWh and 0.85 \$/kWh for peaker replacement and seasonal storage, respectively. Figure 4.2.3 shows that the cost to charge has a larger effect on the LCOS of CAES for both applications, compared to PSH. The variance of the LCOS results are also lower, at 40 % and 45 % for the two storage applications. From Equation 3.3.4, the cost to charge the energy storage system is inversely proportional to the system's round-trip efficiency; which for CAES is nearly half that of PSH at 44 %. In combination with lower investment costs, this might explain why the effect of the charging cost is significantly higher compared to PSH.

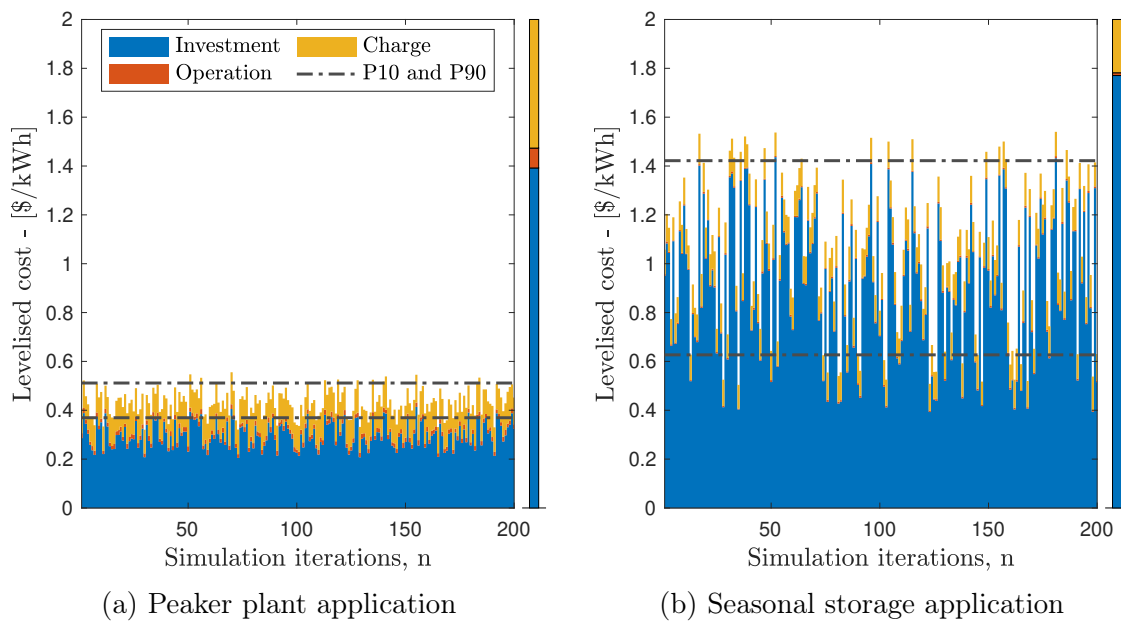


Figure 4.2.3: Levelised cost of compressed air energy storage

4.2.3 Lithium-ion energy storage

Figure 4.2.4 illustrates the LCOS simulation results for lithium-ion battery energy storage. At 1.17 \$/kWh and 13.9 \$/kWh, it has the highest LCOS of the technologies considered in this study. The mean LCOS composition in Figure 4.2.4 illustrates the cost is effectively only driven by the investment cost. While lithium-ion does not have the highest energy or power specific replacement costs, it does have the shortest lifetime compared to the other technologies, meaning that it would need to be replaced more frequently than other technologies. For reference, the life time of PSH and CAES are 33250 and 16250 cycles, respectively, compared to 3250 cycles for lithium-ion (Appendix B). The variance of the results were relatively low at 24 % and 23 % for each of the applications.

4.2.4 Vanadium redox flow battery energy storage

The results for vanadium redox flow battery (VRFB) energy storage are illustrated in Figure 4.2.5 and follow a similar trend to that of lithium-ion. While the investment costs are similar between the two technologies, the shelf life of VRFB is nearly three times longer, which contributes to a slightly lower mean LCOS (1.02 \$/kWh and 13.1 \$/kWh, for peaker replacement and seasonal storage, respectively). The standard deviation of the results for VRFB were the lowest at 19 % and 16 %.

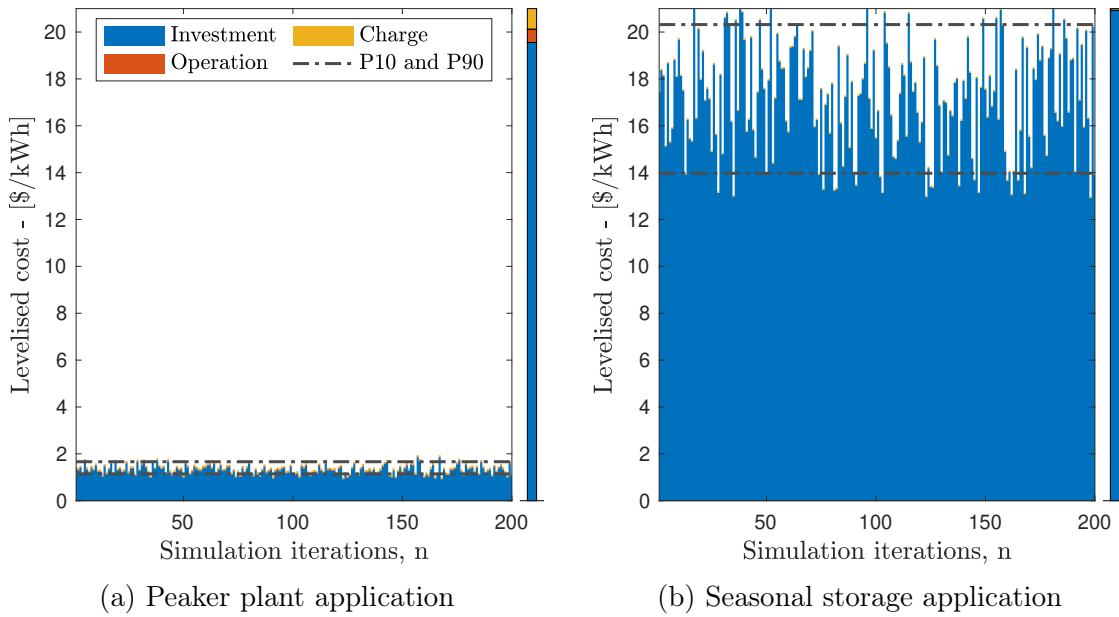


Figure 4.2.4: Levelised cost of lithium-ion energy storage

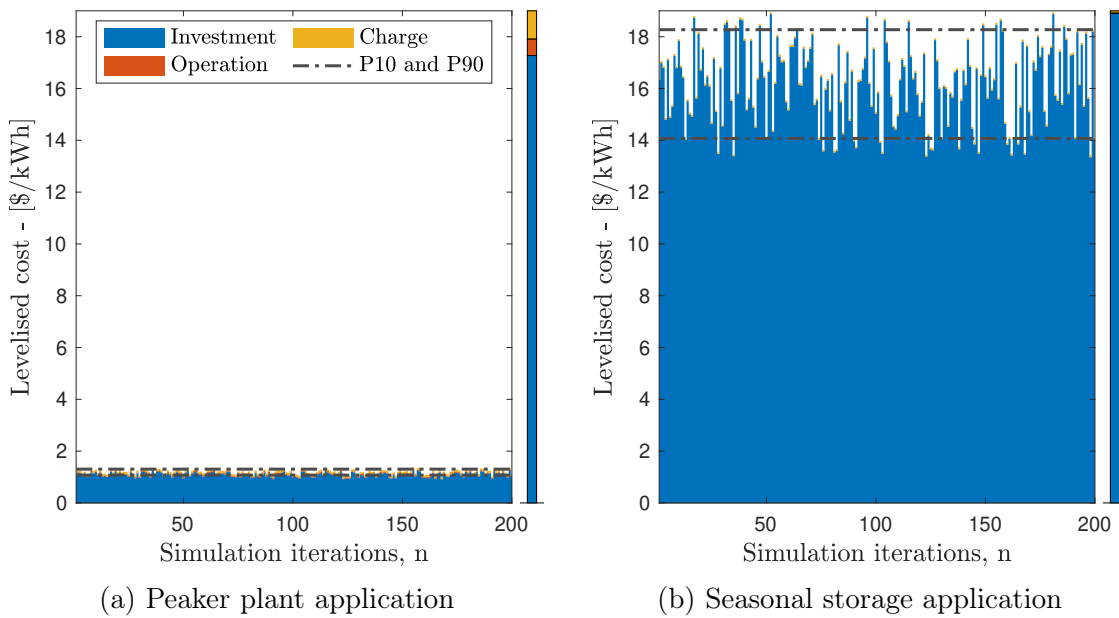


Figure 4.2.5: Levelised cost of vanadium redox flow battery energy storage

4.2.5 Hydrogen energy storage

The results for hydrogen energy storage are presented in 4.2.6. Hydrogen is the only technology that has a lower LCOS for the seasonal energy storage than for peaker replacement (0.78 \$/kWh compared to 1.71 \$/kWh). Hydrogen energy storage has the highest power-specific investment cost, nearly four times greater than that of PSH.

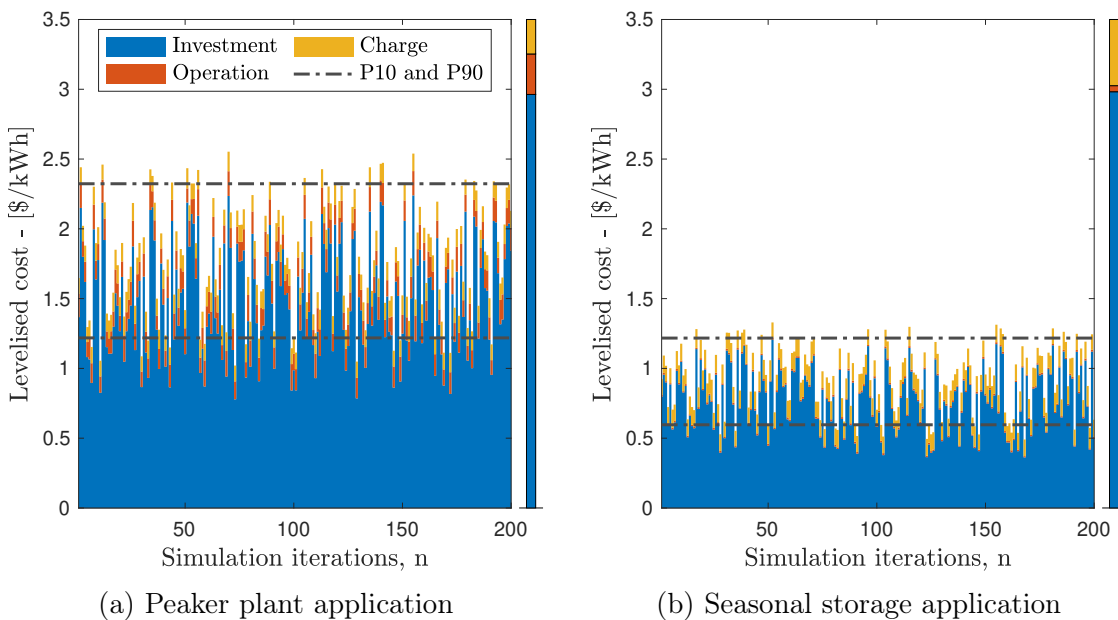


Figure 4.2.6: Levelised cost of hydrogen energy storage

4.2.6 Peaker replacement: comparison of technologies

Here we compare each technology in the application of peaker replacement. Figure 4.2.7 shows a box plot of the LCOS of each technology in the peaker replacement application. The LCOS distribution of PSH, CAES and VRFB are the smallest and hydrogen is the largest.

Although there are noticeably more outliers for Li-ion, it represents a small fraction of the sample size of 500. This difference can be explained by the comparatively high energy-to-power investment cost ratio of Li-ion (1.82), short cycle and shelf life (3250 cycles and 13 years, respectively) and large standard deviation of the latter two variables (38 % in each case). For reference, the energy-to-power investment cost ratio of PSH, CAES, VRFB and hydrogen are 0.07, 0.04, 0.92 and

0.06, respectively. This ratio, as well as the cycle and shelf life, is significant in applications with high cycle frequencies, as is the case with peaker replacement. While the mean of the VRFB input parameters (as explained in Section 3.4) are similar to Li-ion, the standard deviation is significantly smaller, resulting in fewer outliers.

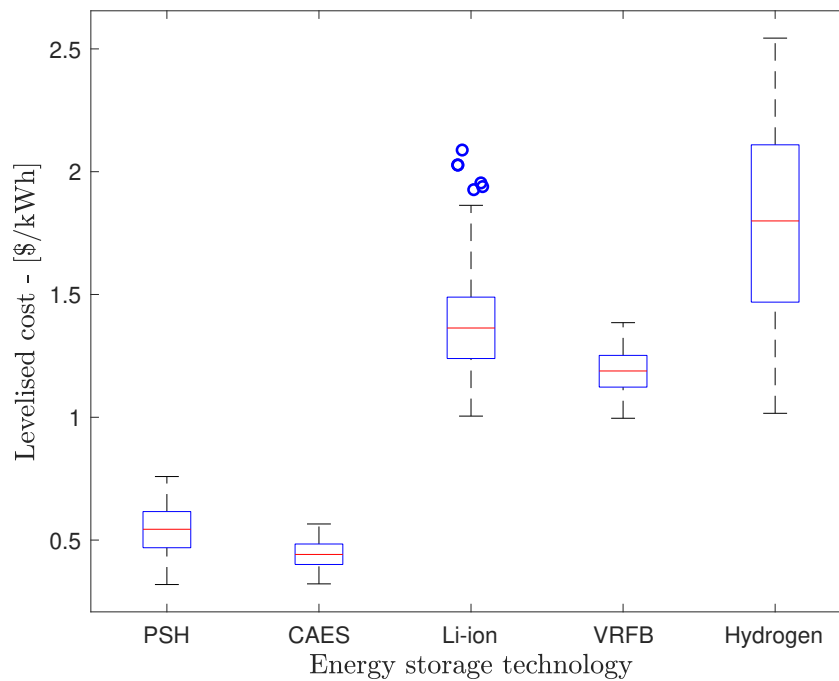


Figure 4.2.7: Comparison of technologies: simulated LCOS (peaker replacement)

4.2.7 Seasonal storage: comparison of technologies

Here we compare each technology in the application of seasonal energy storage. Figure 4.2.8 shows a box plot for the LCOS of each technology in the seasonal energy storage application. In contrast with peaker replacement, hydrogen storage offers the lowest LCOS (and smallest variation) in this application, followed by CAES and PSH. The LCOS of Li-ion and VRFB are the least cost-competitive and the results are distributed relatively widely.

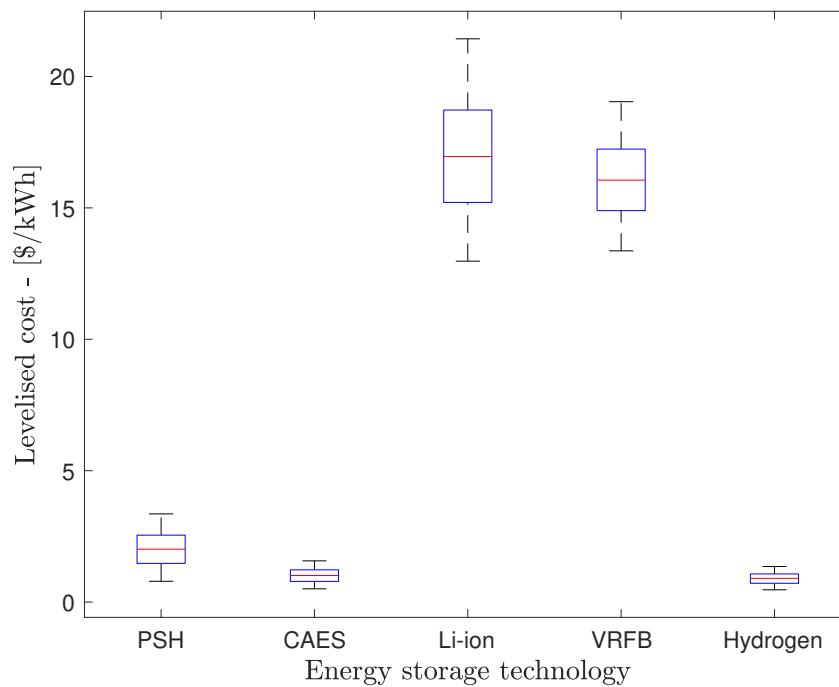


Figure 4.2.8: Comparison of technologies: simulated LCOS (seasonal storage)

4.2.8 Summary of results based on energy storage application

The findings presented above has been summarised in Table 4.2.1 below. In almost every case, the greatest proportion of the LCOS is the investment cost, followed by the replacement and operation costs. In some technologies, like CAES, the replacement cost has a greater impact, while, in others like hydrogen storage, operational costs are more significant. In the seasonal storage application, the contribution of other components beside investment are almost insignificantly small, with hydrogen storage and CAES being the exceptions. In the peaker replacement application, CAES has the lowest LCOS, followed by PSH and then VRFB, Li-ion and hydrogen. In terms of statistical deviation, hydrogen storage had the greatest variability, followed by PSH and CAES. A similar pattern is repeated in the seasonal storage application, with the exception that hydrogen has the lowest cost.

Table 4.2.1: Simulation results for peaker replacement and seasonal storage

Application	Mean LCOS (standard deviation) - [\$/kWh]				
	PSH	CAES	Li-ion	VRFB	Hydrogen
Peaker replacement	0.51 (45.9 %)	0.42 (40.2 %)	1.17 (24.3 %)	1.02 (18.7 %)	1.71 (56.40 %)
Seasonal storage	1.69 (53.8 %)	0.85 (44.87 %)	13.89 (23.26 %)	13.13 (16.27 %)	0.78 (39.05 %)

4.3 Effect of discount rate

The discount rate used in this study was 8 % as discussed in Section 3.1. Figures 4.3.1 and 4.3.2 illustrate the sensitivity of the LCOS for each storage technology and application to variance in the discount rate. The range of discount rate values used for this comparison were 2.5–13.5 %, which includes the discount rates used in other studies of 11 and 12 % (Pan, 2020). The data shows that some technologies are more sensitive to variance in the discount cost compared to others. Sensitivity is represented by the steepness of the gradient in Figures 4.3.1 and 4.3.2. The sensitivity does, however, not hold true for all storage applications, indicating that it is dependent on the system’s capacity, storage duration and annual cycle frequency. In the peaker replacement application, hydrogen energy storage has both the highest LCOS and is the most sensitive to variance in the discount rate, while with PSH and CAES, the opposite is true. The two electrochemical energy storage technologies fit in the middle in terms of LCOS and sensitivity.

The data for seasonal energy storage shows that VRFB and Li-ion have the greatest sensitivity to variance in discount rate and also have the highest LCOS. Hydrogen and CAES have the lowest sensitivity and LCOS.

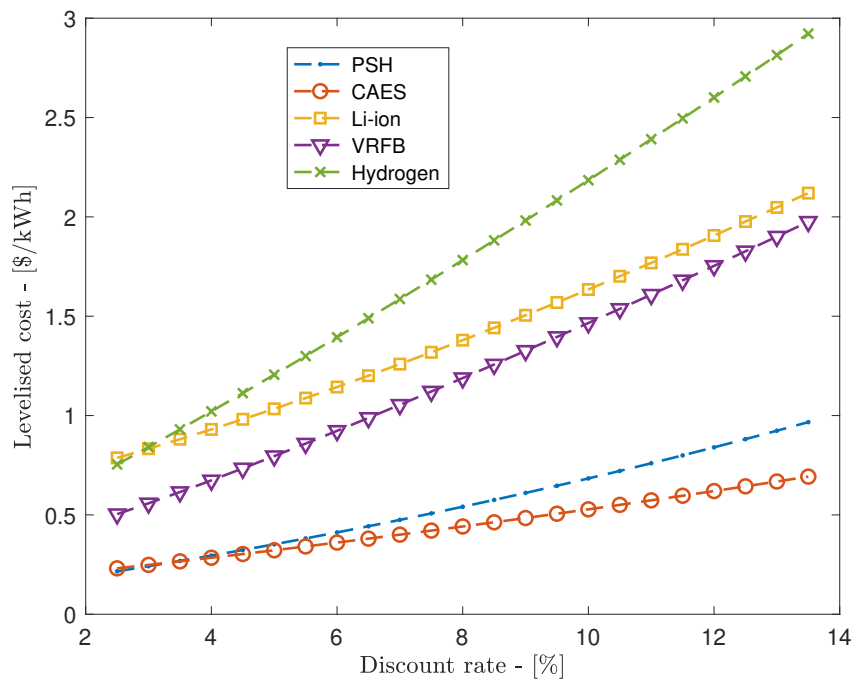


Figure 4.3.1: Effect of variation in discount rate on LCOS (peaker replacement)

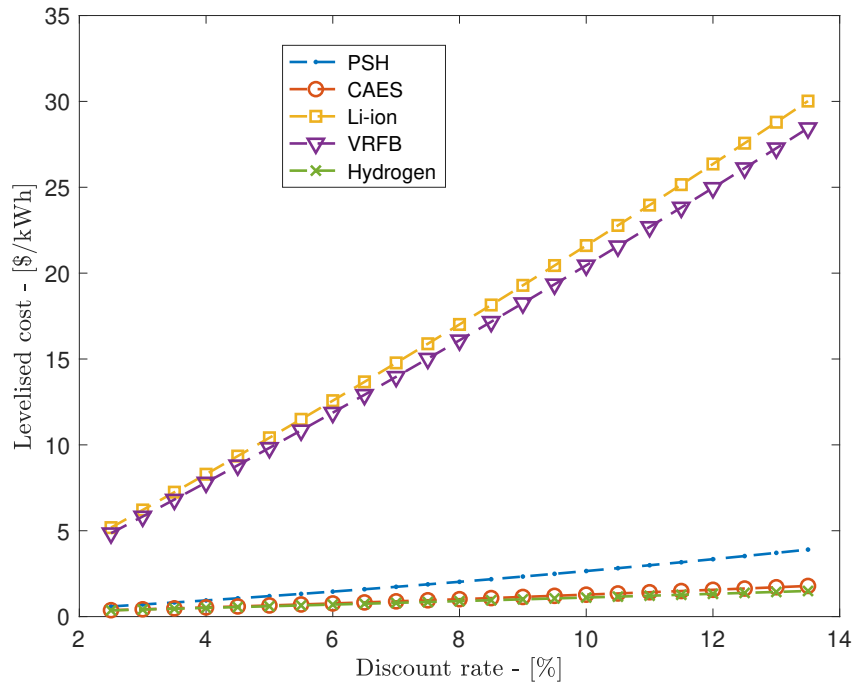


Figure 4.3.2: Effect of variation in discount rate on LCOS (seasonal storage)

4.4 Effect of frequency and discharge duration

As suggested by the literature, the levelised cost of a storage system is strongly dependent on the utilisation rate or the amount of annual full load hours (FLH). With all other parameters fixed, a higher FLH, results in a lower levelised cost. This can be achieved by increasing the energy capacity of the storage system, increasing the cycle frequency, or both. It is therefore valuable to understand how the annual operation of a storage system affects the LCOS. This section presents the results of LCOS calculated across a range of cycle frequencies and discharge duration for each of the preselected energy storage applications and represented by a contour plot. The results for each of the five energy storage technologies are discussed individually. As before, the operating parameters of the peaker replacement application are: discharge duration of 2–6 h and cycle frequencies of 5–100 per year. For long-term seasonal storage these parameters are: discharge duration of 24–2000 h and cycle frequencies of 1–5 per year.

4.4.1 Pumped storage hydroelectricity

The effect of frequency and discharge duration on the levelised cost of PSH is presented in Figure 4.4.1.

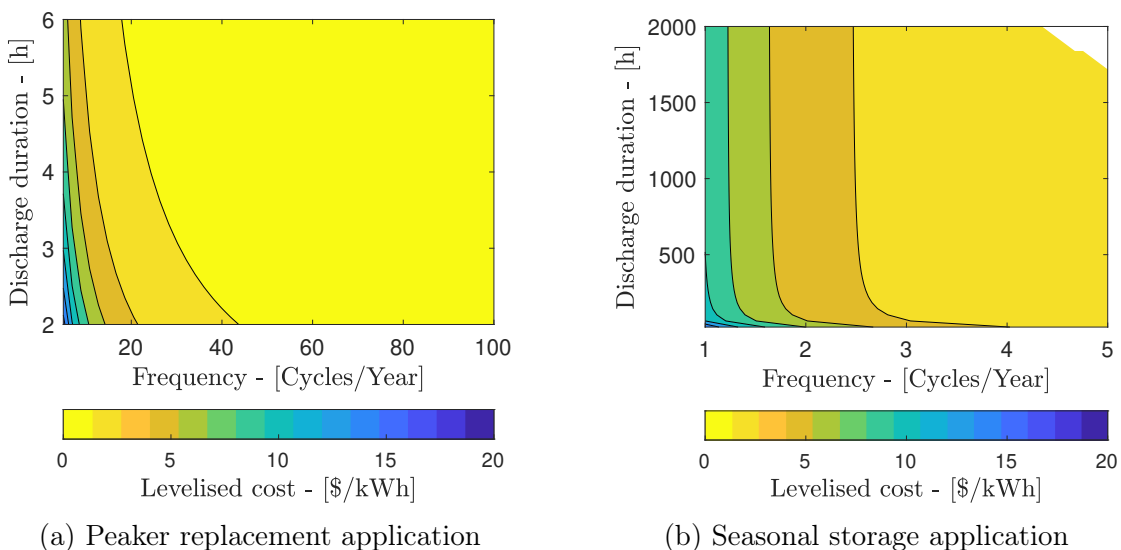


Figure 4.4.1: LCOS contour plot for pumped storage hydroelectricity

From this it can be seen that, in the application of peaker replacement, the levelised cost of pumped hydro storage energy storage is sensitive to the annual cycle fre-

quency. For cycles below 20, the cost increases steeply and after 40, the change in cost becomes more gradual. For a given number of cycles per year, the LCOS is not as sensitive to the change in discharge duration. This might indicate that relative investment of increasing the energy storage capacity is significantly less than the increase in revenue generation associated with an increase in cycle frequency.

In the application of seasonal storage, it could be said that the LCOS is even more sensitive to the cycle frequency, with a more gradual change in cost in the range of 4–5 cycles per year. At discharge durations greater than 500, the effect is more pronounced, with the contour lines approaching vertical asymptotes, illustrating almost no change in levelised cost with increasing discharge durations.

4.4.2 Compressed air energy storage

The effect of frequency and discharge duration on the levelised cost of CAES is presented in Figure 4.4.2. The results appear similar to that of PSH, with a key difference being a lower overall LCOS for both applications. At low cycle frequencies, CAES is more cost-competitive than PSH. This is a promising result as CAES is a relatively new technology, compared to PSH, and may provide a greater reduction in cost with more development.

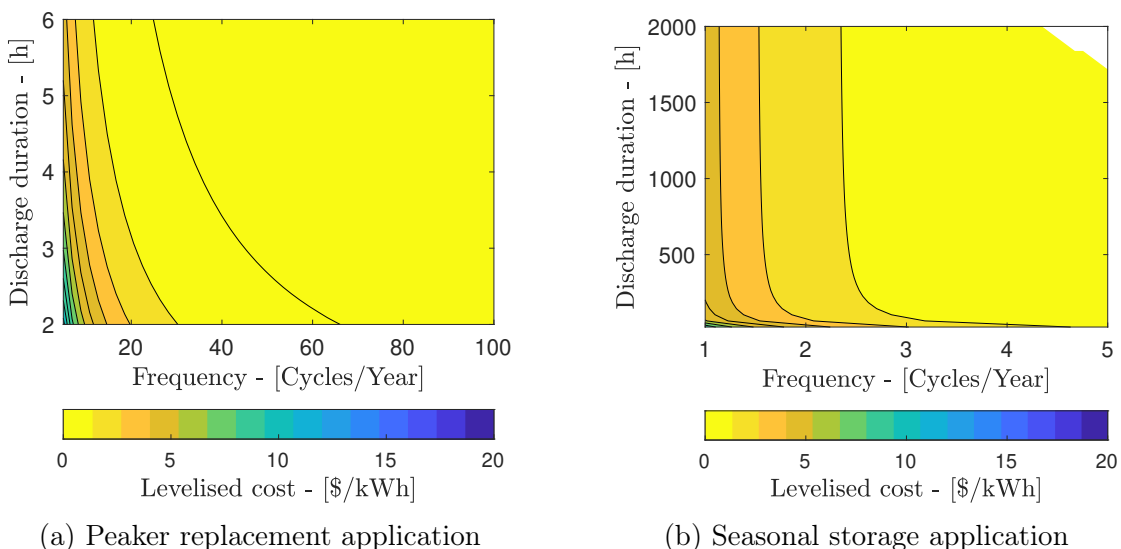


Figure 4.4.2: LCOS contour plot for compressed air energy storage

4.4.3 Lithium-ion battery energy storage

The effect of frequency and discharge duration on the levelised cost of lithium-ion batteries is presented in Figure 4.4.3. Compared to PSH and CAES, the LCOS of lithium-ion batteries are significantly higher and more sensitive to cycle frequency. This result is more prominent in the seasonal storage application, as one might expect, since the specific cost of lithium-ion batteries is relatively high compared to technologies like PSH and CAES. The contour lines between regions are much closer together and the lines appear more vertical, indicating a stronger sensitivity to cycle frequency than discharge duration.

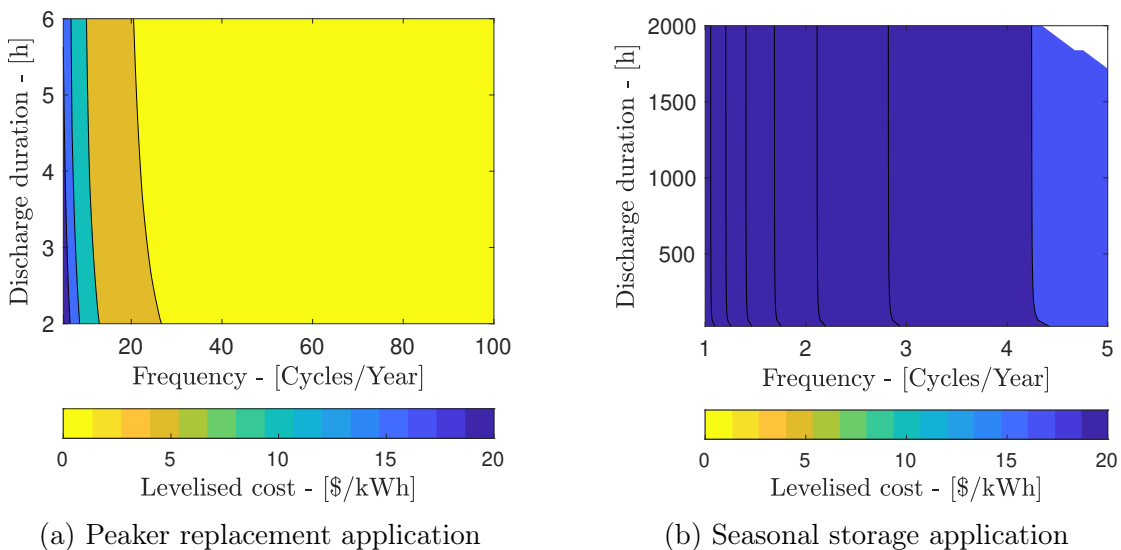


Figure 4.4.3: LCOS contour plot for lithium-ion batteries

4.4.4 Vanadium redox flow batteries

The effect of frequency and discharge duration on the LCOS of VRFB is presented in Figure 4.4.4. These results are relatively similar to that of lithium-ion batteries. Both technologies have high LCOS compared to the other technologies in the two storage applications. Similarly, the LCOS of both technologies exhibit a high sensitivity toward cycle frequency. This could be explained by high cycle frequency combined with relatively short shelf life, resulting in more frequent replacements at higher replacement costs.

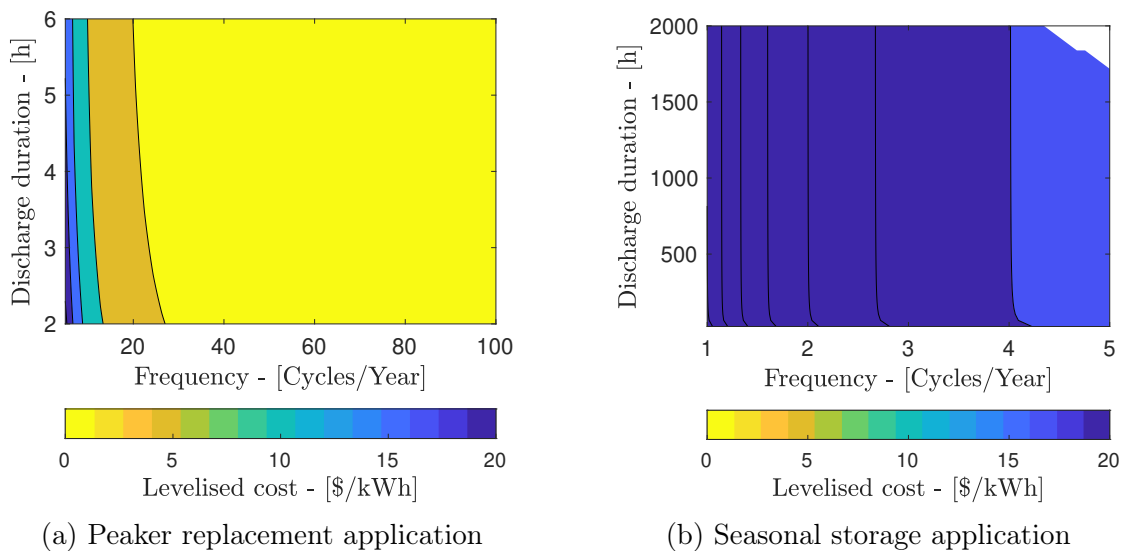


Figure 4.4.4: LCOS contour plot for vanadium redox flow batteries

4.4.5 Hydrogen energy storage

The effect of frequency and discharge duration on the levelised cost of hydrogen energy storage is presented in Figure 4.4.5. Compared to the other technologies considered in this study, the levelised cost of hydrogen energy storage appears to be the least sensitive to cycle frequency, especially in the seasonal energy storage application. Hydrogen also has the lowest LCOS of the chemical storage technologies considered for seasonal storage. This may indicate that it is a good candidate for long-term seasonal energy storage.

4.4.6 Practical limitation

While it is insightful to investigate combined cost effects of discharge duration and frequency of various ESSs, it should be kept in mind that there may exist significant limitations with regard to the recharge capacity of the wider energy system the ESS forms part of. For example, the significantly sized South African PSH systems summarized in Table 2.4.1, while excellently suited to serve morning and evening national grid peak demands or supply failures, often cannot be recharged in the time between demand peaks due to a lack of energy capacity in the system.

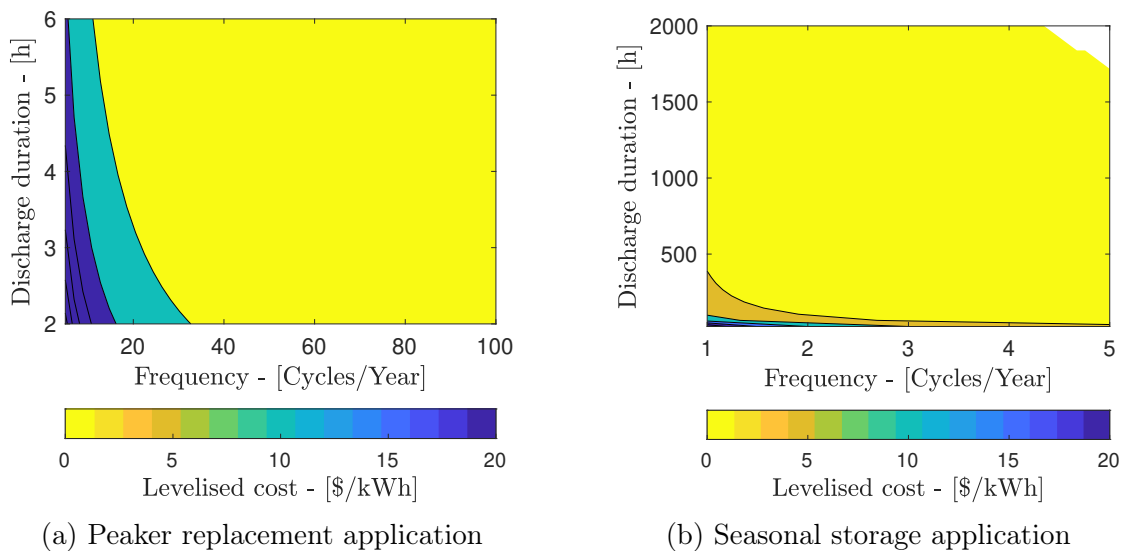


Figure 4.4.5: LCOS contour plot for hydrogen

4.5 Comparison with CSP tariffs

The overall consideration of this study was to examine RE storage technologies, keeping in mind the special nature of CSP. The energy storage technologies considered in the study thus far has only been electrical energy storage systems (EESSs) which does not readily allow for comparison with thermal energy storage (TES) systems, like those used by CSP plants. Due to the near seamless integration of TES systems with modern CSP plants, the performance, and by extension the LCOE, is determined by the operating strategy of the CSP plant and the TES system is very specifically designed around this point. This means that the performance of a TES system would need to be isolated from that of the plant, and the corresponding LCOE for the plant and the TES system would need to be determined. The challenge arises out of the fact that the heat-to-electricity conversion components of the CSP plant are advantageously shared between the use of the heat harvested from the sun directly and the heat from the energy store.

This is beyond the scope of this study, and another method is proposed to compare the cost competitiveness of CSP+TES to EESS. The following section describes the methodology used, the assumptions made, and presents the findings.

4.5.1 Comparison methodology

With greater adoption of energy storage systems, both in scale and number, the question can be asked if EESSs are the most cost-effective solutions simply because they might integrate well with renewable generation technologies like wind and PV plants? Or may another renewable generation source like CSP, with included energy storage in the form of TES, be able to provide a competitive solution, if only in certain applications? As mentioned in Chapter 1, the potential advantage that CSP has is its low-cost thermal energy storage and electricity generating inertia compared to other renewable electricity generating technologies. To investigate the potential value proposition of CSP, the operating parameters of several commercial plants were compared to hypothetical EESSs operating at the same specifications. The following assumptions were made when comparing the energy generation and storage potential of concentrating solar power plants (with included thermal energy storage) and EESSs charged with sources like solar photovoltaic and wind power plants.

The costs of generation and storage components in CSP plants are readily available. However, this study is interested in the final cost of the electricity generated by the system, which is this is a function of each plant's operating strategy and the corresponding PPA. If a plant has been designed to generate electricity during the evening peak, it might have more storage and would use the thermal energy gathered during the day to charge the thermal energy storage system.

The remuneration data for the last three (commissioned between 2018–2019) operational CSP plants in South Africa have been used. These plants include: Ilanga I, Xina Solar One and Kathu Solar Park, all three of which use parabolic trough collector (PTC) technology and 2-tank indirect, molten salt thermal energy storage (TES) systems. The remuneration rate as well as each plant's power capacity and thermal energy storage duration is listed in Table 4.5.1.

Table 4.5.1: South African CSP plants considered (Lilliestam *et al.*, 2020)

Power station	Capacity [MW]	Storage duration [h]	Remuneration [\$/kWh]
Ilanga I	100	4.5	0.179
Xina Solar One	100	5.5	0.168
Kathu Solar Park	100	5	0.157

All data was sourced from the CSP GURU database (Lilliestam *et al.*, 2020). The number of annual cycles was assumed to be 365 (one cycle per day) and the price of electricity used to charge the electrical energy systems was assumed to be 0.033 \$/kWh. This cost was calculated as the average tariff for the 25 onshore wind and solar photovoltaic plants selected as preferred bidders in round 5 of the renewable energy independent power producer procurement programme (REIPPPP). These costs were used because they represent the most relevant tariffs from these renewable generating costs in South Africa.

The plant specifications for each CSP plant listed in Table 4.5.1 was used as an input to calculate a mean LCOS value using the techno-economic model for each of the ESS technologies considered in this study. For example, with Kathu Solar Park (100 MW capacity, 5 h of storage and remuneration of 0.179 \$/kWh) a mean LCOS value of 0.160 \$/kWh was calculated for a 100 MW PSH plant with 5 h of storage.

4.5.2 Direct comparison results

As described by the methodology above, the LCOS for each ESS technology was calculated and compared to CSP plants in South Africa. The results are shown in Table 4.5.2.

Table 4.5.2: CSP tariff comparison with ESSs charged with other VRE

Power station	Mean LCOS - [\$/kWh]				
	PSH	CAES	Li-ion	VRFB	Hydrogen
Ilanga					
0.179	0.170	0.179	0.748	0.432	0.518
Xina Solar One					
0.168	0.152	0.164	0.724	0.416	0.441
Kathu Solar Park					
0.157	0.160	0.171	0.735	0.423	0.476

This presents three interesting observations. Firstly, only PSH and CAES present cost-competitive LCOS figures compared to CSP at discharge durations between 4 and 5 hours. A similar finding was presented by Lovegrove *et al.* (2018) and

Schöniger *et al.* (2021) who found that CSP presents a cost-competitive energy storage solution for durations of 4 hours and longer. More specifically, Schöniger *et al.* (2021) found that a tipping point existed in the cost-competitiveness of PV and battery energy storage systems at 2–3 hours (at 2020 costs) and at 4–10 hours (based on future cost developments). At shorter durations, battery technologies like lithium-ion were the more cost-effective solution.

The second observation that can be made is that lithium-ion has the highest LCOS, followed by hydrogen energy storage and VRFB. From the results presented in Section 4.4, it was determined that these three technologies are the least cost-competitive for storage durations of 4–6 h.

Chapter 5

Discussion of Findings and Limitations

This section presents a summary of the findings in this study and explores its limitations.

5.1 Findings of this study

As discussed in Chapter 1, keeping the special case of CSP in mind, the primary goal of this study was to conduct a literature survey of trends in energy storage. From this fundamental understanding, a techno-economic evaluation was conducted, evaluating 5 key electrical energy storage systems (EESSs). These five technologies are pumped storage hydroelectricity (PSH), compressed air energy storage (CAES), lithium-ion (Li-ion) battery storage, vanadium redox flow batteries (VRFB) and hydrogen energy storage. In the context of this study, the two most relevant energy storage applications were selected in Section 2.5. Following the practises outlined in the literature (Chapter 2), a probabilistic model was developed, verified (Section 3.7) and used to simulate the performance of the selected technologies in the peaker replacement and seasonal storage application.

5.1.1 Energy storage technology recommendations

The levelised cost of storage (LCOS) of 5 EESSs was modelled using a probabilistic model and used Monte Carlo simulations to determine the least-cost option for specific energy storage needs. The Monte Carlo simulations present two areas of investigation. The first is a view into the LCOS model used in this study; through the sensitivity analysis and the contour plots, we are able to understand which variables have the greatest effect on the model output (LCOS). This understand-

ing can help optimise final system specifications, refine the model and optimise for desired operating conditions.

For each of the technologies, investment cost had the greatest influence, while that of replacement and operational costs were far less. From the initial sensitivity analysis, it was shown that the LCOS was sensitive to variation in round-trip efficiency and power specific cost. However, the cost data for each technology used had much smaller variation in this parameter compared to investment cost, resulting in an insignificant contribution in the simulated data.

The second area of investigation was finding the most cost-effective solution for each of the storage applications. In the application of peaker replacement, CAES was the most cost-effective technology, followed by PSH. Hydrogen energy storage was the most cost-effective solution in the seasonal storage application, followed by CAES. Overall, CAES ranks amongst the best performing technologies in terms of cost, and it is worth a closer look for countries with compatible geological features. This result aligns with findings presented by Luke (1996), who found that, compared to PSH, CAES is a cost-competitive energy storage option in South Africa with the system being limited by available storage volume in the form of mines suitable for conversion.

Since 2017, there is great enthusiasm for hydrogen-based economies. As previously mentioned, this excitement comes from the ability to produce hydrogen, powered by renewable energy sources, transport it safely using existing infrastructure and store it in a relatively stable form for later consumption. South Africa is in a prime position to serve as a hydrogen production supplier for other countries, like Japan, who are looking to import the gas as a green energy source. A study from 2022 identified the following advantages for South Africa to achieve economies-of-scale based globally competitively priced hydrogen production: extensive resources in platinum, land, wind and solar, mining, industry, existing international trading partners and geographic location (Arnoldi, 2022). Based on these findings, a recommendation for South Africa's energy sector could be to investigate CAES and hydrogen as longer-term stores of renewable energy generated by sources like solar PV and wind.

5.1.2 A case for CSP in SA's integrated resource plan

As mentioned in this study, CSP plants have a few inherent benefits that are frequently overlooked when a direct comparison is done with PV or wind plants. These benefits include low-cost thermal energy storage and electricity generating inertia compared to other renewable electricity generating technologies. For example, as

part of the power purchase agreement (PPA) between Eskom and Acwa Power, the principle shareholding contractor for the 100 MW Redstone CSP plant (under construction at the time of writing) featuring 12 hour thermal storage, is able to offer short notice ancillary power grid stabilisation services (Buhla, 2021).

While existing CSP is unable to match the levelised cost of electricity (LCOE) generated by solar PV or wind, it was demonstrated by other authors that CSP plays a role in a least cost mix between variable and dispatchable renewable energy sources (Lovegrove *et al.*, 2018; Schöniger *et al.*, 2021). Lilliestam and Pitz-Paal (2018) note that the Aurora CSP plant in Australia has a uniquely low PPA bid of 0.075 \$/kWh and speculate that this is due to its pricing model, which allows for a small portion of the generating capacity to be sold outside the PPA during peak hours when the sun sets and production from the PV fleet slows down. A proposal for CSP in South Africa could include a provision like this, allowing for a small portion of a plant's capacity to be sold during peak evening hours to the highest bidder.

While Section 4.5 demonstrated that EESS technologies like PSH and CAES were able to compete with South Africa's existing CSP plants, these figures made several conservative assumptions in favour of EESSs and did not take state-of-the-art CSP plant costing figures into account. New CSP plants could take advantage of unique PPA similar to those used with Aurora. Interestingly, if the same comparison is conducted with Aurora (150 MW, 8 h storage), neither of the EESSs can compete. PSH and CAES, still the least-cost EESS options, are nearly double that of CSP at 0.127 and 0.143 \$/kWh, respectively.

The 2019 version of the integrated resource plan (IRP) (DoE, 2019) excluded further CSP from bidding rounds, based on its cost non-competitiveness (\$/kWh) with other, non-dispatchable RE (wind and PV). This context all changed when the risk mitigation independent power producer procurement program (RMIPPPP) (DRME, 2020) called for guaranteed dispatchable power delivery in the hours 05h00 to 21h30, technology-agnostic but excluding CSP because it explicitly only permitted technology stipulated in the IRP 2019. This was clearly an unfortunate and misguided policy constraint, as only under such bidding conditions, i.e. which requires storage, the true tariff comparison of CSP, PV and wind power emerges. The RMIPPPP was correctly motivated, as these are the constraint hours troubling the SA grid. IPPs, particular renewable based, as private companies, perform well and deliver. For instance, more RMIPPPP rounds should follow, but CSP must be allowed to bid as well to show its mettle in advancing technology. It is therefore important that the IRP 2019 revision, already announced by Mantashe (2022), takes this into consideration.

5.2 Limitations of this study

A survey of the literature and a review of similar studies, has highlighted several limitations of this study and the methodologies used. This section briefly discusses some of these limitations and recommends remedies where possible.

5.2.1 The LCOS method

While levelised cost is a widely accepted metric for comparing different energy generation and storage technologies, one major limitation is that it does not account for fluctuations in demand and supply; meaning that the value of dispatchability offered by technologies like CSP is undervalued. Joskow (2011) argues that electricity is a temporally heterogeneous good; its value is dependent on when it is generated (and the corresponding demand). Furthermore, LCOS reduces the complexity of comparison between technologies since it narrows many inputs down to a single number, which allows for quick decision-making. This narrow viewpoint also serves as a opportunity for misinterpretation (Kost *et al.*, 2018).

The methodology used in this study considers a standard discount rate across all technologies. While clearly interest rate determining prevalent macroeconomic conditions are important, the credit rating of an engineering contractor is equally so. A more accurate approach would be to calculate a rate on a case-by-case basis for each technology. This study only considers two energy storage applications; peaker replacement and seasonal storage (as defined in Section 2.2.4). Perhaps an interesting study would be to identify the most vital energy storage applications for the South African grid; i.e. which storage applications facilitate the least-cost renewable energy mix or the energy mix with the greatest share of renewable sources. However, for reasons mentioned, and in a rapidly developing commercial technological world and the thankfully rapidly changing South African energy policy climate, this may be a short-lived result to obtain

5.2.2 Thermal energy evaluation

As discussed in Section 4.5, a thorough comparison of TES technologies for CSP requires its decoupling from the rest of the plant. The corresponding economic model used should be able to accommodate various TES systems and change the operating strategy for the CSP plant accordingly. This level of detail is beyond the scope of this study; further investigation into this topic might warrant a more detailed TES economic model. Evaluating thermal energy storage as a standalone energy storage system (ESS) could be done in the form of a Carnot battery model

(discussed in Section 1.2). In that case, the cost of storage does not account for the cost to produce the electricity in the first place.

5.2.3 Energy usage modelling

The energy model used in this study does not take time of use or demand and supply into account or variability of electricity price through the day. By implementing time of use modelling, one would be able to account for the variations in electricity price throughout the day. This kind of model would also be able to predict the supply and demand based on the expected electricity generation supply and would consider the true value in the dispatchability of technologies like CSP with TES. Where this study evaluates the performance of energy storage systems on a high-level, the research questions asked could be even better addressed by using more granular energy modelling techniques. Such a model would employ hourly weather, energy load and generation data, as impacting and reflected in various renewable energy and associated storage technologies deployed.

Chapter 6

Summary, Conclusions and Recommendations

This chapter presents a summary of this study as well as discussing the main findings of this study and outlines recommendations for future work.

6.1 Summary

The objective of this study was to identify and compare energy storage technologies for renewable energy sources using a techno-economic model while also considering the special case of concentrated solar power (CSP). These technologies were identified through an in-depth literature study that sought to develop a thorough knowledge base of state-of-the-art energy storage technologies.

The scope of this study was limited to long-term storage and energy storage durations that will increase the penetration of variable renewable energy (VRE) in South Africa (Section 2.2.4). Since peak loads are most expensive to service from otherwise idle power plants, energy storage to serve peak loads would be the most profitable. Additionally, to minimize energy losses through curtailment and undesirable fossil fuel backup power protecting against intermittency, the largest energy storage is also of interest. Therefore, only technologies that are suitable for peaker replacement and long-term (seasonal storage) applications are considered in this study. The key technical characteristics of these energy storage applications are described by Akhil *et al.* (2015) and IEA (2014) and are summarised in Table 2.2.1.

A literature study was conducted (Chapter 2) which investigated the background of concentrated solar power (CSP), as well as new developments in the field, since in the VRE context, CSP already provides short term cost-effective energy storage.

Various classes of energy were discussed, as well as the most common storage technologies used today. Of the several well-defined energy storage applications found in the literature, peaker replacement and long-term seasonal storage, were identified as the most applicable in the context of this study. The need for storage was identified as well as an internationally growing trend in the type and amount of storage technologies installed in the context of all renewable energy harvesting technologies, with utility scale electricity storage being the most rapidly growing application.

It was found that a high penetration (or higher share of energy mix) of intermittent renewable electricity generation technologies like solar photovoltaic (PV) and wind-powered plants is only viable with enough energy storage. The technical parameters of a storage system were investigated, as well as the timescales of storage necessary for various applications. Discharge durations of 4.5 h and 2160 h were identified (Section 2.2.3) for the purposes of medium (daily) and long-term (seasonal) energy storage and their technical specifications were defined in Section 2.2.4.

Of several techniques identified in the literature used to compare energy storage technologies, levelised cost of storage (LCOS) was selected based on its wide adoption in other studies and relatively well understood best-practices compared to other methods used for the same purpose. The LCOS of five electrical energy storage systems (EESSs) was modelled using a probabilistic model and used Monte Carlo simulations to determine the least-cost option for specific energy storage needs.

Following the example of previous studies, the selection of these technologies were made based on their suitability to meet the technical requirements of peaker replacement and seasonal energy storage applications (Section 2.5). These technologies are: pumped storage hydroelectricity (PSH), compressed air energy storage (CAES), lithium-ion battery energy storage (Li-ion), vanadium redox flow batteries (VRFB) and hydrogen energy storage.

The input data used for this study was sourced from a database created by Schmidt *et al.* (2019) which was derived from a review of academic publications and industry, and verified with industry experts (Section 3.4). Table 3.2.1 summarises the techno-economic parameters considered in this study, as well as those considered in studies from 2013–2019. The technical and economic data of the energy storage systems (ESSs) considered in this study is summarised in Appendix B along with relevant references.

Given the source of the input parameters of this study, it can be expected that certain

technologies might be more expensive in South Africa. However, since this type of information was not accessible, it was assumed that the input parameters are representative of global trends in technology cost and performance, as short-lived as these trends may be.

The method used and motivation for using Monte Carlo simulations are discussed in Sections 3.5 and 3.6. Results of the Monte Carlo simulations are presented in Chapter 4. It was determined that the Monte Carlo simulations present two areas of investigation: a view into the LCOS model (understanding its sensitivities) and the second was finding the most cost-effective solution for each of the two energy storage applications. The sensitivities examined through the Monte Carlo methodology add to the robustness of the results.

The LCOS model used in this study was developed using the mathematical equations described in Section 3.3 and were used in combination with a Monte Carlo simulation script written with Matlab (The MathWorks Inc., 2020), a section of which is presented in Appendix C for the benefit of future research. The LCOS model was verified using publicly available data (Schmidt, 2019).

Section 3.5 explains how variance is introduced into the LCOS model due to the probabilistic nature of the input parameters, and that one method of investigating the model's sensitivity to this variance is to use Monte Carlo simulations. While it is possible to use the mean of these input ranges, the end result is a discrete value and any statistical information is lost.

From initial sensitivity analyses, it was found that the LCOS results showed the greatest sensitivity to round-trip efficiency and power specific cost. The latter is the cost associated with the system's power capacity. The results of the Monte Carlo analysis showed that amongst all 5 technologies, the investment cost component of LCOS had the greatest contribution. In the case of seasonal storage applications, the investment cost component further outweighed the rest, indicating that capital costs make up the bulk of long duration energy storage projects. The Monte Carlo analysis was also used to investigate the relationship between LCOS, discharge duration and annual charge-discharge cycle. The results showed that in each application, the EESS costs strongly depend on the annual cycle frequency and less so on the discharge duration.

Lastly, the LCOS model was used to compare the cost-competitiveness of CSP plants with integrated thermal energy storage (TES) systems to EESSs charged with electricity generated by PV and wind-powered plants commissioned between 2020–2022. While PSH and CAES proved cost-competitive with the last three CSP

plants commissioned in South Africa (between 2018–2019), a comparison with Aurora CSP plant in Australia showed that CSP has a value proposition at storage capacities of 4–8 h. This result confirms the results from similar studies, where CSP with TES was shown to be the least-cost option for dispatchable electricity generation with storage of 4 hours and longer (Lovegrove *et al.*, 2018; Schöniger *et al.*, 2021).

6.2 Findings and conclusions

The literature review highlighted several important aspects of energy storage technologies. Various classes of energy were discussed, as well as the most common storage technologies used today. The study revealed that there is a global trend in the number and diversity of energy storage devices used, with utility scale electricity storage being the most rapidly growing application. It was found that a high penetration (or higher share of energy mix) of intermittent renewable electricity generation technologies like solar photovoltaic (PV) and wind-powered plants is only viable with enough energy storage. Energy storage is the key to decouple renewable energy generation from its consumption. From the energy storage applications identified in the literature review, peaker replacement and long-term seasonal storage were selected as the most appropriate in the context of this study.

For each of the technologies, investment cost had the greatest influence, while that of replacement and operational costs were far less. From the initial sensitivity analysis, it was shown that the LCOS was sensitive to variation in round-trip efficiency and power specific cost. However, the cost data for each technology used had much smaller variation in this parameter compared to investment cost, resulting in an insignificant contribution in the simulated data.

CSP has a role to play in South Africa’s least-cost mix between variable and dispatchable renewable energy generation technologies. Technologies like CAES and hydrogen energy storage can offer least-cost cost solutions to peaker replacement and long-term seasonal storage application and in particular with regard to energy storage via hydrogen, national and international, policy, technological and commercial developments are excitingly accelerating rapidly.

6.3 Recommendations for future work

This study employs the LCOS method, paired with Monte Carlo uncertainty analysis, and presents a guideline for comparing CSP plants with other VRE (like PV

and wind-powered plants) that use EESS technologies. Section 5.2 discusses some of the limitations of this study and assumptions made within its scope. Avenues for further work are based on creating a more detailed comparison between EESSs and TES technologies.

The first being a granular energy model based on real-world inputs like solar resource, electricity consumption profiles, energy storage levels, time of use schedules and variability in electricity demand and price. The value of dispatchability of technologies like CSP would be more apparent with this kind of model.

A second avenue could be to identify the most crucial energy storage applications to facilitate greater penetration of renewable energy generation technologies, i.e. which storage applications facilitate the least-cost renewable energy mix or the energy mix with the greatest share of renewable sources.

Appendices

Appendix A

Inflation Indices and Conversion Rates

The currency exchange rates and inflation indices used for analysis are listed in Tables A.0.1 and A.0.2 respectively. The exchange rate and inflation indices used for 2022 are an average of available values from January to July 2022.

Table A.0.1: Average annual exchange rates: ZAR per USD

Year	ZAR/USD ^a
2013	9.64
2014	10.84
2015	12.77
2016	14.71
2017	13.30
2018	13.26
2019	14.45
2020	16.46
2021	14.79
2022	15.90

^aX-rates (2022)

Table A.0.2: Inflation indices for EUR, USD and ZAR

Year	EUR^a	USD^b	ZAR^c
2008	91.53	215.303	63.6
2009	91.8	214.537	67.8
2010	93.28	218.056	70.7
2011	95.81	224.939	74.2
2012	98.21	229.594	78.4
2013	99.54	232.957	82.9
2014	99.97	236.736	88
2015	100	237.017	92
2016	100.24	240.011	97.8
2017	101.78	245.12	103
2018	103.55	251.107	107.8
2019	104.8	255.657	112.2
2020	105.06	258.811	115.9
2021	107.54	270.25	120.85
2022	114.6	289.5	102.6

^aRate-inflation (2022*b*)

^bRate-inflation (2022*a*)

^cStatistics South Africa (2022)

Appendix B

Technology Cost Data Used

This section presents the cost and performance data used in this study for each of the 5 technologies in Tables B.0.1 to B.0.5. For each technology, the mean value is listed as well as its standard deviation.

Table B.0.1: Stochastic inputs for pumped storage hydroelectricity

Parameter	Symbol	Mean	σ [%]	Units
Investment cost - Power	I_P	1379	45	\$/kW
Investment cost - Energy	I_E	98	63	\$/kWh
Operation cost - Power	C_{P-OM}	9.78	26	\$/kW-yr
Operation cost - Energy	C_{E-OM}	0.001	60	\$/kWh
Replacement cost	C_{REP}	146.6	5	\$/kW
Round-trip efficiency	η_{RT}	78	9	%
Lifetime(100 % DoD)	cy_{Life}	33250	43	cycles
Shelf life	T_{shelf}	55	9	years

Sources: Akhil *et al.* (2015); Zakeri and Syri (2015); Chen *et al.* (2009); Black and Veatch (2012) and Rehman *et al.* (2015)

Table B.0.2: Stochastic inputs for compressed air energy storage

Parameter	Symbol	Mean	σ [%]	Units
Investment cost - Power	I_P	1064	35	\$/kW
Investment cost - Energy	I_E	47.6	58	\$/kWh
Operation cost - Power	C_{P-OM}	4.9	23	\$/kW-yr
Operation cost - Energy	C_{E-OM}	0.005	60	\$/kWh
Replacement cost	C_{REP}	122	5	\$/kW
Round-trip efficiency	η_{RT}	44	16	%
Lifetime(100 % DoD)	cy_{life}	16250	20	cycles
Shelf life	T_{shelf}	30	33	years

Sources: Akhil *et al.* (2015); Zakeri and Syri (2015); Chen *et al.* (2009); Black and Veatch (2012); Elmegaard and Brix (2011) and IRENA (2012)

Table B.0.3: Stochastic inputs for lithium-ion batteries

Parameter	Symbol	Mean	σ [%]	Units
Investment cost - Power	I_P	828	17	\$/kW
Investment cost - Energy	I_E	979	24	\$/kWh
Operation cost - Power	C_{P-OM}	12.21	35	\$/kW-yr
Operation cost - Energy	C_{E-OM}	0.003	60	\$/kWh
Replacement cost	C_{REP}	61.07	5	\$/kW
Round-trip efficiency	η_{RT}	86	7	%
Lifetime(100% DoD)	cy_{life}	3250	38	cycles
Shelf life	T_{shelf}	13	38	years

Sources: Zakeri and Syri (2015); Kleinberg (2016); Black and Veatch (2012); Świerczyński *et al.* (2014)

Table B.0.4: Stochastic inputs for vanadium redox flow batteries

Parameter	Symbol	Mean	σ [%]	Units
Investment cost - Power	I_P	1013	21	\$/kW
Investment cost - Energy	I_E	928	17	\$/kWh
Operation cost - Power	C_{P-OM}	14.7	52	\$/kW-yr
Operation cost - Energy	C_{E-OM}	0.001	60	\$/kWh
Replacement cost	C_{REP}	109.92	5	\$/kW
Round-trip efficiency	η_{RT}	73	9	%
Lifetime(100 % DoD)	cyC_{life}	8272	13	cycles
Shelf life	T_{shelf}	13	20	years

Sources: Akhil *et al.* (2015); Zakeri and Syri (2015); Kleinberg (2016) (Black and Veatch, 2012)

Table B.0.5: Stochastic inputs for hydrogen energy storage

Parameter	Symbol	Mean	σ [%]	Units
Investment cost - Power	I_P	6616	48	\$/kW
Investment cost - Energy	I_E	37.8	60	\$/kWh
Operation cost - Power	C_{P-OM}	56.18	30	\$/kW-yr
Operation cost - Energy	C_{E-OM}	0.0001	60	\$/kWh
Replacement cost	C_{REP}	1832	48	\$/kW
Round-trip efficiency	η_{RT}	40	13	%
Lifetime(100 % DoD)	cyC_{life}	20000	0	cycles
Shelf life	T_{shelf}	18	14	years

Sources: Zakeri and Syri (2015); Black and Veatch (2012); Schmidt *et al.* (2017); Kurtz *et al.* (2015); Kaldellis (2007); Ramsden and Levene (2008) and Karellas and Tzouganatos (2014)

Appendix C

Matlab Script

The function written to perform Monte Carlo simulations and calculate the levelised cost of energy storage, as described in Chapter 3 is printed below.

```
1 function [output_value] = mcFunction(tSim, Tek, rated_power, DD, frequency, pEl,
2     discount)
3 %mcFunction calculates LCOS using monte carlo simulation
4 % This script does the following:
5 % 1. Imports economic data from database file (schmidt, 2019) containing
6 % mean and stdev value for each parameter.
7 % 2. Creates variable rng arrays for each input variable based on mean
8 % value and stdev.
9 % 3. Calculates the LCOS for each sample point and returns data table of
10 % LCOS cost components.
11
12 rng(42)
13
14 % test inputs
15 %tSim = 500; Tek = 1; rated_power = 100e3; DD = 4.5; frequency = 365; pEl =
16     33.33/1000; discount = 8/100;
17
18 % 1. Set up the Import Options and import the data
19 % csvScan is a custom function that reads a CSV file with input data
20 % and returns a data table that corresponds to the selected technology (Tek)
21 data = csvScan(Tek);
22
23 % 2. Creating variable arrays
24 cpi2015 = 237.02;
25 cpi2022 = 289.48;
26 ifc = cpi2022/cpi2015; %inflation constant used to adjust from 2015 to 2022
```

```

27
28 %creating arrays of random inputs within 80% CI
29 p10 = 0.1;
30 p90 = 0.9;
31 arrayFunc = @(num,mp) ...
32     norminv((p10 + (p90 - p10).*rand(tSim,1)),data.x(num)*mp,data.s(num));
33
34 %investment cost – power specific
35 Ip = arrayFunc(1,ifc);
36 %investment cost – energy specific
37 Ie = arrayFunc(2,ifc);
38 %operation and maintenance cost – power specific
39 cPom = arrayFunc(3,ifc);
40 %operation and maintenance cost – energy specific
41 cEom = arrayFunc(4,ifc);
42 %replacement cost
43 rep_power = arrayFunc(5,ifc);
44 %round-trip efficiency
45 nRT = arrayFunc(9,1);
46 cycle_life = arrayFunc(11,1);
47 shelf_life = arrayFunc(12,1);
48
49 % Correcting for NaN caused by zero values
50 if Tek == 3           %if lithium
51     rep_power = zeros(tSim,1);
52 elseif Tek == 4      %if VRF
53     rep_power = zeros(tSim,1);
54 elseif Tek == 5      %if hydrogen
55     cEom = zeros(tSim,1);
56     cycle_life = data.x(11)*ones(tSim,1);
57 end
58
59
60 %Other
61 end_of_life = 0.8; % 80% energy capacity relative to spec
62 cycR = data.x(6);
63 eol_P = data.x(7);
64 eol_E = data.x(13);
65 rep_energy = data.x(17);
66 nSELF = data.x(10);
67 tC = data.x(16);
68 DoD = 1;
69
70 %dependant vars
71 %Replaced by formula below N = ceil(min(shelf_life, cycle_life/cycPa));
72 tR = floor(cycR/frequency);
73 rated_energy = rated_power*DD; %rated energy capacity, kWh
74
75 % 3. Calculation

```

```

76 % Pre-calculations
77 capex = Ip*rated_power + Ie*rated_energy; %precursor to IC
78
79 %declaration of outputs
80 nanArray = NaN(tSim,1); %empty NaN array
81 rep_sum = nanArray;
82 total_capex = nanArray;
83 om_sum = nanArray;
84 elec_sum = nanArray;
85 eol_sum = nanArray;
86 N_array = nanArray;
87
88 qcArray = NaN(tSim,5);
89
90 % start of montecarlo sim
91 for i = 1:tSim
92
93     %dependant variables
94     deg_cyclical = 1 - end_of_life^(1/cycle_life(i));
95     deg_temporal = 1 - end_of_life^(1/shelf_life(i));
96     N = (1-end_of_life)/(deg_cyclical*frequency + deg_temporal);
97     R = floor(N/tR);
98
99
100    %alternate formulae
101    N = cycle_life(i)/frequency;
102    deg_cyclical = (1-end_of_life)/cycle_life(i);
103    deg_temporal = (1-end_of_life)*frequency/cycle_life(i);
104
105    k = 1:N;
106    N_array(i) = N; %determining value of N
107
108    % lcos inputs
109    rep_sum(i) = sum((rep_power(i)*rated_power + rep_energy*rated_energy)...
110        ./ (1+discount).^(tC+(1:R)*tR),2);
111    total_capex(i) = capex(i) + rep_sum(i);
112    om_sum(i) = sum((cPom(i)*rated_power + cEom(i)*(frequency*DoD*rated_energy)...
113        *(1-deg_cyclical).^((k-1)*frequency).*(1-deg_temporal).^(k-1))./(1+
114        discount).^(k+tC)),2);
115    elec_sum(i) = frequency*DoD*rated_energy*(1-nSELF)*...
116        sum(((1-deg_cyclical).^((k-1)*frequency).*(1-deg_temporal).^(k-1))./(1+
117        discount).^(k+tC),2);
118    eol_sum(i) = (eol_P*rated_power + eol_E*rated_energy)./(1+discount).^(N+1);
119
120    qcArray(i,:) = [elec_sum(i), (1-nSELF),(1-deg_cyclical),...
121        N,(1-deg_temporal)];
122 end

```



```
123 charge_sum = pEl./nRT.*elec_sum; % ESS charging cost component
124 lcos = (capex + rep_sum + om_sum + charge_sum + eol_sum)./elec_sum; %USD/kWh
125
126 % 4. Processing
127 % data table output
128 data_table.investment = capex;
129 data_table.replacement = rep_sum;
130 data_table.operation = om_sum;
131 data_table.charge = charge_sum;
132 data_table.eol = eol_sum;
133 data_table.elec = elec_sum;
134 data_table.lcos = lcos;
135 data_table.qcArray = qcArray;
136 output_value = data_table;
137
138 end
```

List of References

- Abdon, A., Zhang, X., Parra, D., Patel, M.K., Bauer, C. and Worlitschek, J. (2017). Techno-economic and environmental assessment of stationary electricity storage technologies for different time scales. *Energy*, vol. 139, pp. 1173–1187.
- Akhil, A.A., Huff, G., Currier, A.B., Kaun, B.C., Rastler, D.M., Chen, S.B., Cotter, A.L., Bradshaw, D.T. and Gauntlett, W.D. (2015). DOE/EPRI Electricity Storage Handbook in Collaboration with NRECA. Tech. Rep. SAND2015-1002, Sandia National Laboratories. Available at: <http://www.sandia.gov/ess/publications/SAND2015-1002.pdf> [19/06/2019].
- Akinyele, D.O. and Rayudu, R.K. (2014). Review of energy storage technologies for sustainable power networks. *Sustainable Energy Technologies and Assessments*, vol. 8, pp. 74–91.
- Allen, K., Von Backström, T., Joubert, E. and Gauché, P. (2016). Rock bed thermal storage: Concepts and costs. In: *SOLARPACES 2015: International Conference on Concentrating Solar Power and Chemical Energy Systems*.
- Arnoldi, M. (2022). South Africa has competitive advantages to develop green hydrogen, says Sasol. Available at: <https://www.engineeringnews.co.za/article/south-africa-has-competitive-advantages-to-develop-green-hydrogen-says-sasol-2022-07-14> [29/07/2022].
- Barlev, D., Vidu, R. and Stroeve, P. (2011). Innovation in concentrated solar power. *Solar Energy Materials and Solar Cells*, vol. 95, pp. 2703–2725.
- Battke, B., Schmidt, T.S., Grosspietsch, D. and Hoffmann, V.H. (2013). A review and probabilistic model of lifecycle costs of stationary batteries in multiple applications. *Renewable and Sustainable Energy Reviews*, vol. 25, pp. 240–250.
- Bellini, E. (2022). State Grid of China switches on world’s largest pumped-hydro station. Available at: <https://www.pv-magazine.com/2022/01/04/state-grid-of-china-switches-on-worlds-largest-pumped-hydro-station/> [06/11/2022].
- Black and Veatch (2012). Cost Report: Cost and Performance for Power Generation Technologies. Tech. Rep., National Renewable Energy Laboratory. Available at: <https://refman.energytransitionmodel.com/publications/1921> [19/06/2020].

- Buhla, N. (2021). Redstone CSP Project. Online Presentation to STERG by Chief Executive Officer of Acwa Power for the Redstone CSP Project, 26 August.
- Çengel, Y.A. and Boles, M.A. (2006). *Thermodynamics: An Engineering Approach*. McGraw-Hill Series in Mechanical Engineering, 5th edn. McGraw-Hill Higher Education, Boston. ISBN 978-0-07-288495-1.
- Chambers, J.M. (2017). *Graphical Methods for Data Analysis*. Chapman and Hall/CRC.
- Chen, H., Cong, T.N., Yang, W., Tan, C., Li, Y. and Ding, Y. (2009). Progress in electrical energy storage system: A critical review. *Progress in Natural Science*, vol. 19, no. 3, pp. 291–312.
- Chueh, W. (2018). The Next Big Opportunities in Energy Storage. Available at: <https://energyinnovation.stanford.edu/next-big-opportunities-energy-storage> [10/01/2019].
- Creamer, T. (2022a). Namibian green hydrogen developer expects implementation agreement on \$10bn project by year-end. Available at: https://www.engineeringnews.co.za/article/namibian-green-hydrogen-developer-expects-implementation-agreement-on-10bn-project-by-year-end-2022-08-18/rep_id:4136 [20/08/2022].
- Creamer, T. (2022b). Scatec Confident R16.4bn Solar-Battery Project Will Lay Renewables ‘Intermittency’ Debate to Rest. Available at: <https://www.engineeringnews.co.za/article/scatec-confident-r164bn-solar-battery-project-will-lay-renewables-intermittency-debate-to-rest-2022-07-20> [20/08/2022].
- Cuskelly, D., Fraser, B., Reed, S., Post, A., Copus, M. and Kisi, E. (2019). Thermal storage for CSP with miscibility gap alloys. *AIP Conference Proceedings*, vol. 2126, p. 200013.
- Denholm, P. and Mai, T. (2019). Timescales of energy storage needed for reducing renewable energy curtailment. *Renewable Energy*, vol. 130, pp. 388–399.
- DNVGL (2017). Safety, operation and performance of grid-connected energy storage systems. Recommended Practice DNVGL-RP-0043, Det Norske Veritas.
- DoE (2019). Integrated resource plan (IRP 2019). Tech. Rep., Department of Energy. Available at: <http://www.energy.gov.za/IRP/2019/IRP-2019.pdf> [12/08/2022].
- DRME (2020). Risk mitigation independent power producer procurement programme (RMIPPPP), bidders’ conference - technical presentation. Available at: <https://www.ipp-rm.co.za> [12/08/2022].

- Eberhard, A. and Naude, R. (2016). The South African Renewable Energy Independent Power Producer Procurement Programme: A Review and Lessons Learned. *Journal of Energy in Southern Africa*.
- Elmegaard, B. and Brix, W. (2011). Efficiency of Compressed Air Energy Storage. In: *International Conference on Efficiency, Cost, Optimization, Simulation and Environmental Impact of Energy Systems*.
- Fernando, J. (2021). Time Value of Money (TVM) Definition. Available at: <https://www.investopedia.com/terms/t/timevalueofmoney.asp> [29/09/2020].
- Gauché, P. (2016). *Spatial-temporal model to evaluate the system potential of concentrating solar power towers in South Africa*. Published doctoral dissertation, Department of Mechanical and Mechatronic Engineering, Stellenbosch University, Stellenbosch. Available at: <https://scholar.sun.ac.za/handle/10019.1/100151> [25/08/2022].
- Guney, M.S. and Tepe, Y. (2017). Classification and assessment of energy storage systems. *Renewable and Sustainable Energy Reviews*, vol. 75, pp. 1187–1197.
- Gür, T.M. (2018). Review of electrical energy storage technologies, materials and systems: Challenges and prospects for large-scale grid storage. *Energy & Environmental Science*, vol. 11, pp. 2696–2767.
- Gutttag, J., Grimson, E. and Bell, A. (2016). Introduction to Computational Thinking and Data Science, lecture 6: Monte Carlo Simulation. Class Lecture. Massachusetts Institute of Technology: MIT OpenCourseWare, Available at: <https://ocw.mit.edu> [27/04/2020].
- Hauschild, M.Z., Rosenbaum, R.K. and Olsen, S.I. (eds.) (2018). *Life Cycle Assessment*. Springer International Publishing. ISBN 978-3-319-56474-6 978-3-319-56475-3.
- Ho, C.K., Albrecht, K.J., Yue, L., Mills, B., Sment, J., Christian, J. and Carlson, M. (2020). Overview and design basis for the Gen 3 Particle Pilot Plant (G3P3). In: *SO-LARPACES 2019: International Conference on Concentrating Solar Power and Chemical Energy Systems*. Daegu, South Korea.
- Huggins, R. (2016). *Energy Storage: Fundamentals, Materials and Applications*. Springer International Publishing. ISBN 978-3-319-21238-8 978-3-319-21239-5.
- IEA (2014). Technology Roadmap- Energy storage. Tech. Rep., International Energy Agency. Available at: <https://www.iea.org/reports/technology-roadmap-energy-storage> [22/04/2022].
- IEA (2021). Electricity generation by source, South Africa 1990-2020. Tech. Rep., International Energy Agency. Available at: <https://www.iea.org/countries/south-africa> [17/08/2022].

- IRENA (2012). Electricity Storage: Technology Brief. Tech. Rep., International Renewable Energy Agency. Available at: <https://www.irena.org/publications/2012/Apr/Electricity-storage> [22/04/2020].
- IRENA (2017). Electricity storage and renewables: Costs and markets to 2030. International Renewable Energy Agency, Abu Dhabi.
- Joskow, P.L. (2011). Comparing the Costs of Intermittent and Dispatchable Electricity Generating Technologies. *American Economic Review*, vol. 101, pp. 238–241.
- Jülch, V. (2016). Comparison of electricity storage options using levelized cost of storage (LCOS) method. *Applied Energy*, vol. 183, pp. 1594–1606.
- Kaldellis, J.K. (2007). Optimum energy storage techniques for the improvement of renewable energy sources-based electricity generation economic efficiency. *Energy*, vol. 32.
- Karellas, S. and Tzouganatos, N. (2014). Comparison of the performance of compressed-air and hydrogen energy storage systems: Karpathos island case study. *Renewable and Sustainable Energy Reviews*, vol. 29.
- Kelly-Detwiler, P. (2020). A Key To The ‘Hydrogen Economy’ Is Carbon-Free Ammonia. Available at: <https://www.forbes.com/sites/peterdetwiler/2020/12/16/maybe-the-hydrogen-economy-will-become-the-ammonia-economy/> [12/01/2021].
- Kleinberg, M. (2016). Battery energy storage study for the 2017 IRP. Tech. Rep. 128197#-P-01-A, DNVG GL.
- Kost, C., Shammugam, S., Jülch, V., Nguyen, H.-t. and Schlegl, T. (2018). Levelized Cost of Electricity - Renewable Energy Technologies. Tech. Rep., Fraunhofer ISE. Available at: <https://www.ise.fraunhofer.de/en/publications/studies/cost-of-electricity.html> [1/10/2020].
- Kurtz, J., Saur, G. and Sprik, S. (2015). Hydrogen fuel cell performance as telecommunications backup power in the united states. Tech. Rep., National Renewable Energy Lab. Available at: <https://www.osti.gov/biblio/1260144>
- Lai, C.S. and McCulloch, M.D. (2017). Levelized cost of electricity for solar photovoltaic and electrical energy storage. *Applied Energy*, vol. 190, pp. 191–203.
- Landman, W.A. (2017). *Optical performance of the reflective surface profile of a Heliostat*. Published doctoral dissertation, Department of Mechanical and Mechatronic Engineering, Stellenbosch University, Stellenbosch. Available at: <https://scholar.sun.ac.za/handle/10019.1/101210> [25/08/2022].

- Lazard (2019). Levelized Cost of Energy and Levelized Cost of Storage 2019. Available at: <http://www.lazard.com/perspective/levelized-cost-of-energy-and-levelized-cost-of-storage-2019/> [10/08/2020].
- Lilliestam, J., Ollier, L., Labordena, M., Pfenninger, S. and Thonig, R. (2020). The near- to mid-term outlook for concentrating solar power: Mostly cloudy, chance of sun. *Energy Sources, Part B: Economics, Planning, and Policy*, pp. 1–19. Available at: <https://csp.guru/> [12/08/2020].
- Lilliestam, J. and Pitz-Paal, R. (2018). Concentrating solar power for less than USD 0.07 per kWh: Finally the breakthrough? *Renewable Energy Focus*, vol. 26, pp. 17–21.
- Lim, S.D., Mazzoleni, A.P., Park, J., Ro, P.I. and Quinlan, B. (2012). Conceptual design of ocean compressed air energy storage system. In: *Proceedings of Oceans, 2012*, pp. 1–8. Hampton Roads, VA.
- Lovegrove, K., James, G., Leitch, D., Milczarek, A., Ngo, A., Rutovitz, J., Watt, M. and Wyder, J. (2018). Comparison of Dispatchable Renewable Electricity Options. Tech. Rep., Australian Renewable Energy Agency (ARENA).
- Lovegrove, K. and Stein, W. (eds.) (2021). *Concentrating Solar Power Technology*. Elsevier. ISBN 978-0-12-819970-1.
- Luke, R. (1996). *Compressed Air Storage for Electricity Generation in South Africa*. Published doctoral dissertation, University of Cape Town.
- Luo, X., Wang, J., Dooner, M. and Clarke, J. (2015). Overview of current development in electrical energy storage technologies and the application potential in power system operation. *Applied Energy*, vol. 137, pp. 511–536.
- Maize, K. (2017). Duck Hunting at the California Independent System Operator. Available at: <http://www.powermag.com/duck-hunting-california-independent-system-operator/> [31/07/2018].
- Mantashe, G. (2022). Minister of Mineral Resources and Energy, as quoted in Mantashe confirms IRP 2019 review, but offers no timing specifics. Available at: <https://www.engineeringnews.co.za/article/mantashe-confirms-irp-2019-review-but-offers-no-timing-specifics-2022-06-02> [31/07/2022].
- Mayr, F. and Beushausen, H. (2016). Navigating the maze of energy storage costs. Available at: https://www.apricum-group.com/wp-content/uploads/2016/06/PV-Tech-Power-May-2016_Navigating-Maze-Storage-Costs_Mayr_Beushausen.pdf [09/11/2020].
- McTigue, J. (2019). 'Carnot Batteries' for Electricity Storage. Available at: <https://www.nrel.gov/docs/fy20osti/75559.pdf> [11/04/2022].

- Microsoft Corporation (2021). Microsoft excel. Available at: <https://office.microsoft.com/excel> [2021-09-24].
- Mostafa, M.H., Abdel Aleem, S.H., Ali, S.G., Ali, Z.M. and Abdelaziz, A.Y. (2020). Techno-economic assessment of energy storage systems using annualized life cycle cost of storage (LCCOS) and levelized cost of energy (LCOE) metrics. *Journal of Energy Storage*, vol. 29, p. 101345.
- NREL (2020). Concentrating Solar Power Projects Database. [Online Database]. Available at: <https://solarpaces.nrel.gov> [12/06/2020].
- NREL (2021). Khi Solar One | Concentrating Solar Power Projects | NREL. <https://solarpaces.nrel.gov/project/khi-solar-one>.
- NTESS (2020). Global Energy Storage Database. [Online Database]. Available at: <https://www.sandia.gov/ess-ssl/global-energy-storage-database-home/> [24/08/2020].
- Obi, M., Jensen, S., Ferris, J.B. and Bass, R.B. (2017). Calculation of levelized costs of electricity for various electrical energy storage systems. *Renewable and Sustainable Energy Reviews*, vol. 67, pp. 908–920.
- Ould Amrouche, S., Rekioua, D., Rekioua, T. and Bacha, S. (2016). Overview of energy storage in renewable energy systems. *International Journal of Hydrogen Energy*, vol. 41, pp. 20914–20927.
- Pan, C.A. (2020). *A Technical and economic assessment of molten salt parabolic trough power plants and operating strategies in Southern Africa*. Published doctoral dissertation, Stellenbosch : Stellenbosch University.
- Pan, C.A., Guédez, R., Dinter, F. and Harms, T.M. (2019). A techno-economic comparative analysis of thermal oil and molten salt parabolic trough power plants with molten salt solar towers. In: *Proceedings of the International Conference on Concentrating Solar Power and Chemical Energy Systems, SOLARPACES 2018*, p. 120014. Casablanca, Morocco.
- Pawel, I. (2014). The cost of storage - How to calculate the levelized cost of stored energy (LCOE) and applications to renewable energy generation. In: *Proceedings of the 8th International Renewable Energy Storage Conference and Exhibition, IRES 2013*. Elsevier Procedia, Berlin.
- Pelay, U., Luo, L., Fan, Y., Stitou, D. and Rood, M. (2017). Thermal energy storage systems for concentrated solar power plants. *Renewable and Sustainable Energy Reviews*, vol. 79, pp. 82–100.
- Raju, M. and Kumar Khaitan, S. (2012). Modeling and simulation of compressed air storage in caverns: A case study of the Huntorf plant. *Applied Energy*, vol. 89, pp. 474–481.

- Ramsden, T., K.B. and Levene, J. (2008). Potential for Opportunities for Hydrogen-Based Energy Storage for Electric Utilities. In: *Proceedings of the NHA Annual Hydrogen Conference*. Sacramento.
- Rate-inflation (2022a). American Historical Consumer Price Index (CPI) - 1913 to 2022. Available at: <https://www.rateinflation.com/consumer-price-index/usa-historical-cpi/> [02/01/2022].
- Rate-inflation (2022b). Euro Area Historical Consumer Price Index (CPI) - 1996 to 2022. Available at: <https://www.rateinflation.com/consumer-price-index/euro-area-historical-cpi/> [02/01/2022].
- Rehman, S., Al-Hadhrami, L.M. and Alam, M.M. (2015). Pumped hydro energy storage system: A technological review. *Renewable and Sustainable Energy Reviews*, vol. 44.
- RenewAfrica (2022). Botswana tenders for two 100 MW concentrated solar power (CSP) plants. Available at: <http://renewafrica.biz/csp/botswana-tenders-for-two-100mw-concentrated-solar-power-csp-plants/> [27/08/2022].
- Reuß, M., Grube, T., Robinius, M., Preuster, P., Wasserscheid, P. and Stolten, D. (2017). Seasonal storage and alternative carriers: A flexible hydrogen supply chain model. *Applied Energy*, vol. 200, pp. 290–302.
- Saunyama, A. (2022). Redstone concentrated solar power project updates. Available at: <https://constructionreviewonline.com/biggest-projects/redstone-concentrated-solar-power-project-developers-make-1st-loan-repayment/> [27/08/2022].
- Schmidt, O. (2019). Lifetime cost of electricity storage online model. Available at: <https://energystorage.shinyapps.io/LCOSApp/> [16/10/2020].
- Schmidt, O. (2020). Electronic mail correspondance with Oliver Schmidt regarding the levelised cost of storage model.
- Schmidt, O., Hawkes, A., Gambhir, A. and Staffell, I. (2017). The future cost of electrical energy storage based on experience rates. *Nature Energy*, vol. 2.
- Schmidt, O., Melchior, S., Hawkes, A. and Staffell, I. (2019). Projecting the Future Levelized Cost of Electricity Storage Technologies. *Joule*, vol. 3, pp. 81–100.
- Schöniger, F., Thonig, R., Resch, G. and Lilliestam, J. (2021). Making the sun shine at night: Comparing the cost of dispatchable concentrating solar power and photovoltaics with storage. vol. 0, pp. 1–20.
- Siemens Gamesa (2019). World first: Siemens Gamesa begins operation of its innovative electrothermal energy storage system. Available at: <https://www.siemensgamesa.com/en-int/newsroom/2019/06/190612-siemens-gamesa-inauguration-energy-system-thermal> [11/03/2022].

- Smil, V. (2017). *Energy and Civilization: A History*. MIT Press. ISBN 978-0-262-33830-1 978-0-262-33831-8.
- Statistics South Africa (2022). Publication | Statistics South Africa. Available at: <http://www.statssa.gov.za/publications/P0141/CPIHistory.pdf?> [02/07/2022].
- Stein, W. and Buck, R. (2017). Advanced power cycles for concentrated solar power. *Solar Energy*, vol. 152, pp. 91–105.
- Świerczyński, M., Stroe, D.I., Stan, A.-I., Teodorescu, R. and Sauer, D.U. (2014). Selection and Performance-Degradation Modeling of $\text{LiMO}_2/\text{Li}_4\text{Ti}_5\text{O}_{12}$ and LiFePO_4/C Battery Cells as Suitable Energy Storage Systems for Grid Integration With Wind Power Plants: An Example for the Primary Frequency Regulation Service. *IEEE Transactions on Sustainable Energy*, vol. 5.
- The MathWorks Inc. (2020). Matlab version 9.9.0.1467703 (R2020b).
- Wright, J.G., Calitz, J.R., Ntuli, N., Fourie, R., Rampokanyo, M.J. and Kamera, P. (2018). Formal comments on the Draft Integrated Resource Plan (IRP) 2018. Available at: <https://researchspace.csir.co.za/dspace/handle/10204/10493> [02/09/2021].
- X-rates (2022). Monthly average exchange rates 2017 (South African Rand per US Dollar). Available at: <https://www.x-rates.com/average/?from=USD&to=ZAR&amount=1&year=2017> [02/01/2022].
- Zakeri, B. and Syri, S. (2015). Electrical energy storage systems: A comparative life cycle cost analysis. *Renewable and Sustainable Energy Reviews*, vol. 42, pp. 569–596.
- Zanganeh, G., Pedretti, A., Zavattoni, S., Barbato, M. and Steinfeld, A. (2012). Packed-bed thermal storage for concentrated solar power – Pilot-scale demonstration and industrial-scale design. *Solar Energy*, vol. 86, pp. 3084–3098.
- Zhang, J.Z., Li, J., Li, Y. and Zhao, Y. (eds.) (2014). *Hydrogen Generation, Storage, and Utilization*. John Wiley & Sons, Inc., Hoboken, NJ, USA.